

Precision-guided Munitions Effects Representation



TRADOC Analysis Center
700 Dyer Road
Monterey, California 93943-0692

This study cost the
Department of Defense approximately
\$186,000 expended by TRAC in
Fiscal Years 16-17.
Prepared on 20170103
TRAC Project Code # 060317.

Precision-guided Munitions Effects Representation

MAJ Cardy Moten III

TRADOC Analysis Center
700 Dyer Road
Monterey, California 93943-0692

This page intentionally left blank.

REPORT DOCUMENTATION PAGE

*Form Approved
OMB No. 0704-0188*

Public reporting burden for this collection of information is estimated to average 1 hour per response, including the time for reviewing instructions, searching existing data sources, gathering and maintaining the data needed, and completing and reviewing this collection of information. Send comments regarding this burden estimate or any other aspect of this collection of information, including suggestions for reducing this burden to Department of Defense, Washington Headquarters Services, Directorate for Information Operations and Reports (0704-0188), 1215 Jefferson Davis Highway, Suite 1204, Arlington, VA 22202-4302. Respondents should be aware that notwithstanding any other provision of law, no person shall be subject to any penalty for failing to comply with a collection of information if it does not display a currently valid OMB control number. **PLEASE DO NOT RETURN YOUR FORM TO THE ABOVE ADDRESS.**

1. REPORT DATE (DD-MM-YYYY) 01-03-2017		2. REPORT TYPE Technical Memorandum		3. DATES COVERED (From - To)	
4. TITLE AND SUBTITLE Precision-guided Munitions Effects Representation				5a. CONTRACT NUMBER	
				5b. GRANT NUMBER	
				5c. PROGRAM ELEMENT NUMBER	
6. AUTHOR(S) MAJ Cardy Moten III				5d. PROJECT NUMBER 060317	
				5e. TASK NUMBER	
				5f. WORK UNIT NUMBER	
7. PERFORMING ORGANIZATION NAME(S) AND ADDRESS(ES) TRADOC Research Analysis Center, Monterey, CA Naval Postgraduate School, Monterey, CA				8. PERFORMING ORGANIZATION REPORT NUMBER TRAC-M-TM-17-007	
9. SPONSORING / MONITORING AGENCY NAME(S) AND ADDRESS(ES) Army G-3/5/7 Munitions Management Division Center for Army Analysis				10. SPONSOR/MONITOR'S ACRONYM(S)	
				11. SPONSOR/MONITOR'S REPORT NUMBER(S)	
12. DISTRIBUTION / AVAILABILITY STATEMENT Approved for public release; distribution is unlimited.					
13. SUPPLEMENTARY NOTES					
14. ABSTRACT The purpose of this memorandum is to provide documentation of research for the Army G3/5/7 Munitions Management Division and Center for Army Analysis (CAA) by the TRADOC Analysis Center, Monterey (TRAC-MTRY). The focus of the research is to improve the current methodology employed by CAA in modeling precision-guided munitions effects into the Joint Integrated Contingency Model (JICM) scenarios to enhance munitions requirements estimate generation, especially for high-cost low-density munitions like Excalibur.					
15. SUBJECT TERMS Training intervention, cognitive state, regret, neurophysiological measures, Wisconsin Card Sorting Test, Iowa Gambling Task					
16. SECURITY CLASSIFICATION OF: Unclassified			17. LIMITATION OF ABSTRACT UL	18. NUMBER OF PAGES 131	19a. NAME OF RESPONSIBLE PERSON MAJ Cardy Moten III
a. REPORT Unclassified	b. ABSTRACT Unclassified	c. THIS PAGE Unclassified			19b. TELEPHONE NUMBER (include area code) 831-656-2452

This page intentionally left blank.

Table of Contents

Report Documentation	iii
Technical Memorandum	1
Appendix A. Study Plan	A-1
Problem Statement	A-1
Project Team	A-1
Constraints, Limitations, & Assumptions	A-2
Methodology	A-2
Timeline	A-3
Appendix B. Progress Report	B-1
Appendix C. Analytic Solution Methodology	C-1
MATLAB Code	C-49
Damage probability for multiple weapons against a unitary target	C-49
Damage probability for area target with M aimpoints placed along an ellipse uniformly in polar angle (EUPA)	C-50
Optimized Damage probability for area target with M aimpoints placed along an ellipse uniformly in polar angle (EUPA)	C-51
Maximum damage probability of M weapons against N targets using the optimized EUPA methodology	C-52
Appendix D. Response Surface Methodology	D-1
Appendix E. References	E-1
Appendix F. Glossary	F-1

This page intentionally left blank.

- 1. Purpose.** The purpose of this memorandum is to provide documentation of research for the Army G3/5/7 Munitions Management Division and Center for Army Analysis (CAA) by the TRADOC Analysis Center, Monterey (TRAC-MTRY). The focus of the research is to improve the current methodology employed by CAA in modeling precision-guided munitions effects into the Joint Integrated Contingency Model (JICM) scenarios to enhance munitions requirements estimate generation, especially for high-cost low-density munitions like Excalibur.
- 2. Background.** The Army Munitions Management Division develops ammunition requirements in support of Army programming and the Army budget. When, as usually happens, there are not sufficient resources to fill 100% of requirements, this office also offers analysis on the risks associated with not filling the full requirement by munition. Currently, CAA supports the Munitions Management office by using JICM to do Army level analysis to support requirements and risks associated with tradeoffs in filling requirements. CAA uses effects data provided by the Army Material Systems Analysis Activity (AMSAA) and tactics, techniques, and procedures (TTPs) and related data from subject matter experts at the Fires Center of Excellence (FCoE) to inform the development of requirements for precision guided munitions (PGMs). Given the critical role that PGMs play in modern Joint warfare, it is of great importance to ensure that CAA's modeling represents PGM usage and effectiveness in an operationally appropriate manner to inform risk analysis for not filling precision munitions to 100% of requirements.
- 3. Methodology.** The research team used two approaches to solve the JICM precision-munitions effects modeling problem: an analytic model for the Carleton damage function, and a response surface model to predict the probability of damage, wounded personnel, suppression effects. Appendix A shows constraints, limitations, and assumptions used for our research methodology.
 - (a) The first approach refined the analytical solution to the Carleton damage function to compute the damage probability for multiple munitions fired at a unitary target and area targets. Wang et al. in detail the derivation of their equations (See Appendix C). First, Wang et al. determined the requisite parameters to determine an exact damage probability using the Carleton damage function of M weapons fired at a unitary target. Next, they utilized this solution to optimize the aim-point distribution that provides the greatest probability of damage to the target.¹ The results of this research will allow the JICM developers to improve their modeling methodology which does not evaluate the optimal probability of multiple weapons systems fired at a unitary target. After determining the optimal damage probability against a unitary target, Wang et al. identified the optimal probability against an area target.² Essentially, this research extends their previ-

¹Hongyun Wang et al. "Explicit Exact Solution of Damage Probability for Multiple Weapons against a Unitary Target". In: *American Journal of Operations Research* 6.06 (2016a), p. 450.

²Hongyun Wang et al. *Average damage caused by multiple weapons against an area target of normally distributed elements*. Tech. rep. TRAC-Monterey, 2016b.

ous work to multiple target engagements and provides added capability for the JICM developers to implement in their combat model.

- (b) Although, the analytic methodology provided added benefits to the JICM model by improving the number of munitions expended in the model, it still does not ensure the fidelity of Battlefield effects required by the Army G-3/5/7 munitions management personnel. The response surface modeling methodology addresses this issue by computing a predicted probability of damage, wounded personnel, and suppression based on the current inputs used in the JICM model. (See Appendix D). To start, Ahner and McCarthy computed a damage probability using the Klopocic damage function, which is a combination of the Carleton damage function and the cookie cutter function.³ Next, they used this damage function and the JICM input parameters to build a design of experiments and a meta-model to compute a predicted probability of damage based on the munition type and target distance. They also developed a similar methodology to compute a predicted probability of suppression and wounded personnel.⁴ Finally, Ahner and McCarthy developed a risk value to model a commander's risk tolerance for collateral damage. Using this parameter will give a decision maker insight into the amount of certainty they can have of damaging, wounding, or suppressing a particular target which is currently not a capability within the JICM model. Another benefit of their methodology is that the CAA JCIM developers can implement this algorithm into their current model or use a separately developed spreadsheet model as a supplemental analysis tool.

4. **Results.** The project team briefed the final results to the sponsor on 27 October 2016 and the slides and notes from this briefing are contained in Appendix B.

³Darryl Ahner and Andrew McCarthy. *Algorithm Development for the Combat Sample Generator (COSAGE) Model*. Tech. rep. Air Force Institute of Technology, 2016.

⁴Ibid.

Appendix A

Study Plan

Problem Statement

To improve the current methodology employed by the Center for Army Analysis (CAA) in modeling precision-guided munitions effects into JICM scenarios in order to enhance munitions requirements estimate generation, especially for high-cost low-density munitions like Excalibur.

Project Team

Sponsor Agency:	Robert Grubbs Munitions Management Division, HQDA G-3/5/7 robert.a.grubbs.civ@mail.mil
Project Stakeholder:	David Knudson Campaign Analysis Division Chief Center for Army Analysis, Fort Belvoir, VA 22060 david.b.knudson.civ@mail.mil
TRAC Lead:	Cardy Moten III MAJ, LG/FA49 TRADOC Analysis Center - Monterey cardy.moten3.mil@mail.mil
NPS Faculty:	Dr. Hong Zhou Applied Mathematics Department Naval Postgraduate School, Monterey, CA hzhou@nps.edu
AFIT Faculty:	Dr. Darryl Ahner Operations Research Department Air Force Institute of Technology, Dayton, OH darryl.ahner@afit.edu

Constraints, Limitations, & Assumptions

- Constraint

- The project completion date is no later than 30 September 2016.

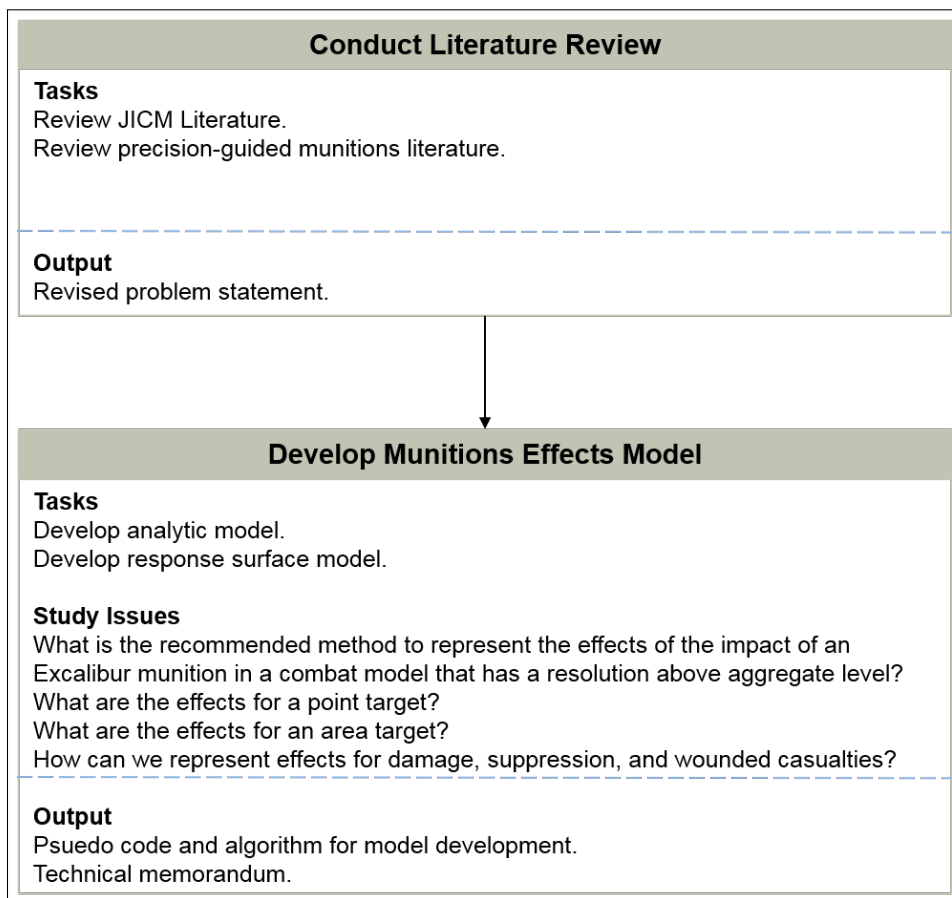
- Limitation

- The project will focus only on precision-guided munitions estimates and effects.

- Assumption

- THe project methodology can be implemented for other types of munitions within JICM.

Methodology



Timeline

- | | |
|------------------|---|
| 06 JAN 16 | IPR #1: Restated problem statement approval. |
| 15 JAN 16 | Complete literature review. |
| 18 JAN 16 | Develop modeling methodology. |
| 9 MAR 16 | IPR #2: Brief initial findings to CAA. |
| 17 MAY 16 | IPR #3: Brief initial findings to G3 Munitions. |
| 27 SEP 16 | Final IPR to CAA. |
| 27 OCT 16 | Final IPR to G3 munitions. |
| 16 DEC 16 | Deliver project documentation. |

This page intentionally left blank.

Appendix B

Progress Report

The final IPR, presented to the sponsor on 27 October 2016, for this phase of the project is on the following pages.



UNCLASSIFIED

Precision-guided Munitions Effects Representation

Final IPR



**Briefing to Army Munitions Management
Division**

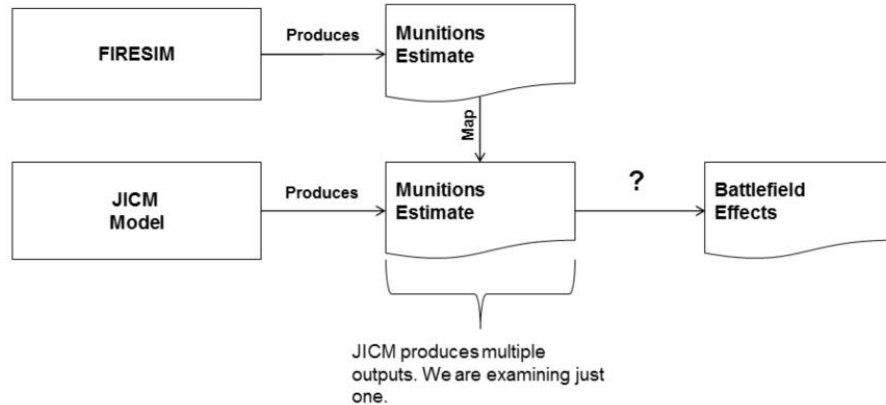
27 October 2016

DISTRIBUTION STATEMENT A: Approved for public release; distribution is unlimited. Release of this information in this brief does not imply any commitment or intent on the part of the U.S. Government to provide any additional public information on any topic presented herein or to participate in any wargame or experiment.

UNCLASSIFIED



Currently, JICM does not adequately adjudicate the effects of Excalibur rounds fired.



25 October 2016

UNCLASSIFIED

Precision-guided Munitions Effects

2

In the current process, JICM produces an estimate of Excalibur rounds fired. This estimate is manually mapped to FIRESIM results. The problem with this method is that FIRESIM and JICM do not adjudicate their effects at the same resolution.

Since FIRESIM is a higher resolution model than COSAGE, the current process requires more subjective analysis of the results.



CAA needs this capability to provide robust munitions estimates to the Army G3 Munitions Division.



25 October 2016

UNCLASSIFIED

Precision-guided Munitions Effects

3

This slide makes a simple depiction of why this problem is important. In essence, CAA sends an estimation of munitions requirements to the Army G3 Munitions office for their follow-on analysis.

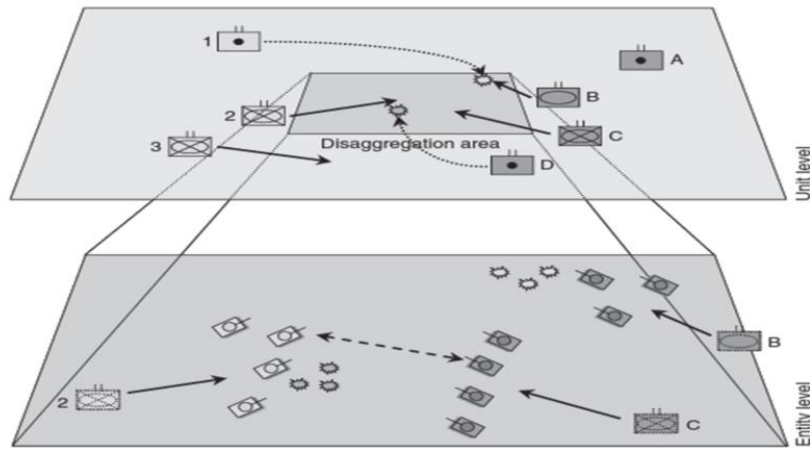
The Army G3 munitions office provides feedback to CAA in the form of updated munitions constraints for CAA to model and then provide updated munitions estimates.

Since the estimates for precision-guided munitions are not adjudicated in enough detail to provide the Army G3 munitions division an assessment of the relative risk to mission, the Army G3 munitions office is having difficulty in providing adequate constraints model for CAA to improve the munitions estimates.

Thus, our proposed model should provide a potential solution to this problem.



COSAGE needs an improved effects modeling methodology for precision-guided munitions.



25 October 2016

UNCLASSIFIED

Precision-guided Munitions Effects

4

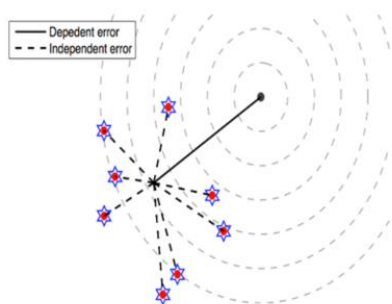
The current COSAGE methodology is as follows.

- Select 1 piece of critical equipment to target at random
- Based on range from target a lethal area and associated round errors are determined for the piece of equipment selected at random
- Calculation of PK for 1 round
 - Center point of piece of equipment is the aim point (0,0)
 - Target size is based on the largest dimension of the target equipment size
 - Use a D_0 value of 1.0
 - Use the Carlton Damage Function from ME to determine a PK
- Draw a random number to determine if the piece of equipment was killed or not
- There is no Collateral targets under consideration

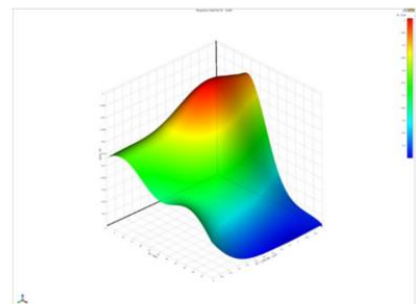
To improve this methodology, we are going to explore more robust damage functions, and improve the target location algorithms.



Use our models to guide your development of a precision-guided munitions effects model in COASE.



Analytical Effects Model



Response Surface Effects Model

25 October 2016

UNCLASSIFIED

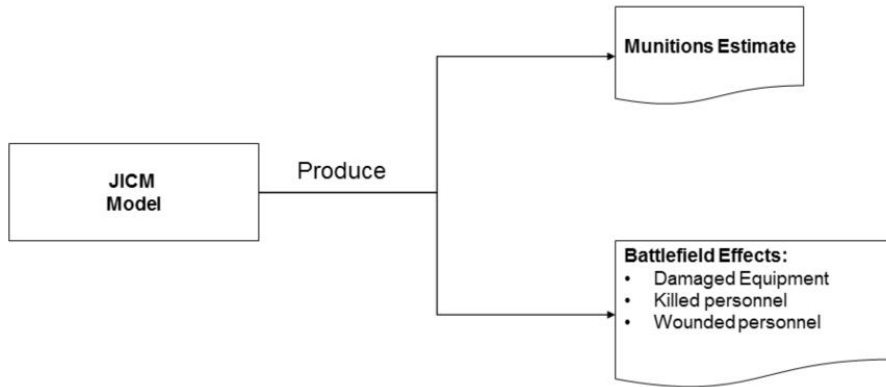
Precision-guided Munitions Effects

5

The bottom line is that we feel that using our proposed model will help CAA to fill its current gap in adjudicating precision-munitions effects in COSAGE.



At endstate, CAA will have the methods to develop an improved effects model for precision-guided munitions.



25 October 2016

UNCLASSIFIED

Precision-guided Munitions Effects

6

The intent of our modeling methodology is to not only provide information on how many rounds were fired, but also other battlefield effects such as: damaged equipment, personnel killed, and wounded personnel.



Our modeling approach is broad in perspective to ensure we analyze the most important issues.



Conduct Literature Review

Review JICM literature.
Review precision-guided munitions literature.

Revised problem statement.

Develop munitions effects model

Develop analytical model.
Develop response surface model.

What is the recommended method to represent the effects of the impact of an Excalibur munition in a combat model that has a resolution above aggregate level?
What are the effects for a point target?
What are the effects for an area target?
How can we represent effects for damage, suppression, and wounded casualties?
Pseudo code and algorithm for model development.
Technical memorandum.



We used the following constraint, limitation, and an assumption to scope our problem.



Constraint.

The project completion date is no later than 30 September 2016.

Limitation.

The project will focus only on precision-guided munitions estimates and effects.

Assumption.

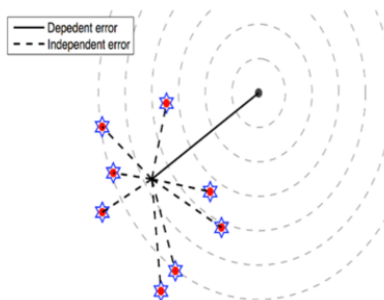
The project methodology can be implemented for other types of munitions within JICM.



Analytical Model Results



Hong Zhou, PhD
Professor of Applied Mathematics



UNIVERSITY OF CALIFORNIA
SANTA CRUZ

Hongyun Wang, PhD
Professor of Applied Mathematics

25 October 2016

UNCLASSIFIED

Precision-guided Munitions Effects



We started our approach by analyzing multiple weapons against a unitary target.



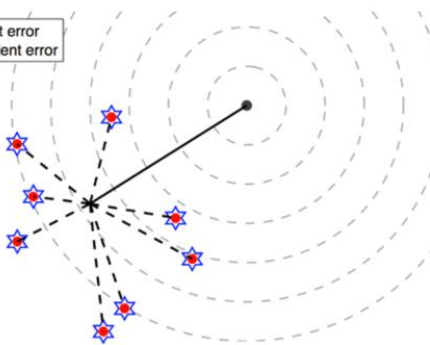
M weapons = either multiple weapons or multiple shots from one weapon

Effect of each weapon is modeled by Carleton damage function

Dependent error = one error deviating impact points of all M weapons

Independent errors = M independent errors, one affecting each of M weapons

— Dependent error
- - - Independent error



Impact point of weapon j :

$$\underbrace{\vec{W}_j}_{\text{Impact point}} = \underbrace{\vec{r}_j}_{\text{Aiming point}} + \underbrace{\vec{Y}}_{\text{Dependent error}} + \underbrace{\vec{X}_j}_{\text{Independent error}}$$

25 October 2016

UNCLASSIFIED

Precision-guided Munitions Effects

10

For this case we consider the problem of shooting multiple weapons against a single target. We model the effects of the munitions using the Carleton damage function. We also will model the effects by analyzing both dependent error (aiming error) and independent error (ballistics errors).

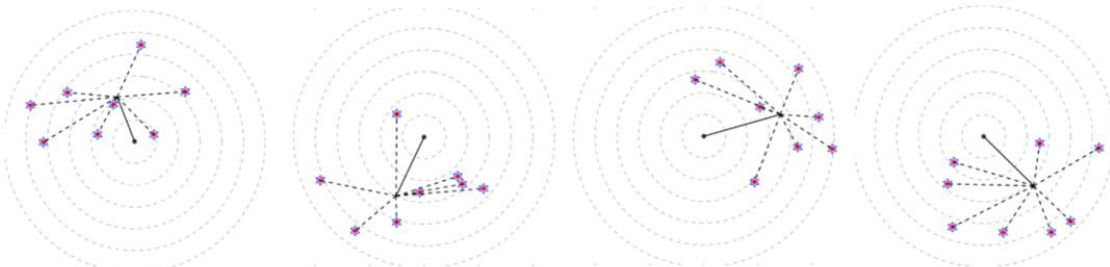
In short, the impact point for the round is a combination of the aiming point and the effects from both the dependent and independent error.



Next, we computed the kill probability in the presence of dependent and independent errors.



Many realizations of firing M weapons:



Kill probability = average over all realizations

Exact solution for the kill probability:

fast and accurate calculation of kill probability

making it possible to optimize aiming points of M weapons

25 October 2016

UNCLASSIFIED

Precision-guided Munitions Effects

11

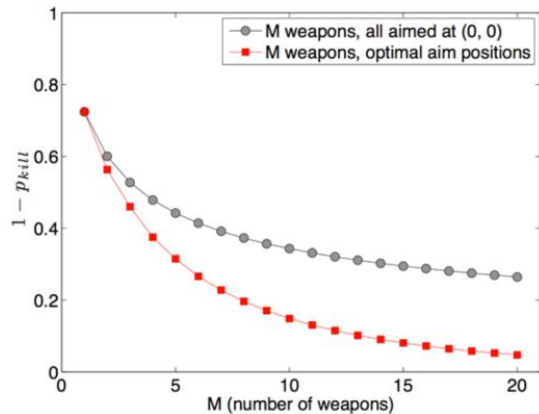
We derived our kill probability solution from the Carleton damage function and will use this solution to examine the kill probability corresponding to various distributions of the aimpoints of M weapons.



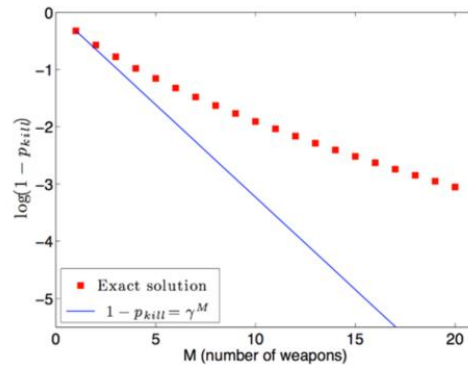
Essentially, spreading out aiming points is effective in countering dependent error.



Survival probability = $1 - (\text{kill probability})$



Survival probability does not decay exponentially with number of weapons.



25 October 2016

UNCLASSIFIED

Precision-guided Munitions Effects

12

The left panel shows a comparison of the case of all M weapons aimed at $(0,0)$ vs the case of using the optimal distribution of aim positions in the decay of $1-p_{kill}$. With the optimal distribution of aim points for M weapons, we expect that $1-p_{kill}(M)$ decays faster than in the case of aiming all M weapons at the same position, which the left side chart confirms.

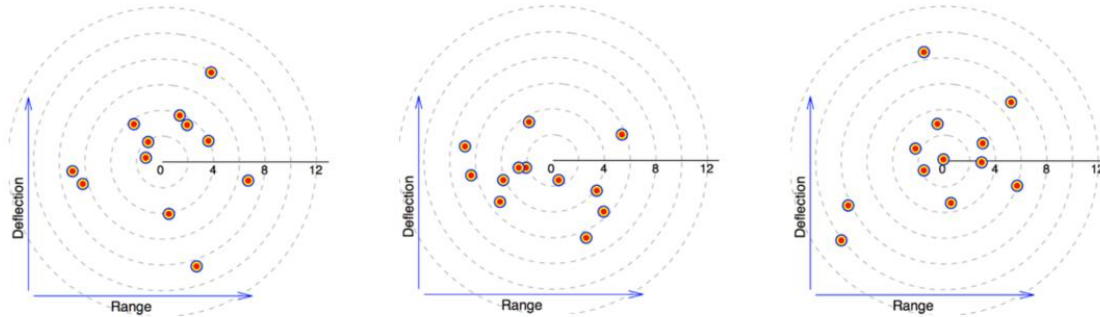
In the right panel, we plot $\log(1-p_{kill})$ vs. M . It is clear that in the presence of dependent error, the survival probability decreases slower than the geometric decay.



Next, we analyzed an area target with randomly distributed elements.



Many realizations of target elements distribution



s: **radius of area target**

= standard deviation of target elements distribution

Average damage fraction:

$$q_{\text{damage}}(\text{area target}, M \text{ weapons}) = \text{Average over all realizations}$$

25 October 2016

UNCLASSIFIED

Precision-guided Munitions Effects

13

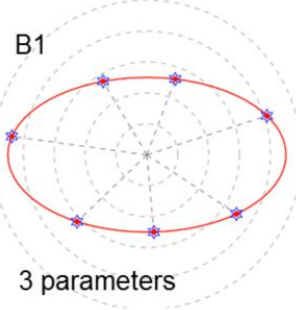
This chart shows an example of the type of problem we analyzed. In each graphic, there are 12 targets normally distributed around the center of the target located at (0,0). Similar to the point target problem, the solution for the damage to these area targets are an average over all realizations of the targets.



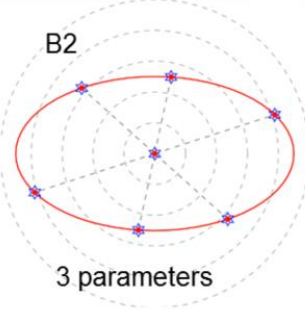
Next, we analyzed a constrained optimization over various patterns of aiming points.



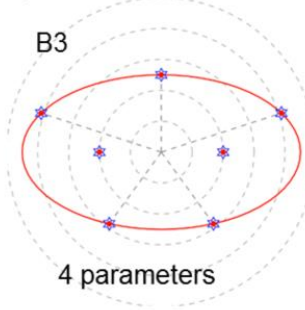
Patterns of B-family: uniform in polar (geometric) angle along an ellipse



3 parameters



3 parameters



4 parameters

In contrast, unconstrained optimization of 12 weapons has 24 parameters!

Patterns of A-family:

uniform in parametric angle along an ellipse $\theta_j = \theta_1 + \frac{(j-1)}{M} 2\pi, \quad \begin{cases} x_j = r_x \cos \theta_j \\ y_j = r_y \sin \theta_j \end{cases}$

A1

A2

A3

25 October 2016

UNCLASSIFIED

Precision-guided Munitions Effects

14

The goal of our method is to find simple and efficient “empirical” methods for calculating nearly optimal aiming positions. This approach greatly simplifies the numerical complexity of finding the optimal aiming points at the price of obtaining an approximate optimum. We considered 6 constrained patterns. The patterns of B-family aimpoints are M points on an ellipse that are uniform in polar angle. The pattern of A-family aimpoints analyzed M points along an ellipse that are uniform in parametric angle.

Pattern 1 for both groups, depict M points uniform in either parameter or polar angle. Pattern two depicts one target located at (0,0) and the remaining (M-1) targets uniform in either parameter or polar angle. Pattern 3 depicts two targets along the x-axis and the remaining (M-2) targets uniform in either parameter or polar angle.

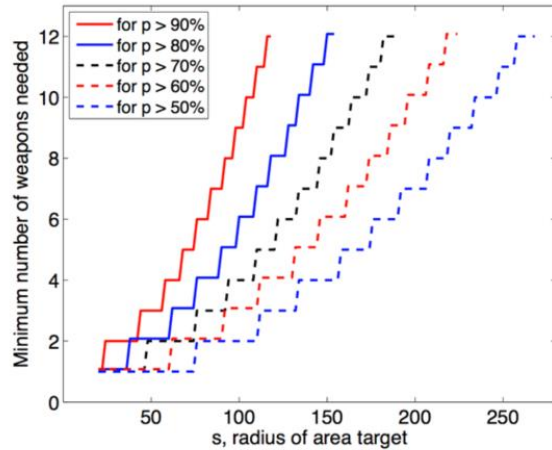
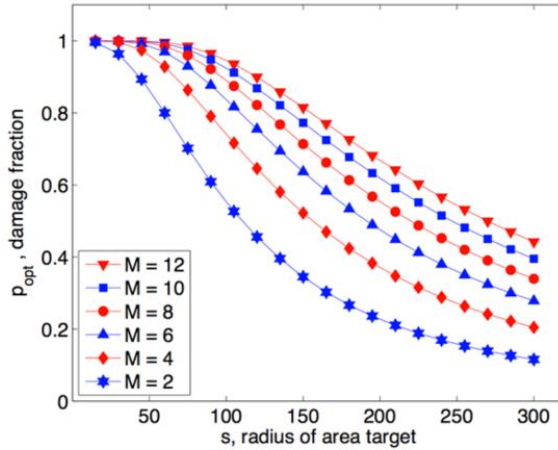
Patterns 1 and 2 have three parameters: the parameter/polar weapon angle, effective radius of the ellipse, and the aspect ration of the ellipse. Patter 3 also contains these three parameters plus a fourth parameter for the aiming point for the x-axis targets.



For a fixed number of weapons, the optimal damage decreases with as the target radius increases.



Number of weapons needed for a given level of damage fraction increases much less than quadratically with area target radius.



25 October 2016

UNCLASSIFIED

Precision-guided Munitions Effects

15

The left panel plots the optimal target damage fraction as a function of several values for the target radius (s) and a fixed value for the number of weapons M .

A practical question regarding resource allocation is the following. Given the radius of area target (s), what is the minimum number of weapons needed to achieve a given threshold of damage fraction? This question is answered in the chart on the right. This graphic shows that for any given threshold of damage fraction, the minimum number of weapons needed is an increasing function of the area target radius (i.e., larger area target requires larger number of weapons), which again is reasonable and consistent with our intuition.

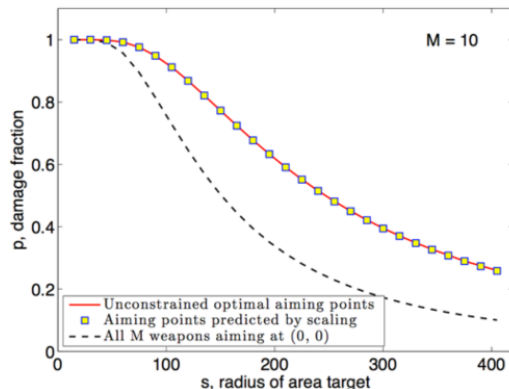
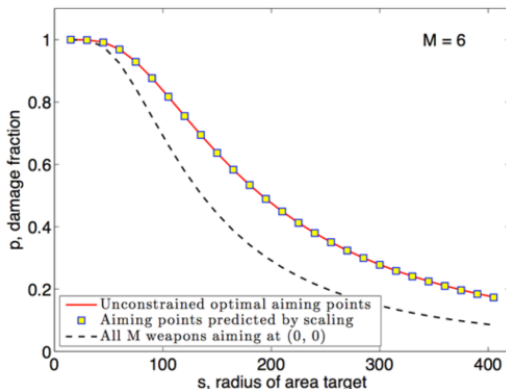


Thus, aiming points predicted by scaling are very efficient and accurate for area targets.



We need to calculate only one set of optimal aiming points

$$\underbrace{\left\{ \bar{r}_j(s), j=1, 2, \dots, M \right\}}_{\text{aiming points predicted by scaling law}} = \sqrt{\frac{s}{s_0}} \cdot \left\{ \bar{r}_j(s_0), j=1, 2, \dots, M \right\}$$



25 October 2016

UNCLASSIFIED

Precision-guided Munitions Effects

16

For an area target of radius s , we simply calculate/predict a set of nearly optimal aiming points using the scaling law shown above. We evaluate the performance of this efficient method by examining the damage fraction values achieved by these sets of nearly optimal aiming points. Specifically, for each area target, we calculate the damage fraction values corresponding to three sets of aiming points:

- Aiming points calculated in the unconstrained optimization.
- Aiming points calculated using the scaling law.
- All aiming points = (0,0).

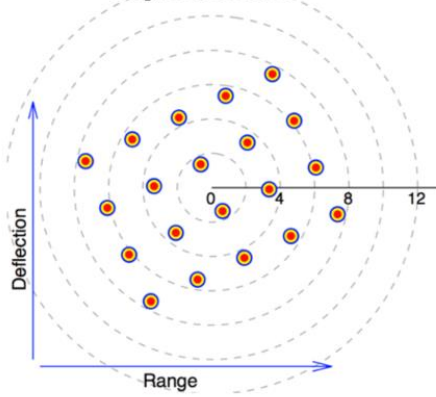
The charts in the slide compare the damage fraction values caused by the 3 sets of aiming points described above for $M = 6$ weapons (left panel) and for $M = 10$ weapons (right panel). The damage fraction achieved by the set of nearly optimal aiming points calculated using scaling is indistinguishable from that achieved in the unconstrained optimization (true optimum) while the damage fraction corresponding to all weapons aiming at (0; 0) is much lower. Therefore, we conclude that the scaling law is an efficient and accurate method for calculating a set of nearly optimal aiming points.



Work in progress: Area target with uniform (deterministic) distribution of elements

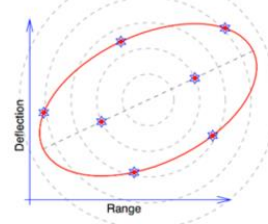
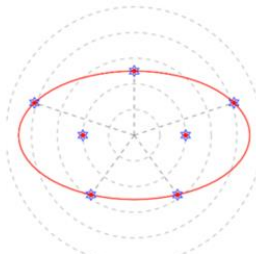


Deterministic distribution of target elements



Constrained optimization over prescribed patterns

Patterns of modified B-family:
uniform in polar (geometric) angle
along a **rotated ellipse**



25 October 2016

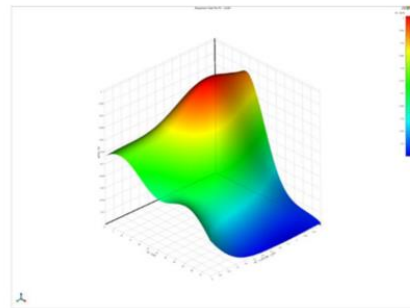
UNCLASSIFIED

Precision-guided Munitions Effects

17



Response Surface Model



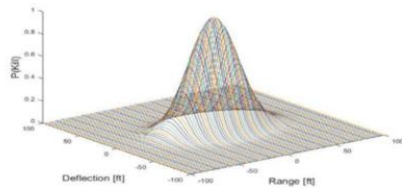
Darryl Ahner, PhD, PE

Associate Professor of Operations Research

UNCLASSIFIED

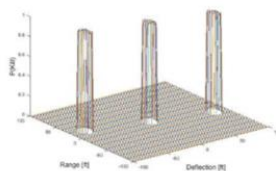


Goals are to find an approximate solution to the kill probability for a known set of conditions and expected munition requirements

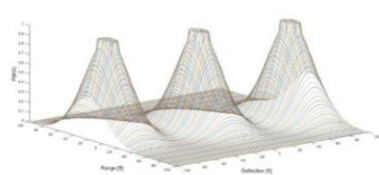


Carlton Damage Function tends to underestimate damage in close proximity to the detonation point.

Does an excellent job approximating damage far from detonation point



Cookie Cutter Function is simple to implement, but underestimates effects of munitions on distant targets



Klopocic Hybrid Function uses best of both functions

Source: Klopocic, 1990

25 October 2016

UNCLASSIFIED

Precision-guided Munitions Effects

19

Carlton Damage Functions calculates P_K as a function of
distance from blast
munition impact angle
direct hit effectiveness
& weapon lethal area

But the Carlton damage function tends to underestimate damage in close proximity to the detonation point but does an excellent job approximating damage far from detonation point

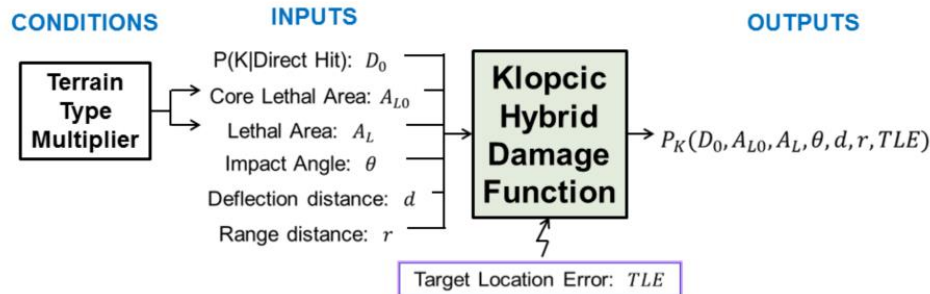
In contrast, the cookie cutter function estimates damage a constant damage for close proximity points and $P_K = 0$ for points farther away.

This becomes especially important when analyzing fratricide and collateral damage, damage far away from detonation is an important consideration, which is more appropriate modeled by the Carlton Damage Function.

We therefore combine them taking the best characteristics from each.



The damage function accounts for all key inputs which can be adjusted to account for terrain.



25 October 2016

UNCLASSIFIED

Precision-guided Munitions Effects

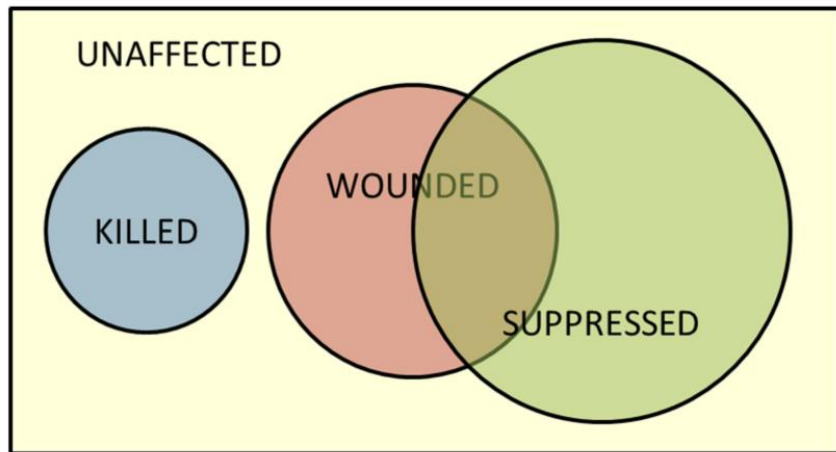
20

The damage function accounts for typical inputs to produce the effects of one munition. For multiple munitions, the effects are considered as independent events and is applied repetitively. Terrain affects are accounted for through the Lethal Area and Core Lethal Area inputs.

Target location area is the only uncertain factor entering into our equation. We treat it as a random variable that is distributed uniformly from 0 to its maximum value in all directions. This requires a simulation to determine the average effect since our damage function is nonlinear.



Munitions affect targets and nontargeted objects in various ways



25 October 2016

UNCLASSIFIED

Precision-guided Munitions Effects

21

Precision munitions can affect any object in their area. A target or other object, such as a civilian, can be affected over the entire spectrum from unaffected to killed. An enemy who is suppressed is unable to fire and there may be a time dependent component to this effect.

An enemy who is **wounded** may perform at less than peak effectiveness, but may or may not be suppressed

An enemy who is **killed** is eliminated from the scenario

The probability of being wounded or suppressed is modeled similarly to P(K), using a scaler to determine the size of the “wounding lethal area”



Inputs are varied to ensure coverage of all operational possibilities when constructing the simulation runs



Input Variable	Minimum	Maximum
Deflection Distance	0 meters	50 meters
Range Distance	0 m	50 m
D_0	0.05	1.0
Lethal Area (A_L)	100 m ²	1500 m ²
Core Lethal Area	10% of A_L	60% of A_L
Terrain factor	0.5	1.0
Impact Angle	30°	90°
Target Location Error	2 m	91 m
Wound LA factor	1.1	2.5
Suppression LA factor	1.1	2.5

25 October 2016

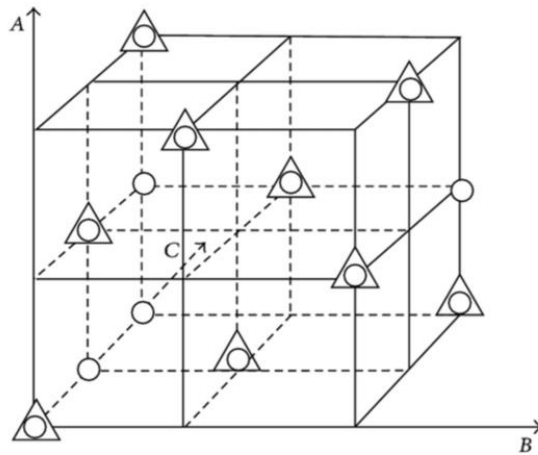
UNCLASSIFIED

Precision-guided Munitions Effects

22



Nearly orthogonal Latin hypercube is used on inputs to create response surface over entire space of inputs.



Source: Cioppa and Lucas, 2007

25 October 2016

UNCLASSIFIED

Precision-guided Munitions Effects

23

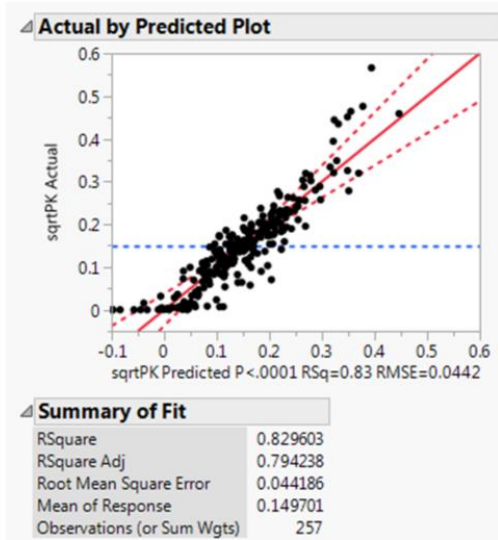
The experimental design is a Nearly Orthogonal Latin Hypercube (NOLH), which is a space covering design that ensures the correlation between input variables will be negligible which has better space-filling properties than completely randomized variable selection

Variable correlation is restricted to being in the range (-.03, .03)

A minimum and maximum value must be set for each input variable



Initial fit to transformed response is good statistically over all P_k values but poor practically for large P_k values



25 October 2016

UNCLASSIFIED

Precision-guided Munitions Effects

24

Notice that we end up modeling the square root of P_k in order to satisfy fitting a linear model. R², the measure of model fit want close to one, changes from 0.66 to 0.79 with normal distribution of errors around the solid red line.

Unfortunately, there are still too many small values of P_k that affect fit resulting in poor predicted larger P_k values that we care about most. We therefore decided to use regression trees to construct the model piece wise.

Models were developed for different maximum values of TLE, Lethal Area, and distance from the origin (d and r)

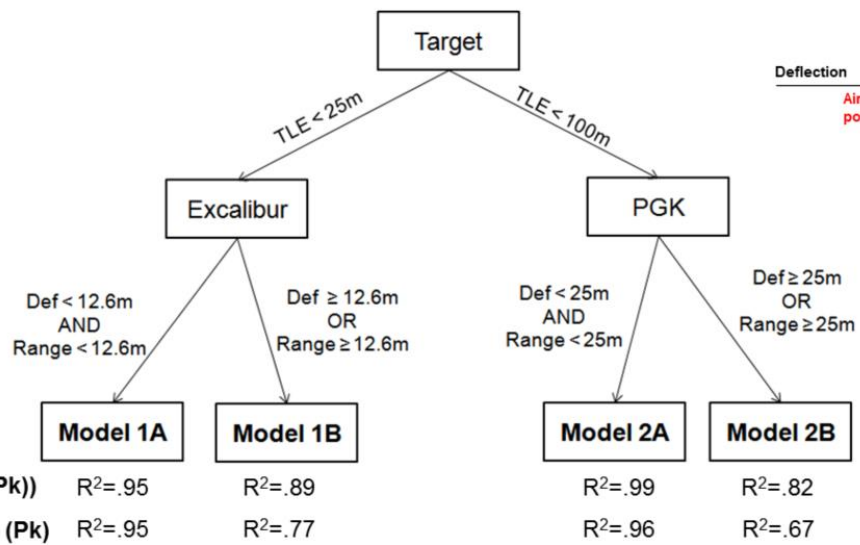
Max TLEs of 15m, 50m, and 91m

Max Lethal Areas of 500m², 1000m², and 1500m²

Max d and r of 10m, 15m, 20m, 25m, and 50m



Approaching the modeling piecewise greatly increases the operational realism of the model results.



25 October 2016

UNCLASSIFIED

Precision-guided Munitions Effects

25

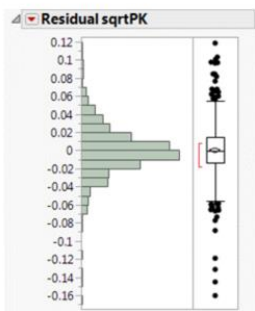
The regression tree analysis showed that Deflection and Range were the two factors that accounted for the most variance in the prediction. Additionally, the analysis led to construct models by munition type. This resulted in four models as shown with the best models, 1A and 2A, which are the most operationally relevant.



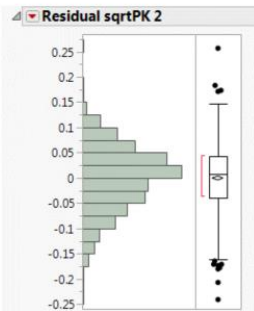
The distribution of simulated results versus predicted values provide for risk averse adjustments



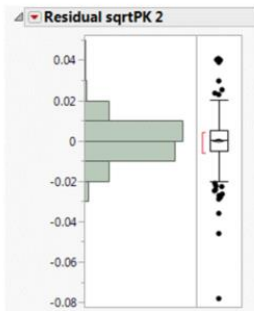
Model 1A



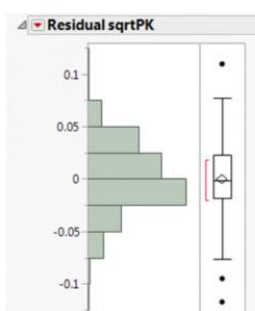
Model 1B



Model 2A



Model 2B



Model	75% Adj	90% Adj	99% Adj
1A	0.014	0.032	0.10
1B	0.04	0.077	0.15
2A	0.005	0.011	0.04
2B	0.022	0.041	0.10

$$\sqrt{P_K} = f(d, r, D_0, A_L, A_{L0}, T, \theta, TLE)$$

$$\sqrt{P_K} = f(d, r, D_0, A_L, A_{L0}, T, \theta, TLE) + C$$

$$P_K = [f(d, r, D_0, A_L, A_{L0}, T, \theta, TLE) + C]^2$$

25 October 2016

UNCLASSIFIED

Precision-guided Munitions Effects

26

Significant push in recent conflicts to reduce non-enemy damage (collateral damage and fratricide)

In order to meet this effort, a conservative adjustment can be made to better protect the safety of non-enemies

Based on the Model in use, a constant based on error distribution can be added to the model before it is squared

Example: To be 90% certain that P_K is this value or less, add a civilian adjustment C



The response surface modeling provides a flexible approach that is also in the form of an equation.



Using simulation results based on selected factors, using the Carleton Damage Function, quality generalized results are achieved.

The developed model provides a robust and flexible capability for modeling effects and tradeoffs between precision and conventional munitions.

Methodology is adaptable for determining killed, wounded, and suppression effects.

The model is easily modified for risk-averse effects on non-combat populations.



In summary, both models provide CAA a robust precision-munitions effects modeling capability.



Our research team developed two methods to model precision-guided munitions effects.

The analytical models improve ultimately on munitions estimates from the model output.

The response surface models provide additional risk analysis capabilities for exploration.



Questions?



Project Team



Sponsor: US Army Munitions Management Division

Project Funding Agency: ASPMO

Project Lead:

MAJ Cardy Moten III (TRAC-MTRY)

Phone: 831-656-2452

Email: cardy.moten3.mil@mail.mil

Technical POCs:

Applied approach:

Dr. Hong Zhou (NPS Applied Mathematics)

Phone: 831-656-2600

Email: hzhou@nps.edu

Response surface methodology:

Dr. Darryl Ahner (AFIT Operations Research)

Phone: 931-255-6565 x4708

Email: Darryl.Ahner@afit.edu

Stakeholders:

CAA Campaign Operations Team

25 October 2016

UNCLASSIFIED

Precision-guided Munitions Effects

28



Backups





Analytical Method

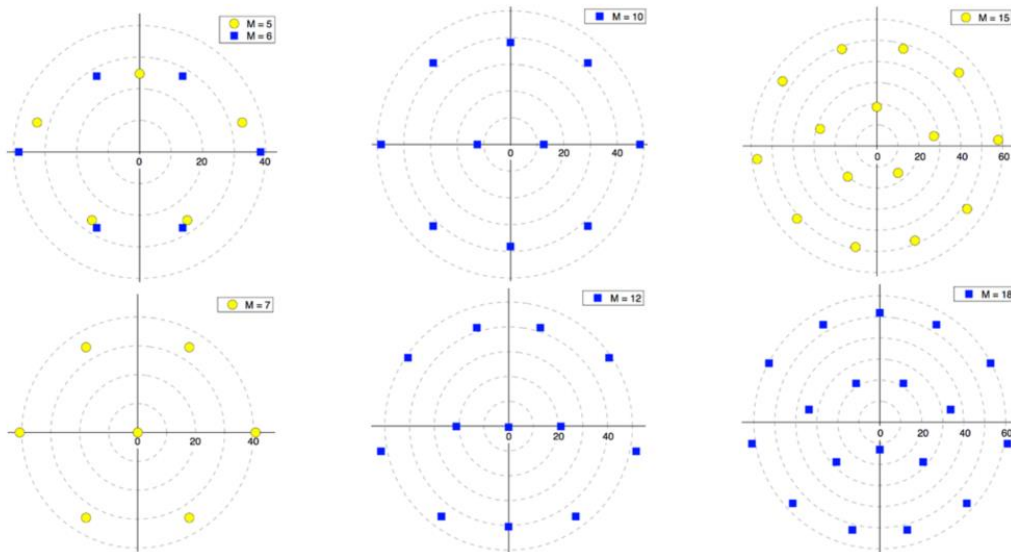
UNCLASSIFIED



We then analyzed optimal aiming points of M weapons in the presence of dependent and independent errors.



Optimal aiming points for maximizing kill probability:



25 October 2016

UNCLASSIFIED

Precision-guided Munitions Effects

32

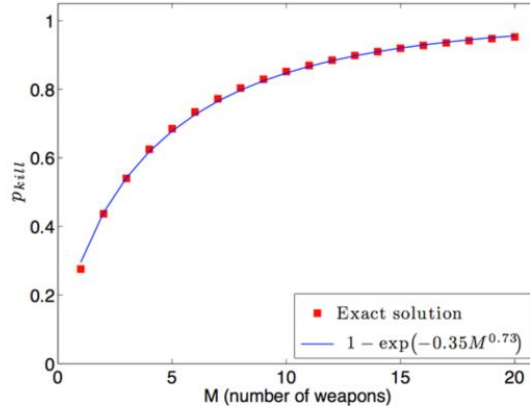
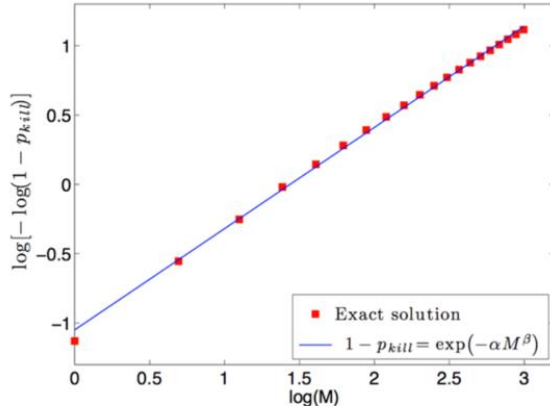
We analyzed the optimal distribution of aim points initially for circular and elliptical shaped aiming areas. The series of graphics on this slide depict our final analysis of aim position distribution without constraint to the target area. We varied the number of weapons to aim at a target located at (0,0) from a minimum of five weapons to a maximum of 18 weapon systems firing a single round at the target.



Also, the scaling law for the decay of survival probability showed a linear fitting.



$\log(-\log(1-p_{kill}))$ vs. $\log M$ is approximately linear.



$$\text{Scaling law: } p_{kill} = 1 - \gamma^{M^\beta}, \quad \beta < 1$$

25 October 2016

UNCLASSIFIED

Precision-guided Munitions Effects

33

To find a phenomenological fitting to the decay of survival probability as a function of M , we consider the form of $1 - p_{kill}(M) = \exp(-\alpha M^\beta)$. If the survival probability approximately satisfies this relation, then the plot of $\log[-\log(1 - p_{kill})]$ vs. $\log(M)$ would approximately follow a straight line. In other words $\log[-\log(1 - p_{kill})] = \log(\alpha) + \beta \log(M)$. The left panel shows the plot is very close to a straight line.

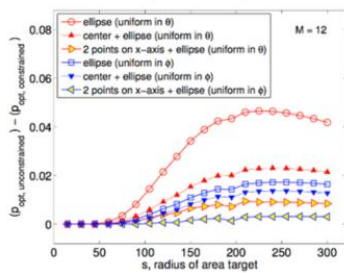
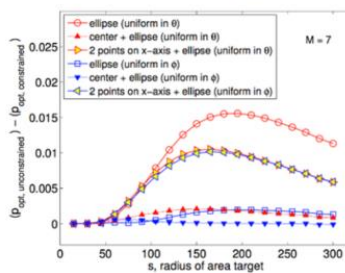
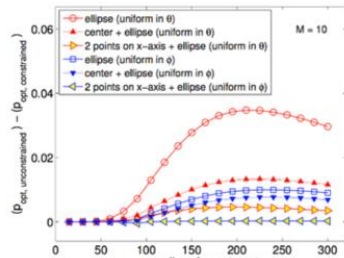
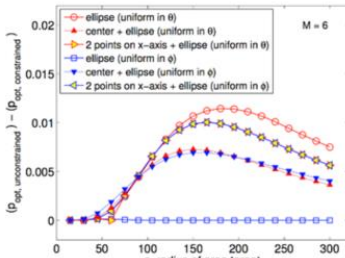
In the right panel, we plot p_{kill} vs. M and the fitting function $1 - \exp(-0.35M^{0.73})$. For the set of parameters values used, phenomenologically we have the approximation of $p_{kill} \approx 1 - \exp(-0.35M^{0.73})$.



Our results show that constrained optimization is more efficient and accurate compared to unconstrained opt.



Patterns of B-family yield results very close to the true optimum



25 October 2016

Precision-guided Munitions Effects

34

As M increases, the best pattern of aiming points goes from patterns B1 to B2 to B3.

UNCLASSIFIED

We compare the results of optimization over constrained patterns with those of the overall optimization. The charts show plots of the difference in optimal (maximal) damage fractions (p_{opt}) between constrained and unconstrained optimizations as a function of area target radius (s) for various number of weapons (M). The difference shows how accurate it is to optimize over a given pattern. For $M \leq 6$ (top left panel), the best approximate optimal damage fraction is achieved by distributing the aiming points over an ellipse, uniformly in polar angle (Pattern B1). At $M = 7$ (lower left panel), the best approximate optimal damage fraction is achieved by placing an aiming point at center and placing the rest six aiming points over an ellipse, uniformly in polar angle (Pattern B2). This is also true for $M = 8$ and $M = 9$. As the number of weapons increases, at $M = 10$ (top right panel), the best approximate optimal damage fraction is achieved by placing two aiming points on the x-axis and the rest eight aiming points over an ellipse, uniformly in polar angle (Pattern B3). The constrained optimum over Pattern B3 remains very accurate at $M = 12$ weapons (lower right panel).

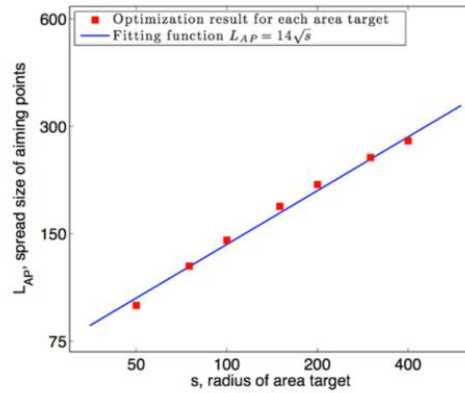
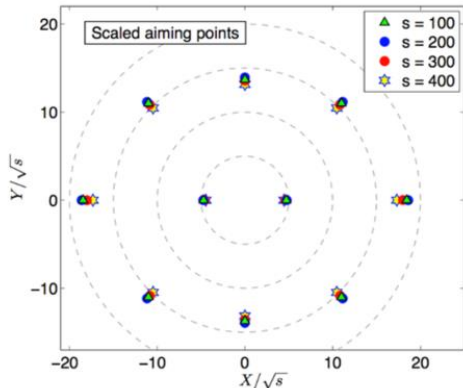


We also analyzed the scaling law for optimal aiming points vs area target size.



s: radius of area target = standard deviation of target elements distribution

optimal aiming points $\nearrow \frac{\{\vec{r}_j(s), j=1,2,\dots,M\}}{\sqrt{s}}$ is invariant with respect to s.



25 October 2016

UNCLASSIFIED

Precision-guided Munitions Effects

35

To explore how the size of optimal aiming points scales with the area target radius, we plotted these two quantities against each other in a log-log plot. The left panel compares sets of scaled optimal aiming points of pattern B3 for $s = 100$, $s = 200$, $s = 300$, and $s = 400$. The comparison demonstrates that not only the spread of optimal aiming points scales as \sqrt{s} , the distribution of optimal aiming points after scaling is approximately invariant with respect to the area target radius.

The right panel shows that the size of the optimal aiming points is approximately proportional to the square root of the area target radius (s). This observation suggests that we should normalize the aiming points by the square root of the area target radius.

Appendix C

Analytic Solution Methodology

This appendix contains the technical report for the analytical solution of firing precision-guided munitions at point and area targets, supporting MATLAB code used to implement the methodologies, and finally a white paper detailing the functions produced in MATLAB.

Explicit exact solution of damage probability for multiple weapons against a unitary target

Hongyun Wang

Department of Applied Mathematics and Statistics

University of California, Santa Cruz, CA 95064

Cardy Moten

TRADOC Analysis Center

Naval Postgraduate School, Monterey, CA 93943

Morris Driels

MAE Department

Naval Postgraduate School, Monterey, CA 93943

Don Grundel

Armament Directorate, Eglin AFB

Hong Zhou *

Department of Applied Mathematics

Naval Postgraduate School, Monterey, CA 93943

April 27, 2016

Abstract

We study the damage probability when M weapons are used against a unitary target. We use the Carleton damage function to model the distribution of damage probability caused by each weapon. The deviation of the impact point from the aimpoint is attributed to both the dependent error and independent errors. The dependent error is one random variable affecting M weapons the same way while independent errors are associated with individual weapons and are independent of each other. We consider the case where the dependent error is significant, non-negligible relative to independent errors. We first derive an explicit exact solution for the damage probability caused by M weapons for any M . Based on the exact solution, we find the optimal aimpoint distribution of M weapons to maximize the damage probability in several cases where the aimpoint distribution is constrained geometrically with a few free parameters, including uniform distributions around a circle or around an ellipse. Then, we perform unconstrained optimization to obtain the overall optimal aimpoint distribution and the overall maximum damage probability, which is carried out for different values of M , up to 20 weapons. Finally, we derive a phenomenological approximate expression for the damage probability vs M , the number of weapons, for the parameters studied here.

Keywords: Damage probability; Carleton damage function; multiple weapons with dependent errors; exact solution; optimal distribution of aimpoint

1 Introduction

The probability of killing or damaging a target depends heavily on how close a weapon is delivered to the target. This delivery accuracy of a weapon may be affected by many components. In general, the errors are usually divided into two main groups: the dependent

*Corresponding author, hzhou@nps.edu

error and independent errors. The dependent error is related to the aiming error that results from a miscalculation of latitude, longitude, distance, wind effect, or uncertainty in locating the target position. The dependent error results in the armament impacting away from the desired target point and it affects all weapons the same way. The independent errors refer to ballistic dispersion errors, which may result from variations in bullet shape, variations in gun barrels, or variations in amount of explosive used inside each bullet [1].

Due to many uncertainties in the field of weapon effectiveness, Monte Carlo simulations have been widely employed to estimate the probability of target damage [2]. Even though Monte Carlo simulations can provide reasonable estimates, exact solutions are mathematically more attractive and practically more useful. The objectives of this paper are i) to derive explicit exact solution for the damage probability caused by multiple weapons against a single target, ii) to use the exact solution to maximize the damage probability with respect to the aimpoint distribution of weapons, with or without geometric constraint(s) on the aimpoint distribution, and iii) to study the relation of damage probability to the number of weapons when the dependent error is significant. The results obtained here can be applied to indirect fire artillery, or GPS/INS-guided weapons.

The remainder of this paper will progress as follows. Section II provides the detailed mathematical formulation and explicit exact solution for the kill probability. Section III considers the performances of various aimpoint distributions. Finally, Section IV presents conclusions and future work.

2 Mathematical formulation

We consider a single point target in the two dimensional space. We establish the coordinate system such that the target is located at the origin point $\vec{x}_{target} = (0, 0)$. We use M weapons with dependent and independent errors to fire on the target. Due to the presence of significant dependent error, if all M weapons are aimed at $\vec{x}_{target} = (0, 0)$, the M impact points may be uniformly shifted away from the target by a significant distance, resulting in a small damage probability. To make the damage probability less susceptible to the dependent

error, we aim the M weapons at M different points distributed around the target. When the dependent error shifts some impact points away from the target, it simultaneously shifts the some other impact points toward the target. In this study all weapons are assumed to be perfectly reliable. Gross errors due to anomalies such as catastrophic weapon system failure, adverse weapon separation effects, and GPS jamming are neglected.

Let

- \vec{r}_j = the aiming point of weapon j .
- \vec{Y} = miss distance from the aimpoint due to the dependent error of M weapons, affecting the impact points of all M weapons uniformly.
- \vec{X}_j = miss distance from the aimpoint due to the independent error of weapon j , affecting only the impact point of weapon j individually. We assume that $\{\vec{X}_j, j = 1, 2, \dots, M\}$ are independent of each other and independent of random variable \vec{Y} .

The impact point of weapon j is given by

$$\vec{w}_j = \vec{r}_j + \vec{Y} + \vec{X}_j$$

We model the dependent error \vec{Y} as a normal random variable with zero mean:

$$\vec{Y} \sim N \left(\begin{pmatrix} 0 \\ 0 \end{pmatrix}, \begin{pmatrix} \sigma_1^2 & 0 \\ 0 & \sigma_2^2 \end{pmatrix} \right)$$

where σ_1 and σ_2 are standard deviations, respectively, in the two coordinate directions, which give an indication of the spread of the dependent error in the two directions. We model each independent error \vec{X}_j as a normal random variable with zero mean:

$$\vec{X}_j \sim N \left(\begin{pmatrix} 0 \\ 0 \end{pmatrix}, \begin{pmatrix} d_1^2 & 0 \\ 0 & d_2^2 \end{pmatrix} \right)$$

Further, we assume that the independent errors of individual weapons $\{\vec{X}_j, j = 1, 2, \dots, M\}$ are independent of each other and are independent of the dependent error \vec{Y} .

We use the mathematical fact that the sum of two independent normal random variables is a normal random variable. Suppose $U \sim N(0, \sigma^2)$ and $V \sim N(0, s^2)$. We have

$$Z \equiv V + U \sim N(0, s^2 + \sigma^2) \quad (1)$$

The probability density functions of U and V are given by

$$\begin{aligned} \rho_U(u) &= \frac{1}{\sqrt{2\pi\sigma^2}} \exp\left(\frac{-u^2}{2\sigma^2}\right) \\ \rho_V(v) &= \frac{1}{\sqrt{2\pi s^2}} \exp\left(\frac{-v^2}{2s^2}\right) \end{aligned}$$

In terms of the probability density functions, we write equation (1) as

$$\begin{aligned} &\int \frac{1}{\sqrt{2\pi s^2}} \exp\left(\frac{-(z-u)^2}{2s^2}\right) \frac{1}{\sqrt{2\pi\sigma^2}} \exp\left(\frac{-u^2}{2\sigma^2}\right) du \\ &= \frac{1}{\sqrt{2\pi(s^2 + \sigma^2)}} \exp\left(\frac{-z^2}{2(s^2 + \sigma^2)}\right) \quad \text{for any } z \end{aligned}$$

Applying a change of variables $u_{new} = -u$, denoting u_{new} still by u for simplicity and multiplying the equation by $\sqrt{2\pi s^2}$, we get

$$\begin{aligned} &\int \exp\left(\frac{-(z+u)^2}{2s^2}\right) \frac{1}{\sqrt{2\pi\sigma^2}} \exp\left(\frac{-u^2}{2\sigma^2}\right) du \\ &= \left(\frac{s^2}{s^2 + \sigma^2}\right)^{\frac{1}{2}} \exp\left(\frac{-z^2}{2(s^2 + \sigma^2)}\right) \quad \text{for any } z \end{aligned}$$

We rewrite the equation above in terms of expected values:

$$E_U \left[\exp\left(\frac{-(z+U)^2}{2s^2}\right) \right] = \left(\frac{s^2}{s^2 + \sigma^2}\right)^{\frac{1}{2}} \exp\left(\frac{-z^2}{2(s^2 + \sigma^2)}\right) \quad (2)$$

Here the notation E_U indicates the average with respect to random variable U while z and s^2 are fixed, not varying with U . Equation (2) is valid for any normal random variable $U \sim N(0, \sigma^2)$, and for any z and $s^2 > 0$. In the analysis below, we will use equation (2) extensively.

We use the Carleton damage function to model the probability of killing by an individual weapon. Let $\vec{w} = (w(1), w(2))$ be the impact point of a weapon where $w(1)$ and $w(2)$ describe

the impact points in the range and deflection directions from the target. The probability of the target being killed by an weapon at impact point \vec{w} is modeled mathematically as

$$\Pr(\text{target being killed by one weapon at impact point } \vec{w})$$

$$= \exp\left(\frac{-w(1)^2}{2b_1^2}\right) \exp\left(\frac{-w(2)^2}{2b_2^2}\right) \quad (3)$$

This is called the Carleton damage function or the diffuse Gaussian damage function [3]. The two parameters b_1 and b_2 in the Carleton damage function (3) represent the effective weapon radii in the range and deflection directions, respectively. With the impact points of the M weapons given by $\vec{w}_j = \vec{r}_j + \vec{Y} + \vec{X}_j$, $j = 1, 2, \dots, M$, the probability of the target located at the origin being killed by the M weapons is

$$\Pr(\text{target being killed by } M \text{ weapons at impact points } \{\vec{w}_j, j = 1, 2, \dots, M\})$$

$$\begin{aligned} &= 1 - \prod_{j=1}^M \left(1 - \exp\left(\frac{-w_j(1)^2}{2b_1^2}\right) \exp\left(\frac{-w_j(2)^2}{2b_2^2}\right) \right) \\ &= - \sum_{k=1}^M (-1)^k \sum_{\substack{\text{all k-combinations} \\ (j_1, j_2, \dots, j_k) \\ \text{from } (1, 2, \dots, M)}} \prod_{l=1}^k \exp\left(\frac{-w_{j_l}(1)^2}{2b_1^2}\right) \exp\left(\frac{-w_{j_l}(2)^2}{2b_2^2}\right) \\ &= - \sum_{k=1}^M (-1)^k \underbrace{\sum_{(j_1, \dots, j_k)} \prod_{l=1}^k \exp\left(\frac{-(r_{j_l}(1) + Y(1) + X_{j_l}(1))^2}{2b_1^2}\right)}_{F_1(j_1, \dots, j_k)} \\ &\quad \times \underbrace{\prod_{l=1}^k \exp\left(\frac{-(r_{j_l}(2) + Y(2) + X_{j_l}(2))^2}{2b_2^2}\right)}_{F_2(j_1, \dots, j_k)} \end{aligned} \quad (4)$$

We calculate the probability of the target being killed averaged over independent errors $\{\vec{X}_j, j = 1, 2, \dots, N\}$ and averaged over the dependent error \vec{Y} . For that purpose, we only need to calculate the average of each term inside the summation: $E[F_1(j_1, \dots, j_k) \times F_2(j_1, \dots, j_k)]$. Notice that $F_1(j_1, \dots, j_k)$ involves only the horizontal components and $F_2(j_1, \dots, j_k)$ involves only the vertical components of $\{\vec{X}_j\}$ and \vec{Y} . Since the horizontal components and vertical

components are independent of each other, we have

$$E [F_1(j_1, \dots, j_k) \times F_2(j_1, \dots, j_k)] = E [F_1(j_1, \dots, j_k)] \times E [F_2(j_1, \dots, j_k)]$$

Since $F_1(j_1, \dots, j_k)$ and $F_2(j_1, \dots, j_k)$ have exactly the same format, we only need to derive the analytical expression for one. For conciseness, we denote $r_{ji}(1)$, $Y(1)$, and $X_{ji}(1)$ simply by r_{ji} , Y , and X_{ji} in the calculation of $E [F_1(j_1, \dots, j_k)]$. We first average $F_1(j_1, \dots, j_k)$ over independent errors $\{X_j \sim N(0, d_1^2)\}$.

$$\begin{aligned} E_{\{X_j\}} [F_1(j_1, \dots, j_k)] &= E_{\{X_j\}} \left[\prod_{l=1}^k \exp \left(\frac{-(r_{jl} + Y + X_{jl})^2}{2b_1^2} \right) \right] \\ &= \prod_{l=1}^k E_{X_{jl}} \left[\exp \left(\frac{-(r_{jl} + Y + X_{jl})^2}{2b_1^2} \right) \right] \end{aligned} \quad (5)$$

Each term in the product is an average of the form on the left hand side of (2). Applying equation (2), we write each average as

$$E_{X_{jl}} \left[\exp \left(\frac{-(r_{jl} + Y + X_{jl})^2}{2b_1^2} \right) \right] = \left(\frac{b_1^2}{b_1^2 + d_1^2} \right)^{\frac{1}{2}} \exp \left(\frac{-(r_{jl} + Y)^2}{2(b_1^2 + d_1^2)} \right)$$

Substituting this result into equation (5), we obtain

$$\begin{aligned} E_{\{X_j\}} [F_1(j_1, \dots, j_k)] &= \prod_{l=1}^k \left(\frac{b_1^2}{b_1^2 + d_1^2} \right)^{\frac{1}{2}} \exp \left(\frac{-(r_{jl} + Y)^2}{2(b_1^2 + d_1^2)} \right) \\ &= \left(\frac{b_1^2}{b_1^2 + d_1^2} \right)^{\frac{k}{2}} \exp \left(\frac{-\sum_{l=1}^k (r_{jl} + Y)^2}{2(b_1^2 + d_1^2)} \right) \\ &= \left(\frac{b_1^2}{b_1^2 + d_1^2} \right)^{\frac{k}{2}} \exp \left(\frac{-\left(Y^2 + 2Y \sum_{l=1}^k r_{jl}/k + \sum_{l=1}^k r_{jl}^2/k\right)}{2(b_1^2 + d_1^2)/k} \right) \\ &= \left(\frac{b_1^2}{b_1^2 + d_1^2} \right)^{\frac{k}{2}} \exp \left(\frac{\left(\sum_{l=1}^k r_{jl}/k\right)^2 - \sum_{l=1}^k r_{jl}^2/k}{2(b_1^2 + d_1^2)/k} \right) \exp \left(\frac{-\left(Y + \sum_{l=1}^k r_{jl}/k\right)^2}{2(b_1^2 + d_1^2)/k} \right) \end{aligned}$$

Next we average over the dependent error $Y \sim N(0, \sigma_1^2)$. Again, the average is of the form on the left hand side of (2). Applying equation (2), we arrive at

$$E_Y \left[\exp \left(\frac{-\left(Y + \sum_{l=1}^k r_{jl}/k\right)^2}{2(b_1^2 + d_1^2)/k} \right) \right] = \left(\frac{(b_1^2 + d_1^2)/k}{(b_1^2 + d_1^2)/k + \sigma_1^2} \right)^{\frac{1}{2}} \exp \left(\frac{-\left(\sum_{l=1}^k r_{jl}/k\right)^2}{2((b_1^2 + d_1^2)/k + \sigma_1^2)} \right)$$

Thus, the overall average of $F_1(j_1, \dots, j_k)$ has the expression

$$E [F_1(j_1, \dots, j_k)] = \left(\frac{b_1^2}{b_1^2 + d_1^2} \right)^{\frac{k}{2}} \left(\frac{(b_1^2 + d_1^2)/k}{(b_1^2 + d_1^2)/k + \sigma_1^2} \right)^{\frac{1}{2}} \\ \times \exp \left(\frac{\left(\sum_{l=1}^k r_{j_l}(1)/k \right)^2 - \sum_{l=1}^k r_{j_l}(1)^2/k}{2(b_1^2 + d_1^2)/k} - \frac{\left(\sum_{l=1}^k r_{j_l}(1)/k \right)^2}{2((b_1^2 + d_1^2)/k + \sigma_1^2)} \right) \quad (6)$$

Similarly, the overall average of $F_2(j_1, \dots, j_k)$ has the expression

$$E [F_2(j_1, \dots, j_k)] = \left(\frac{b_2^2}{b_2^2 + d_2^2} \right)^{\frac{k}{2}} \left(\frac{(b_2^2 + d_2^2)/k}{(b_2^2 + d_2^2)/k + \sigma_2^2} \right)^{\frac{1}{2}} \\ \times \exp \left(\frac{\left(\sum_{l=1}^k r_{j_l}(2)/k \right)^2 - \sum_{l=1}^k r_{j_l}(2)^2/k}{2(b_2^2 + d_2^2)/k} - \frac{\left(\sum_{l=1}^k r_{j_l}(2)/k \right)^2}{2((b_2^2 + d_2^2)/k + \sigma_2^2)} \right) \quad (7)$$

The probability of target being killed, averaged over independent errors and dependent error, is called kill probability, and is denoted by p_{kill} (M weapons). It has the expression

$$p_{\text{kill}}(M \text{ weapons}) = - \sum_{k=1}^M (-1)^k \sum_{(j_1, \dots, j_k)} E [F_1(j_1, \dots, j_k)] E [F_2(j_1, \dots, j_k)] \quad (8)$$

where $E [F_1(j_1, \dots, j_k)]$ and $E [F_2(j_1, \dots, j_k)]$ are given in (6) and (7) above. Together, equations (6), (7), and (8), give us an explicit analytical expression for calculating the kill probability.

After the completion of the above derivation, we discovered that similar approaches had been taken separately by von Neumann [4] and by Washburn [5].

3 Performances of various aimpoint distributions of multiple weapons against a single target

Now we apply the exact solution to examine the kill probability corresponding to various distributions of the aimpoints of M weapons.

Let A_L denote the weapon lethal area or the fragmentation mean area of the effectiveness. It describes the effect of a warhead against a target and includes the effects of direct hit, blast, and fragmentation. We can calculate A_L from the Carleton damage function (3) as

$$A_L = \int_{-\infty}^{\infty} \int_{-\infty}^{\infty} \exp\left(-\frac{x^2}{2b_1^2} - \frac{y^2}{2b_2^2}\right) dx dy = 2\pi b_1 b_2 \quad (9)$$

The aspect ratio of the weapon radii of the Carleton damage function $a = \frac{b_1}{b_2}$ is described by the empirical formula:

$$a = \max(1 - 0.8 \cos \theta, 0.3) \quad (10)$$

where θ is the impact angle.

Once the lethal area A_L and the aspect ratio a are given, one can calculate the weapon radii for the Carleton damage function (3) as follows:

$$b_1 = \sqrt{\frac{a \times A_L}{2\pi}} \quad (11)$$

$$b_2 = \frac{b_1}{a} \quad (12)$$

For all the cases considered in this paper, we choose $A_L = 2270 \text{ ft}^2$, $\theta = 65^\circ$. This yields $b_1 = 15.4640 \text{ ft}$ and $b_2 = 23.3628 \text{ ft}$. Furthermore, we choose $\sigma_1 = \sigma_2 = 30$ for the dependent error and $d_1 = d_2 = 5$ for the independent errors.

We first consider the case of M weapons with aimpoints uniformly distributed on a circle as formulated below

$$\vec{r}_j = \left(r \cos\left(\theta + \frac{2\pi(j-1)}{M}\right), r \sin\left(\theta + \frac{2\pi(j-1)}{M}\right) \right)$$

where r is the radius and θ the phase off-set angle of the distribution. These are parameters that we can tune to maximize the kill probability.

For each value of M , we maximize the kill probability with respect to (r, θ) . This unconstrained nonlinear optimization can be achieved by using MATLAB built-in function *fminsearch* which is based on a direct search method of Lagarias et al. [6]. The results are listed in Table 1.

Table 1: The optimal distribution for M aimpoints when they are uniformly distributed around a circle and the corresponding probability of kill. Here r is the radius and θ is the phase off-set angle.

M	r_{opt}	θ_{opt}	p_{kill}
1	0	***	0.27597
2	16.246	0	0.43690
3	22.960	$\frac{\pi}{6}$	0.53834
4	26.948	0	0.62291
5	29.192	$\frac{\pi}{10}$	0.68212
6	31.086	$\frac{\pi}{6}$	0.72869
7	32.529	$\frac{\pi}{14}$	0.76474
8	33.731	0	0.79360
9	34.747	$\frac{\pi}{18}$	0.81702
10	35.63	$\frac{\pi}{10}$	0.83635
11	36.409	$\frac{\pi}{22}$	0.85251
12	37.105	0	0.86617

Note that the Carleton damage function we use is not isotropic. It has different effective radii in the range and deflection directions. To accommodate this anisotropic property of the Carleton damage function, we consider the case of M weapons with aimpoints distributed on an ellipse as formulated below

$$\vec{r}_j = \left(q\sqrt{\eta} \cos \left(\phi + \frac{2\pi(j-1)}{M} \right), \frac{q}{\sqrt{\eta}} \sin \left(\phi + \frac{2\pi(j-1)}{M} \right) \right)$$

where η is the aspect ratio of the ellipse. In the formulation above, we elongate one axis by $\sqrt{\eta}$ and simultaneously shrink the other axis by the same factor. In this way, the area of the

Table 2: The optimal distribution for M aimpoints when they are uniformly distributed around an ellipse and the corresponding probability of kill. Here ϕ is the off-set value in the parametric equation of the ellipse. The cases of $M = 1$ and $M = 2$ are not affected by aspect ratio.

M	(major axis) _{opt}	(minor axis) _{opt}	ϕ_{opt}	p_{kill}
1	0	0	***	0.27597
2	16.246	16.246	0	0.43690
3	25.637	17.639	$\frac{\pi}{6}$	0.53989
4	29.621	23.068	0	0.62477
5	30.411	27.235	$\frac{\pi}{10}$	0.68264
6	32.859	28.548	$\frac{\pi}{6}$	0.72958
7	34.292	30.095	$\frac{\pi}{14}$	0.76560
8	35.848	30.967	0	0.79469
9	37.135	31.75	$\frac{\pi}{18}$	0.81829
10	38.342	32.349	$\frac{\pi}{10}$	0.83784
11	39.436	32.861	$\frac{\pi}{22}$	0.85420
12	40.457	33.29	0	0.86806

ellipse is maintained at πq^2 , independent of the aspect ratio η . Parameter q has the meaning

$$q = \sqrt{\frac{\text{area of ellipse}}{\pi}} = \sqrt{(\text{major axis}) \times (\text{minor axis})}$$

From q and η , we can determine the major axis and the minor axis as

$$\begin{aligned} \text{major axis} &= q\sqrt{\eta} \\ \text{minor axis} &= \frac{q}{\sqrt{\eta}} \end{aligned}$$

We should point out that parameter ϕ is not the polar angle of the aimpoint of weapon 1. ϕ is the angular value used in the parametric equation of the ellipse to calculate the aimpoint

of weapon 1. ϕ is the phase angle before the major axis is elongated and before the minor axis is shrunk.

Table 3: The optimal distribution for M aimpoints when one of them is aimed at the origin while the rest of aimpoints are uniformly distributed around an ellipse, and the corresponding probability of kill. Here ϕ is the off-set value in the parametric equation of the ellipse. For the cases of $M \leq 5$, the kill probability is not improved by moving one of the M aimpoints to the center.

M	$(\text{major axis})_{\text{opt}}$	$(\text{minor axis})_{\text{opt}}$	ϕ_{opt}	p_{kill}
1	***	***	***	0.27597
2	22.161	22.161	0	0.40957
3	25.412	25.412	0	0.53737
4	32.918	23.814	$\frac{\pi}{6}$	0.60947
5	34.369	30.581	0.1407π	0.67798
6	36.213	33.451	$\frac{\pi}{10}$	0.73052
7	38.374	34.765	0	0.77123
8	39.45	36.17	$\frac{\pi}{14}$	0.80221
9	40.859	36.86	$\frac{\pi}{8}$	0.8274
10	41.814	37.655	$\frac{\pi}{18}$	0.84766
11	42.838	38.163	0	0.86449
12	43.709	38.648	$\frac{\pi}{22}$	0.87853

For each value of M , we maximize the kill probability with respect to (q, ϕ, η) . We obtain the results in Table 2.

In the above, we calculated the performance of placing the aimpoints of M weapons along a circle or an ellipse. We now examine the case of aiming one weapon at the center and aiming the rest ($M - 1$) weapons at positions distributed on an ellipse. The aimpoints of M

weapons are distributed as formulated below.

$$\vec{r}_j = \left(q\sqrt{\eta} \cos \left(\phi + \frac{2\pi(j-1)}{M-1} \right), \frac{q}{\sqrt{\eta}} \sin \left(\phi + \frac{2\pi(j-1)}{M-1} \right) \right), \quad j = 1, 2, \dots, M-1$$

$$\vec{r}_M = (0, 0)$$

For each value of M , we maximize the kill probability with respect to (q, ϕ, η) . The optimal results are reported in Table 3.

Next, we fully optimize the distribution of M aimpoints without constraining them on a circle or an ellipse. We represent the M aimpoints in polar coordinates.

$$(r_j, \theta_j), \quad j = 1, 2, \dots, M$$

The optimal solutions for $M = 1$, $M = 2$, $M = 3$ and $M = 4$ are listed in Table 4.

Figure 1 shows the optimal distributions of aimpoints for $M = 1$ (yellow circles) and $M = 2$ (blue squares) while the optimal distributions for the cases of $M = 3$ (yellow circles) and $M = 4$ (blue squares) are displayed in Figure 2.

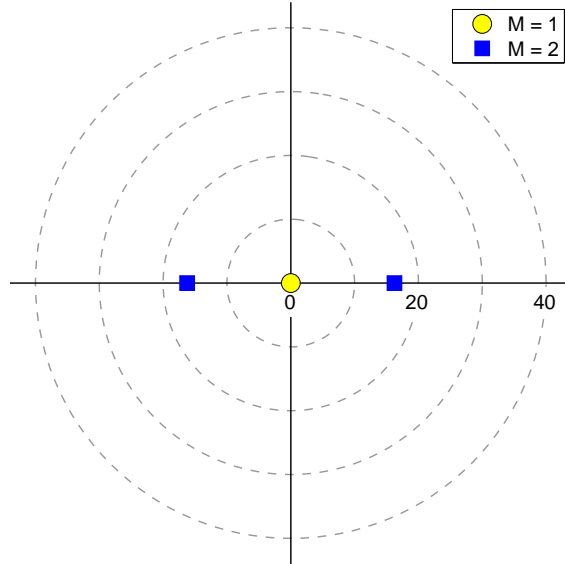


Figure 1: Optimal distributions of aimpoints for $M = 1$ (yellow circles) and $M = 2$ (blue squares).

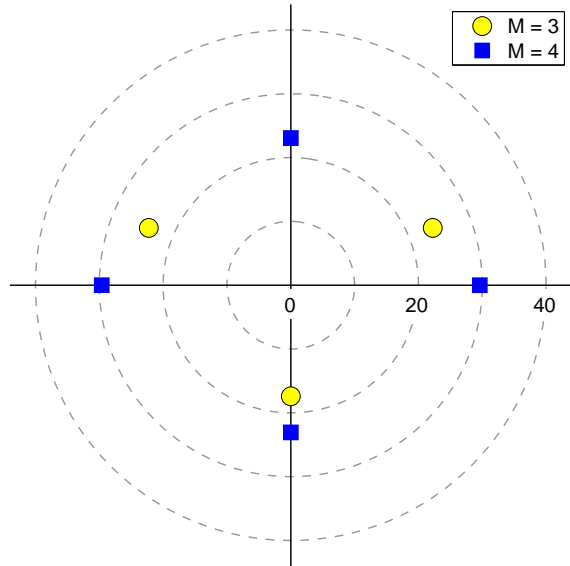


Figure 2: Optimal distributions of aimpoints for $M = 3$ (yellow circles) and $M = 4$ (blue squares).

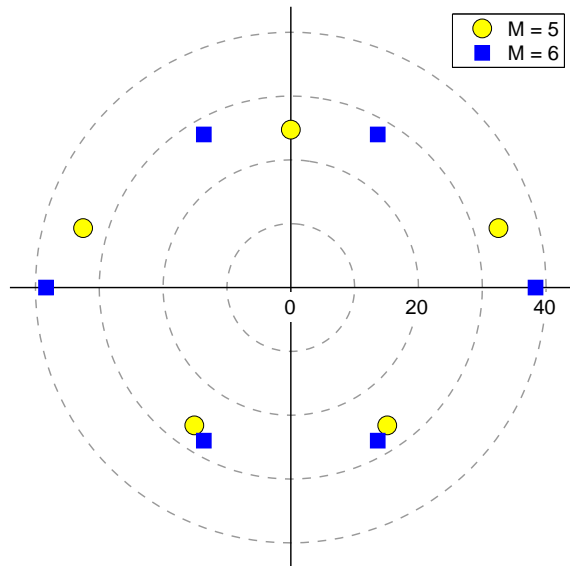


Figure 3: Optimal distributions of aimpoints for $M = 5$ (yellow circles) and $M = 6$ (blue squares).

The optimal solutions for $M = 5$, $M = 6$, $M = 7$ and $M = 8$ are given in Table 5.

Table 4: Optimal distributions of aimpoints and the corresponding probabilities of kill for $M = 1$, $M = 2$, $M = 3$ and $M = 4$.

	M = 1		M = 2		M = 3		M = 4	
	$p_{kill} = 0.27597$		$p_{kill} = 0.4369$		$p_{kill} = 0.53989$		$p_{kill} = 0.62477$	
j	r_j	θ_j	r_j	θ_j	r_j	θ_j	r_j	θ_j
1	0		16.246	0	23.975	0.12211π	29.621	0
2			16.246	π	23.975	0.87789π	23.068	0.5π
3					17.411	1.5π	29.621	π
4							23.068	2π

Table 5: Optimal distributions of aimpoints and the corresponding probabilities of kill for $M = 5$, $M = 6$, $M = 7$ and $M = 8$.

	M = 5		M = 6		M = 7		M = 8	
	$p_{kill} = 0.68505$		$p_{kill} = 0.73391$		$p_{kill} = 0.77218$		$p_{kill} = 0.80341$	
j	r_j	θ_j	r_j	θ_j	r_j	θ_j	r_j	θ_j
1	33.839	0.08879π	38.334	0	40.69	0	43.43	0
2	24.734	0.5π	27.589	0.33554π	34.456	0.32695π	36.016	0.28566π
3	33.839	0.91121π	27.589	0.66446π	34.456	0.67305π	34.191	0.5809π
4	26.353	1.3057π	38.334	π	40.69	π	40.507	0.85228π
5	26.353	1.6943π	27.589	1.3355π	34.456	1.327π	40.507	1.1477π
6			27.589	1.6645π	34.456	1.673π	34.191	1.4191π
7					0		36.016	1.7143π
8							0.6587	0

Figure 3 illustrates the optimal distributions of aimpoints for $M = 5$ (yellow circles) and $M = 6$ (blue squares); Figure 4 shows the optimal distributions of aimpoints for $M = 7$ (yellow circles) and $M = 8$ (blue squares).

The optimal solutions for $M = 9$, $M = 10$, $M = 11$ and $M = 12$ are listed in Table 6.

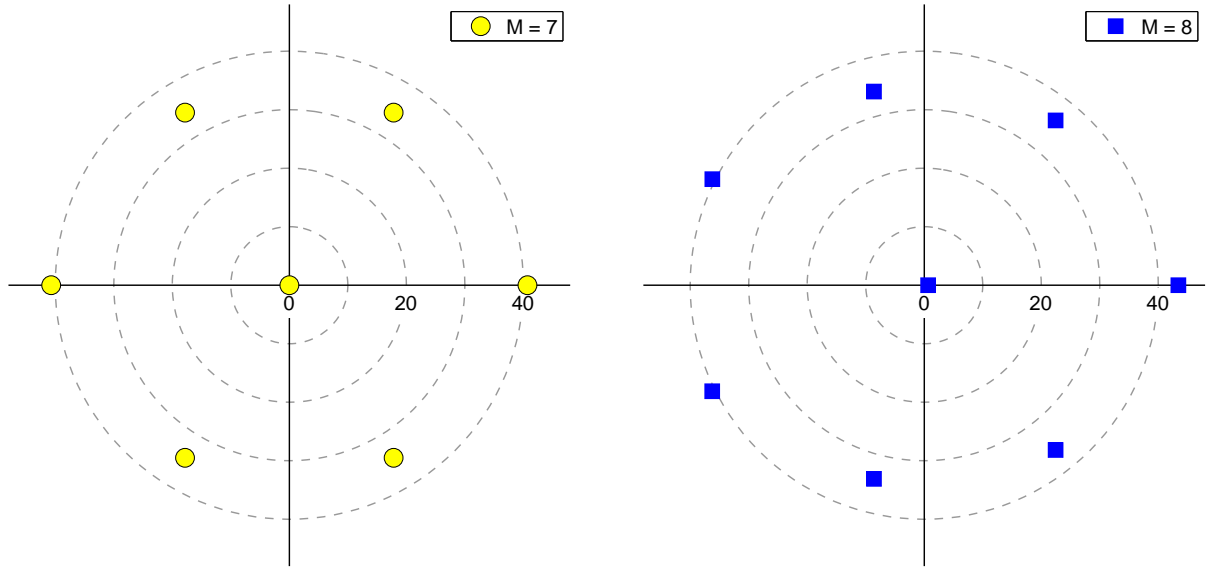


Figure 4: Optimal distributions of aimpoints for $M = 7$ (yellow circles) and $M = 8$ (blue squares).

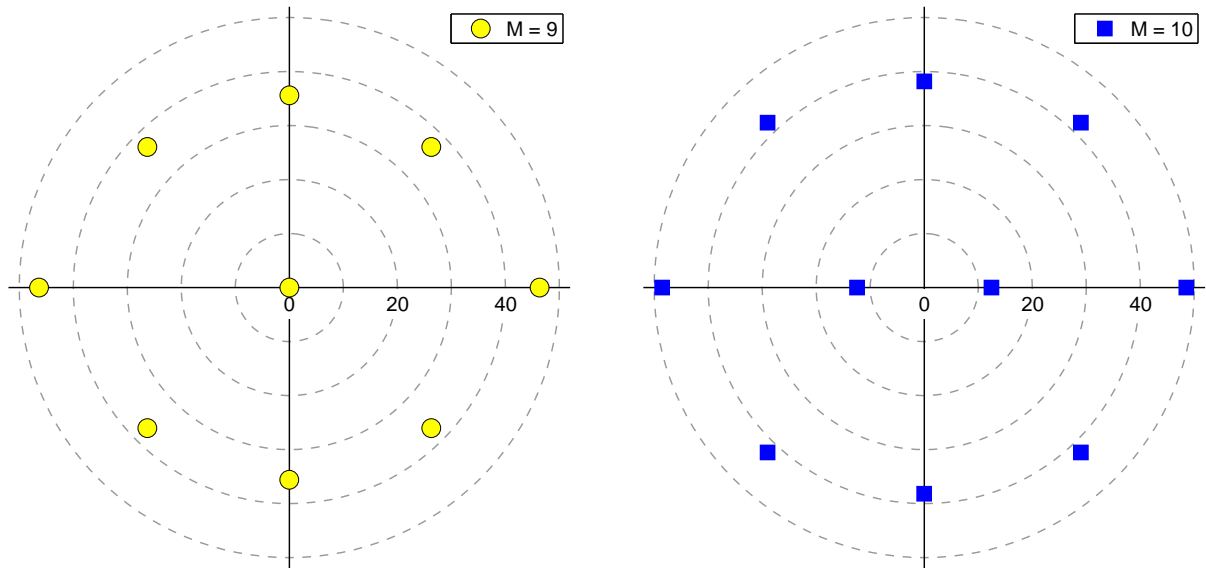


Figure 5: Optimal distributions of aimpoints for $M = 9$ (yellow circles) and $M = 10$ (blue squares).

Figure 5 displays the optimal distributions of aimpoints for $M = 9$ (yellow circles) and $M = 10$ (blue squares); the optimal distributions for $M = 11$ (yellow circles) and $M = 12$

Table 6: Optimal distributions of aimpoints and the corresponding probabilities of kill for $M = 9$, $M = 10$, $M = 11$ and $M = 12$.

	M = 9		M = 10		M = 11		M = 12	
	$p_{kill} = 0.82935$		$p_{kill} = 0.85158$		$p_{kill} = 0.86957$		$p_{kill} = 0.88499$	
j	r_j	θ_j	r_j	θ_j	r_j	θ_j	r_j	θ_j
1	46.336	0	48.534	0	50.078	0.05606π	49.091	0.18972π
2	36.994	0.24837π	42.116	0.25814π	42.093	0.28098π	41.676	0.40044π
3	35.587	0.5π	38.162	0.5π	38.939	0.5π	41.675	0.59952π
4	36.994	0.75163π	42.116	0.74186π	42.093	0.71902π	49.089	0.81023π
5	46.336	π	48.534	π	50.078	0.94394π	52.524	1.062π
6	36.994	1.2484π	42.116	1.2581π	45.328	1.1852π	45.409	1.296π
7	35.587	1.5π	38.162	1.5π	38.882	1.395π	40.554	1.5π
8	36.994	1.7516π	42.116	1.7419π	38.882	1.605π	45.407	1.9379π
9	0		12.452	0	45.328	1.8148π	52.523	1.7578π
10			12.452	π	12.535	0.02372π	21.097	1.9977π
11					12.535	0.97628π	0.44808	1.5002π
12							21.097	1.0023π

(blue squares) are plotted in Figure 6.

As M (the number of weapons) increases, the optimal distribution of aimpoints has more layers, covering a larger area with a more uniform distribution over the area. In Figure 7, we plot the optimal distributions of aimpoints for $M = 15$ (yellow circles) and $M = 18$ (blue squares).

Next, we study the optimal kill probability as a function of M . Let $p_{kill}(M)$ denote the kill probability corresponding to the optimal distribution of aimpoints for the case of M weapons. As M increases, the survival probability of the target, $(1 - p_{kill}(M))$, decreases. In the absence of dependent error and when the aimpoints are all fixed at one point, the outcome of each weapon affected by its independent error is statistically independent of the

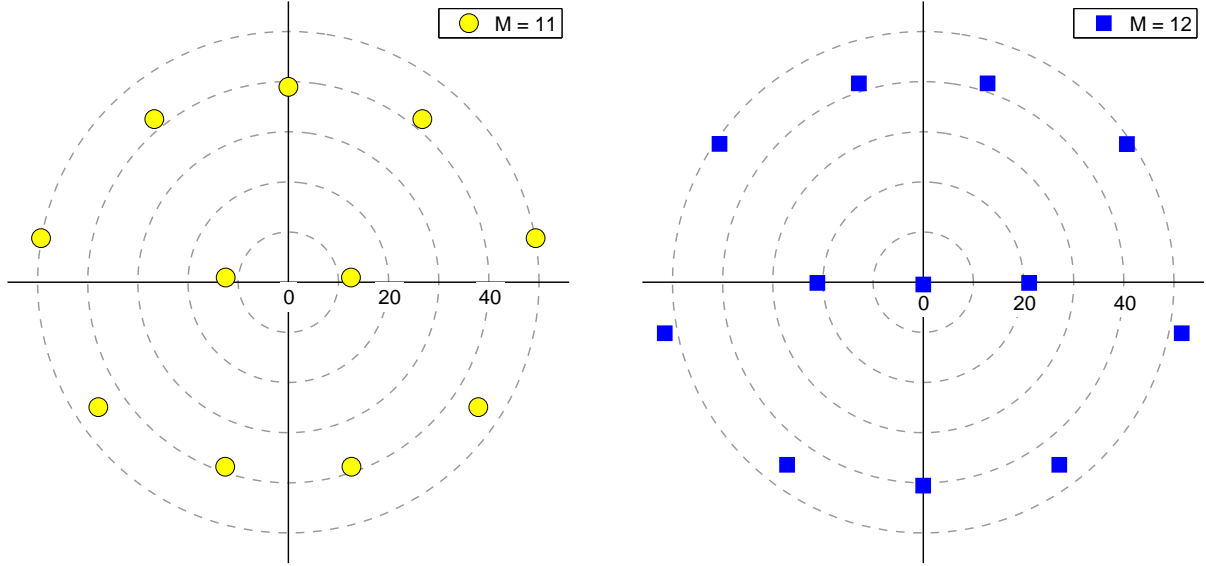


Figure 6: Optimal distributions of aimpoints for $M = 11$ (yellow circles) and $M = 12$ (blue squares).

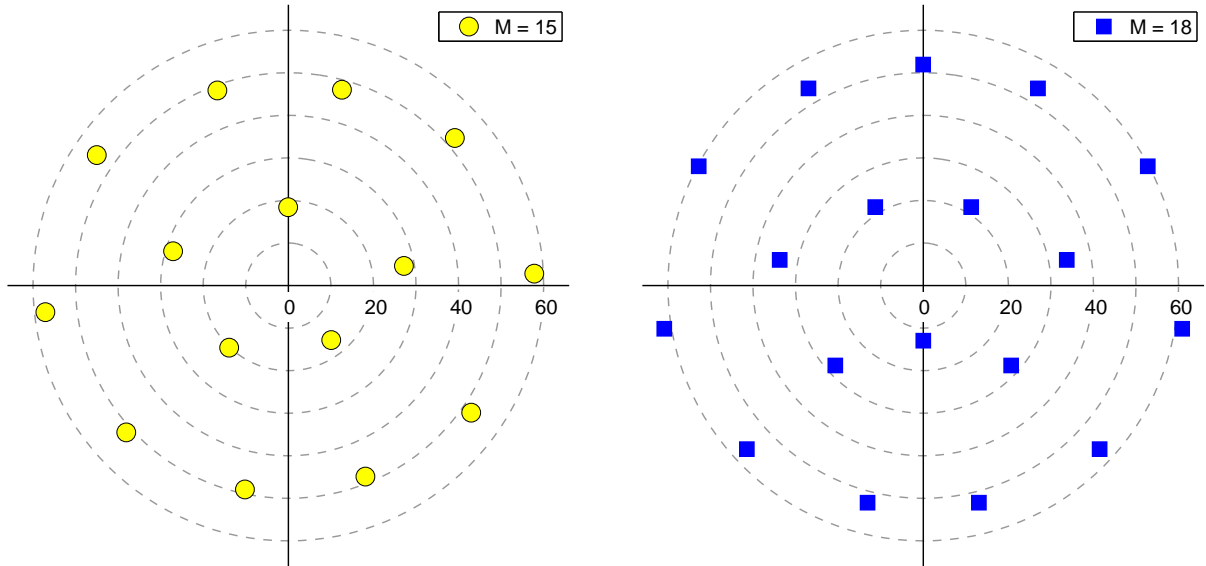


Figure 7: Optimal distributions of aimpoints for $M = 15$ (yellow circles) and $M = 18$ (blue squares).

outcome of other weapons affected by their own independent errors. In this situation, the probability of surviving M weapons is simply the M -th power of the probability of surviving

one weapon: $1 - p_{kill}(M) = (1 - p_{kill}(1))^M$. In other words, in the absence of dependent error, the log survival probability is a linear function of M .

$$\log(1 - p_{kill}(M)) = M \log(1 - p_{kill}(1))$$

In the presence of dependent error, however, the situation is completely different. The same dependent error affects all M weapons. The outcomes of individual weapons are no longer independent of each other. As a matter of fact, when the M weapons are all aimed at the same position, the outcomes of individual weapons are highly correlated with each other. As an example, we examine the case of aiming all M weapons at the origin. The averages of $F_1(j_1, \dots, j_k)$ and $F_2(j_1, \dots, j_k)$ are calculated from equations (6) and (7) as

$$E [F_1(j_1, \dots, j_k)] = \left(\frac{b_1^2}{b_1^2 + d_1^2} \right)^{\frac{k}{2}} \left(\frac{(b_1^2 + d_1^2)/k}{(b_1^2 + d_1^2)/k + \sigma_1^2} \right)^{\frac{1}{2}}$$

$$E [F_2(j_1, \dots, j_k)] = \left(\frac{b_2^2}{b_2^2 + d_2^2} \right)^{\frac{k}{2}} \left(\frac{(b_2^2 + d_2^2)/k}{(b_2^2 + d_2^2)/k + \sigma_2^2} \right)^{\frac{1}{2}}$$

The kill probability is

$$p_{kill}(M) = - \sum_{k=1}^M (-1)^k \sum_{(j_1, \dots, j_k)} E [F_1(j_1, \dots, j_k)] E [F_2(j_1, \dots, j_k)]$$

$$= - \sum_{k=1}^M (-1)^k \binom{M}{k} \left(\frac{b_1 b_2}{\sqrt{(b_1^2 + d_1^2)(b_2^2 + d_2^2)}} \right)^k \sqrt{\frac{b_1^2 + d_1^2}{b_1^2 + d_1^2 + k\sigma_1^2}} \sqrt{\frac{b_2^2 + d_2^2}{b_2^2 + d_2^2 + k\sigma_2^2}}$$

In the absence of dependent error, we have $\sigma_1 = \sigma_2 = 0$, and the kill probability is

$$1 - p_{kill}(M) = \left(1 - \frac{b_1 b_2}{\sqrt{(b_1^2 + d_1^2)(b_2^2 + d_2^2)}} \right)^M$$

In the presence of dependent error, to simplify the analysis, we assume that the independent errors are zero ($d_1 = d_2 = 0$) and assume that $\frac{\sigma_1^2}{b_1^2} = \frac{\sigma_2^2}{b_2^2} \equiv \omega^2$. The kill probability becomes

$$1 - p_{kill}(M) = 1 + \sum_{k=1}^M (-1)^k \binom{M}{k} \frac{1}{1 + k\omega^2}$$

For the first few values of M , we obtain

$$1 - p_{kill}(1) = \frac{\omega^2}{1 + \omega^2}$$

$$1 - p_{kill}(2) = \left(\frac{\omega^2}{1 + \omega^2} \right) \left(\frac{2\omega^2}{1 + 2\omega^2} \right)$$

$$1 - p_{kill}(3) = \left(\frac{\omega^2}{1 + \omega^2} \right) \left(\frac{2\omega^2}{1 + 2\omega^2} \right) \left(\frac{3\omega^2}{1 + 3\omega^2} \right)$$

Using mathematical induction, we can prove that

$$1 - p_{kill}(M) = \prod_{k=1}^M \left(\frac{k\omega^2}{1 + k\omega^2} \right)$$

Clearly, when all M weapons are aimed at the same positon, $1 - p_{kill}(M)$ decays less than geometrically with M .

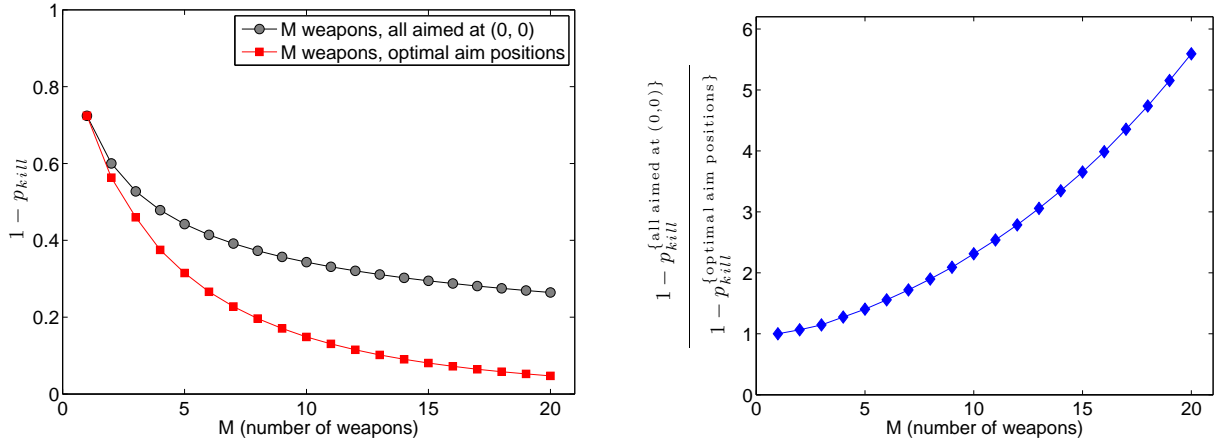


Figure 8: Left panel: Comparison in the decay of survival probability ($1 - p_{kill}$), of the case of aiming all M weapons at $(0, 0)$ vs the case of using optimal distribution of aimpoints. Right panel: Enhancement in the decay of survival probability ($1 - p_{kill}$) attributed to optimizing the distribution of M aimpoints.

With the optimal distribution of aimpoints for M weapons, we may expect that $1 - p_{kill}(M)$ decays faster than in the case of aiming all M weapons at the same position. Indeed, as demonstrated in the left panel of Figure 8, when the M weapons are aimed according to the optimal distribution of aimpoints, $1 - p_{kill}(M)$ decays much faster than in the case of aiming all M weapons at $(0, 0)$. The right panel of Figure 8 shows the enhancement in the decay of survival probability ($1 - p_{kill}(M)$) attributed to the optimal distribution of aimpoints. Specifically, in the right panel of Figure 8, we plot the quantity below as a

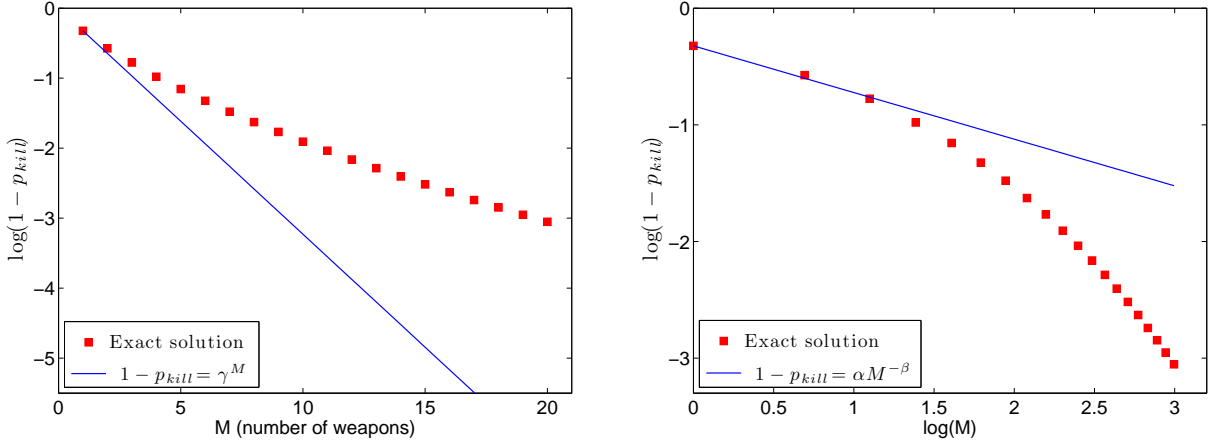


Figure 9: Left panel: plot of $\log(1 - p_{kill})$ vs M . Right panel: plot of $\log(1 - p_{kill})$ vs $\log(M)$

function of M

$$\frac{1 - p_{kill}^{\{\text{all aimed at } (0,0)\}}}{1 - p_{kill}^{\{\text{optimal aim positions}\}}}$$

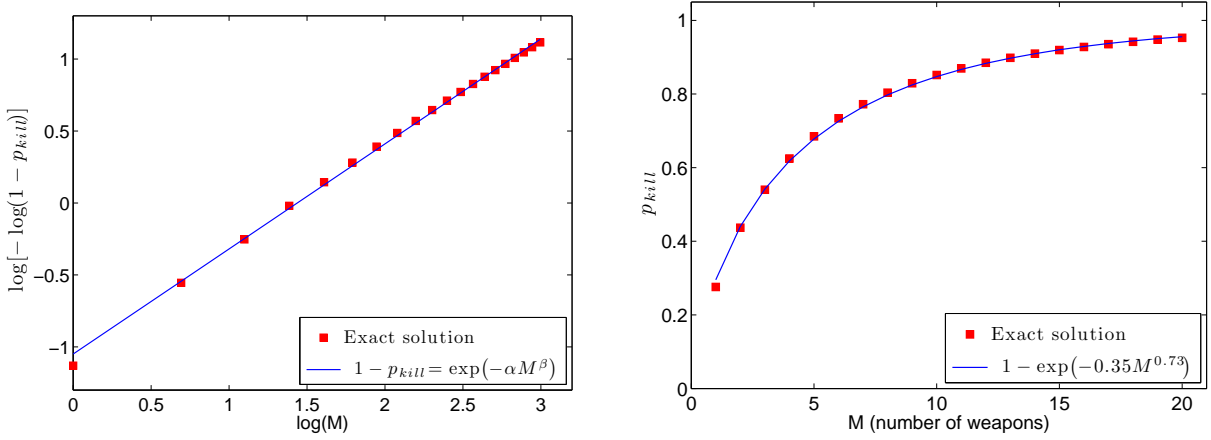


Figure 10: Left panel: plot of $\log[-\log(1 - p_{kill})]$ vs $\log(M)$. Right panel: plot of p_{kill} vs M

Even with the optimal distribution of aimpoints, however, the log survival probability, $\log(1 - p_{kill}(M))$, does not decrease linearly with respect to M in the presence of dependent error. In the left panel of Figure 9, we plot $\log(1 - p_{kill})$ vs M . It is clear that in the presence of dependent error, the survival probability decreases slower than the geometric decay.

After excluding the geometric decay, we explore the possibility of a power law decay for the survival probability. Specifically we examine whether or not the survival probability

obeys the power law $1 - p_{kill}(M) = \alpha M^{-\beta}$. If the survival probability follows this power law relation, then the plot of $\log(1 - p_{kill})$ vs $\log(M)$ would be a linear function

$$\log(1 - p_{kill}) = \log(\alpha) - \beta \log(M)$$

In the right panel of Figure 9, we plot $\log(1 - p_{kill})$ vs $\log(M)$. The plot demonstrates clearly that the survival probability does not follow a power law decay.

To find a phenomenological fitting to the decay of survival probability as a function of M , we consider the form of $1 - p_{kill}(M) = \exp(-\alpha M^\beta)$. If the survival probability approximately satisfies this relation, then the plot of $\log[-\log(1 - p_{kill})]$ vs $\log(M)$ would approximately follow a straight line.

$$\log[-\log(1 - p_{kill})] = \log(\alpha) + \beta \log(M)$$

In the left panel of Figure 10, we plot $\log[-\log(1 - p_{kill})]$ vs $\log(M)$. The plot is very close to a straight line. In the right panel of Figure 10, we plot p_{kill} vs M and the fitting function $1 - \exp(-0.35M^{0.73})$. For the set of parameter values used, phenomenologically we have the approximation:

$$p_{kill} \approx 1 - \exp(-0.35M^{0.73})$$

4 Conclusion

We have considered the damage probability caused by multiple weapons against a single target. Explicit exact solution was derived for the damage probability in the case of M weapons with both dependent error and independent errors. Then we applied the explicit exact solution to maximize the damage probability and find the corresponding optimal distribution of aimpoints. We observed that in the presence of significant dependent error, the decay of the survival probability corresponding to the optimal aimpoints distribution (i.e., $1 - \text{optimal damage probability}$) is slower than the exponential decay with respect to M , the number of weapons. This observation demonstrates that increasing M is much less effective in overcoming the dependent error than in overcoming independent errors. We found that

phenomenologically the survival probability decays exponentially with respect to a fractional power of M . Presumably, the fraction power varies with the parameter values of the problem. The mathematics behind this phenomenological expression and the dependence of the fraction power on the parameter values will be investigated in future studies.

5 Disclaimer

H. Zhou would like to thank TRAC-M for supporting this work. The views expressed in this document are those of the authors and do not reflect the official policy or position of the Department of Defense or the U.S. Government.

References

- [1] Driels, M. (2014). *Weaponeering: Conventional Weapon System Effectiveness*, 2nd edition, American Institute of Aeronautics and Astronautics (AIAA) Education Series, Reston, VA.
- [2] Chusilp, P., Charubhun, W., and Koanantachai, P. (2014) Monte Carlo simulations of weapon effectiveness using Pk matrix and Carleton damage function, International Journal of Applied Physics and Mathematics, 4(4): 280-285
- [3] Washburn, A. and Kress, M. (2009). *Combat Modeling*. Dordrecht; New York; Springer.
- [4] von Neumann, J. (1941). Optimum aiming at an imperfectly located target, appendix to optimum spacing of bombs or shots in the presence of systematic errors, Ballistic Research Laboratory, Report 241, July 3.
- [5] Washburn, A. (2003) Diffuse Gaussian multiple-shot patterns, Military Operations Research, 8(3): 59-64

- [6] Lagarias, J.C., Reeds, J.A., Wright, M.H., Wright, P.E. (1998) Convergence properties of the Nelder-Mead simplex method in low dimensions, SIAM Journal of Optimization, 9(1): 112-147

Average damage caused by multiple weapons against an area target of normally distributed elements

Hongyun Wang and George Labaria

Department of Applied Mathematics and Statistics

University of California, Santa Cruz, CA 95064

Cardy Moten

TRADOC Analysis Center

Naval Postgraduate School, Monterey, CA 93943

Hong Zhou *

Department of Applied Mathematics

Naval Postgraduate School, Monterey, CA 93943

October 8, 2016

Abstract

This paper investigates the effect of launching multiple weapons against an area target of normally distributed elements. We provide an analytical form of the average damage fraction and then apply it to obtain optimal aimpoints. To facilitate the computational efforts in practice, we also consider optimizations over given constrained

*Corresponding author, hzhou@nps.edu

patterns of aimpoints. Finally, we derive scaling laws for optimal aimpoints and optimal damage fraction with respect to the radius of the area target.

Military OR application area: Strike Warfare

OR methodology: Probabilistic Operations Research; Decision in the presence of uncertainty

1 Introduction

The theory of firing, which mainly concerns about aiming, kill probability and allocation of munitions, was inspired by World War II and has been progressed significantly in the past decades [1]. A brief history of firing theory can be found in Washburn and Kress's book [2] where the authors also presented a detailed discussion on shooting without feedback or with feedback. Another good reference on weaponeering is given by Driels [3].

In this paper we are interested in studying the effect of precision-guided munitions such as Excaliburs. These coordinate-seeking munitions are usually guided by radio, radar, or laser and launched by a cannon. They are intended to hit a target accurately and cause minimal collateral damage to civilians, friendly forces and infrastructure, especially hospitals, schools, churches, and residential homes. The precision-guided weapons are in general subject to target-location errors and ballistic dispersion errors. The target-location errors, or aiming errors, result from inaccuracies associated with identifying a target's location. In contrast, the ballistic dispersion errors are caused by random weapons effects, which may vary from one weapon to another and are assumed to be independent from shot to shot. When a single weapon is fired, it is natural to aim it at the expected center of the target. However, when multiple weapons are launched against a unitary target, the probability of damaging the target can be improved significantly by spreading the aimpoints around the target and the optimal distribution of aimpoints has been investigated in our recent work [4]. Our goal here is to extend our previous studies to estimate the probability of destroying an area target of normally distributed elements with multiple weapons. We will seek optimal aimpoints for various number of weapons.

The plan of this paper is to first review our previous analytical results for the case of multiple weapons against a single target in section 2. Section 3 introduces the mathematical problem of multiple weapons being released against an area target consisting of normally distributed elements. Exact solution for the average damage fraction is then derived. Section 4 calculates the optimal aiming points and examines the relation among the radius of area target, the number of weapons and the optimal (maximum) damage fraction. In addition to the unconstrained overall optimization of the damage fraction, we also study empirical, fast and robust constrained optimization over several prescribed patterns. The goal is to reduce the computational complexity of optimization and to compute a set of nearly optimal aiming points efficiently. Section 5 provides scaling laws for optimal aimpoints and optimal damage fraction with respect to the radius of area target. Section 6 highlights conclusions.

2 Review of our previous analytical results for the case of multiple weapons against a single target

Even though the world is three-dimensional, most targets are known to be on the surface of the Earth and therefore the targets are assumed to be in a two-dimensional ground space. Conventionally, we use two coordinates to define this ground plane: the range direction and the deflection direction. The range direction is defined by the direction of the weapon's velocity vector, whereas the deflection direction is perpendicular to the range direction.

Previously [4] we have studied the case of multiple weapons with both dependent and independent errors against a single target at $\vec{x}_{target} = (0, 0)$. For reader's convenience, we review briefly the mathematical formulation of the problem. Let

- \vec{r}_j = the aiming point of weapon j for $j = 1, 2, \dots, M$.
- \vec{Y} = the dependent error of M weapons, affecting the impact points of all M weapons uniformly. We assume Y is a normal random variable.
- \vec{X}_j = independent error of weapon j , affecting only the impact point of weapon j

individually. We assume that $\{\vec{X}_j, j = 1, 2, \dots, M\}$ are normal random variables, independent of each other and independent of normal random variable \vec{Y} .

We model the dependent error \vec{Y} as a normal random variable with zero mean:

$$\vec{Y} \sim N \left(\begin{pmatrix} 0 \\ 0 \end{pmatrix}, \begin{pmatrix} \sigma_1^2 & 0 \\ 0 & \sigma_2^2 \end{pmatrix} \right)$$

where σ_1 and σ_2 are standard deviations, respectively, in the range and the deflection directions, which give an indication of the spread of the dependent error in these two directions. We model each independent error \vec{X}_j as a normal random variable with zero mean:

$$\vec{X}_j \sim N \left(\begin{pmatrix} 0 \\ 0 \end{pmatrix}, \begin{pmatrix} d_1^2 & 0 \\ 0 & d_2^2 \end{pmatrix} \right)$$

The impact point of weapon j is given by

$$\vec{w}_j = \vec{r}_j + \vec{Y} + \vec{X}_j$$

We use the Carleton damage function to model the probability of killing by an individual weapon. Let $\vec{w} = (w(1), w(2))$ be the impact point of a weapon where $w(1)$ and $w(2)$ describe the impact point in the range and deflection directions from the target. The probability of the target being killed by an weapon at impact point \vec{w} is modeled mathematically as

$$\begin{aligned} & \Pr(\text{target being killed by one weapon at impact point } \vec{w}) \\ &= \exp \left(\frac{-w(1)^2}{2b_1^2} \right) \exp \left(\frac{-w(2)^2}{2b_2^2} \right) \end{aligned} \tag{1}$$

This is the well-known Carleton damage function or the diffuse Gaussian damage function [2]. The two parameters b_1 and b_2 in the Carleton damage function (1) represent the effective weapon radii in the range and deflection directions, respectively.

The probability of a target being killed by the M weapons, averaged over all random errors (i.e., dependent and independent errors), is called the kill probability and is mathematically denoted by $p_{\text{kill}}(\text{target}, M \text{ weapons})$. Note that in the notation for the kill probability, the target identity is explicitly included. This will be very convenient later in the discussion of

an area target with multiple target elements, in which we can study the kill probability for each individual element.

With the impact points of the M weapons given by $\{\vec{w}_j = \vec{r}_j + \vec{Y} + \vec{X}_j, j = 1, 2, \dots, M\}$, we derived an analytical expression for the kill probability as a function of quantities $(\sigma_1, \sigma_2, d_1, d_2, b_1, b_2, \{\vec{r}_j, j = 1, 2, \dots, M\})$.

$$p_{\text{kill}}(\text{target}, M \text{ weapons}) = G(\sigma_1, \sigma_2, d_1, d_2, b_1, b_2, \{\vec{r}_j, j = 1, 2, \dots, M\}) \quad (2)$$

where function G is defined as

$$\begin{aligned} & G(\sigma_1, \sigma_2, d_1, d_2, b_1, b_2, \{\vec{r}_j, j = 1, 2, \dots, M\}) \\ &= - \sum_{k=1}^M (-1)^k \sum_{(j_1, \dots, j_k)} E[F_1(j_1, \dots, j_k)] E[F_2(j_1, \dots, j_k)] \end{aligned} \quad (3)$$

$$\begin{aligned} E[F_1(j_1, \dots, j_k)] &= \left(\frac{b_1^2}{b_1^2 + d_1^2} \right)^{\frac{k}{2}} \left(\frac{(b_1^2 + d_1^2)/k}{(b_1^2 + d_1^2)/k + \sigma_1^2} \right)^{\frac{1}{2}} \\ &\times \exp \left(\frac{\left(\sum_{l=1}^k r_{j_l}(1)/k \right)^2 - \sum_{l=1}^k r_{j_l}(1)^2/k}{2(b_1^2 + d_1^2)/k} - \frac{\left(\sum_{l=1}^k r_{j_l}(1)/k \right)^2}{2((b_1^2 + d_1^2)/k + \sigma_1^2)} \right) \end{aligned} \quad (4)$$

$$\begin{aligned} E[F_2(j_1, \dots, j_k)] &= \left(\frac{b_2^2}{b_2^2 + d_2^2} \right)^{\frac{k}{2}} \left(\frac{(b_2^2 + d_2^2)/k}{(b_2^2 + d_2^2)/k + \sigma_2^2} \right)^{\frac{1}{2}} \\ &\times \exp \left(\frac{\left(\sum_{l=1}^k r_{j_l}(2)/k \right)^2 - \sum_{l=1}^k r_{j_l}(2)^2/k}{2(b_2^2 + d_2^2)/k} - \frac{\left(\sum_{l=1}^k r_{j_l}(2)/k \right)^2}{2((b_2^2 + d_2^2)/k + \sigma_2^2)} \right) \end{aligned} \quad (5)$$

Mathematically, $F_1(j_1, \dots, j_k)$ is the product, over k weapons $\{j_1, \dots, j_k\}$, of all factors involving only components in the range direction (i.e., $\sigma_1, d_1, b_1, r(1)$) while $F_2(j_1, \dots, j_k)$ is the product, over k weapons $\{j_1, \dots, j_k\}$, of all factors involving only components in the deflection direction (i.e., $\sigma_2, d_2, b_2, r(2)$). Together, equations (2), (3), (4) and (5) form an explicit analytical expression for the kill probability of the target, $p_{\text{kill}}(\text{target}, M \text{ weapons})$.

3 Mathematical formulation: multiple weapons against an area target of normally distributed elements

Now let us examine the situation where M weapons are used against an area target centered at $\vec{x}_{target} = (0, 0)$, consisting of N discrete elements, normally distributed around the center. Let

- \vec{Z}_k = the location of element k of the area target, for $k = 1, 2, \dots, N$.
- \vec{r}_j , \vec{X}_j , and \vec{Y} are the same as defined above. They are respectively, the aiming point, the independent error, and the dependent error of weapon j .

In this situation, \vec{Z}_k , the location of element k of the area target, is modeled as a normal random variable with zero mean:

$$\vec{Z}_k \sim N \left(\begin{pmatrix} 0 \\ 0 \end{pmatrix}, \begin{pmatrix} s_1^2 & 0 \\ 0 & s_2^2 \end{pmatrix} \right) \quad (6)$$

We assume that $\{\vec{Z}_k, k = 1, 2, \dots, N\}$ are independent of each other, and are independent of \vec{X}_j and \vec{Y} .

Figure 1 shows a sample distribution for an area target of 20 elements normally distributed with $s_1 = s_2 = 4$.

To study the damage fraction caused by the M weapons on the area target, we examine the kill probability of element k caused by the M weapons. The impact point of weapon j relative to element k of the area target is given by

$$\begin{aligned} \vec{w}_j^{(k)} &= \vec{r}_j + \vec{Y} + \vec{X}_j - \vec{Z}_k \\ &\equiv \vec{r}_j + \vec{Y}^{(k, \text{eff})} + \vec{X}_j \end{aligned} \quad (7)$$

where the effective dependent error of the M weapons relative to element k is defined as

$$\vec{Y}^{(k, \text{eff})} \equiv \vec{Y} - \vec{Z}_k$$

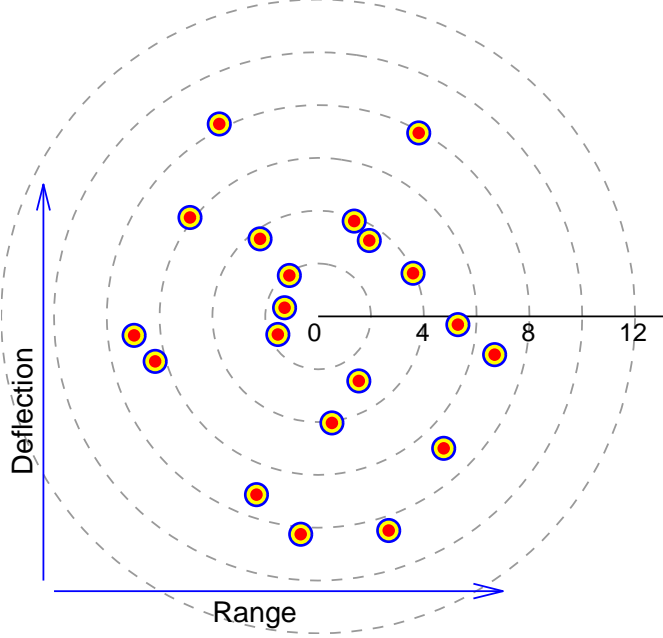


Figure 1: A sample distribution for an area target consisting of 20 random elements normally distributed with $s_1 = s_2 = 4$, as described by (6).

Note that $\vec{Y}^{(k,\text{eff})}$ is a normal random variable with zero mean

$$\vec{Y}^{(k,\text{eff})} \sim N \left(\begin{pmatrix} 0 \\ 0 \end{pmatrix}, \begin{pmatrix} \sigma_1^2 + s_1^2 & 0 \\ 0 & \sigma_2^2 + s_2^2 \end{pmatrix} \right)$$

The kill probability of element k caused by the M weapons (averaged over random independent errors $\{\vec{X}_j, j = 1, 2, \dots, M\}$, over the random dependent error \vec{Y} , and over the random element location \vec{Z}_k) is given by

$$\begin{aligned} p_{\text{kill}}(\text{element } k, M \text{ weapons}) \\ = G(\sqrt{\sigma_1^2 + s_1^2}, \sqrt{\sigma_2^2 + s_2^2}, d_1, d_2, b_1, b_2, \{\vec{r}_j, j = 1, 2, \dots, M\}) \end{aligned} \quad (8)$$

where function G is defined in equations (3), (4) and (5). Notice that in the case of an area target of normally distributed elements, the kill probability of element k has exactly the same form as in the case of a single target at $(0,0)$ with the exception that all instances of σ_1^2 be replaced by $(\sigma_1^2 + s_1^2)$ and σ_2^2 be replaced by $(\sigma_2^2 + s_2^2)$.

Let χ_k be the Bernoulli random variable indicating whether or not element k is killed (“1” corresponding to “killed”). The damage fraction (random variable) of the area target

is the number of elements killed normalized by the total number of elements.

$$q_{\text{damage}}(\text{area target}, M \text{ weapons}) \equiv \frac{1}{N} \sum_{k=1}^N \chi_k$$

The average damage fraction has the expression

$$\begin{aligned} E \left[q_{\text{damage}}(\text{area target}, M \text{ weapons}) \right] &= E \left[\frac{1}{N} \sum_{k=1}^N \chi_k \right] \\ &= \frac{1}{N} \sum_{k=1}^N p_{\text{kill}}(\text{element } k, M \text{ weapons}) \\ &= G(\sqrt{\sigma_1^2 + s_1^2}, \sqrt{\sigma_2^2 + s_2^2}, d_1, d_2, b_1, b_2, \{\vec{r}_j, j = 1, 2, \dots, M\}) \end{aligned} \quad (9)$$

Expression (9) gives the exact solution for the case of an area target of normally distributed elements.

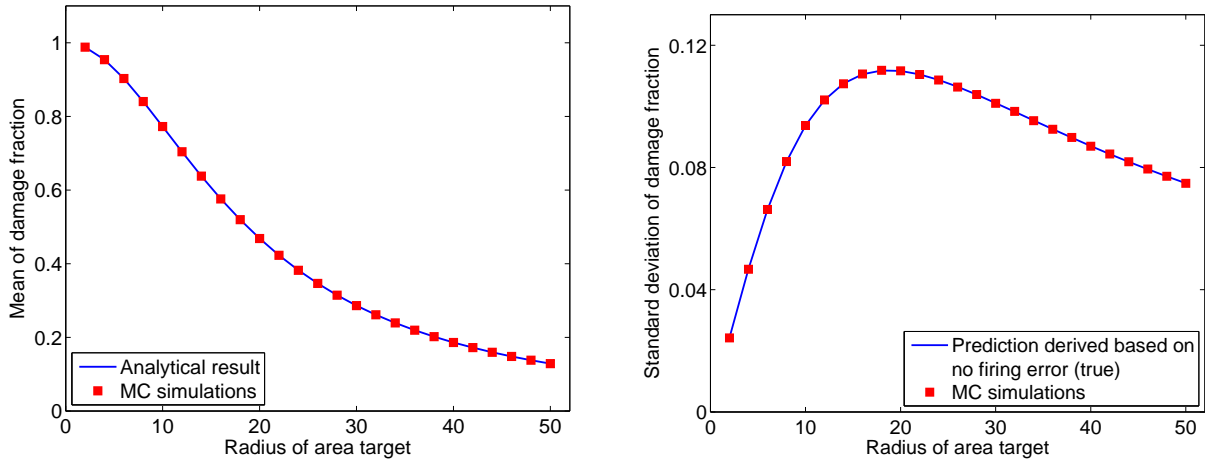


Figure 2: Statistics of the damage fraction for the case of a single shot against $N = 20$ normally distributed target elements with no firing error $(\sigma_1, \sigma_2, d_1, d_2) = 0$ and $(b_1, b_2) = (15, 25)$. The radius of area target is defined as $s_1 = s_2$ (the standard deviation of the elements distribution). Left panel: mean of damage fraction vs radius of area target. The analytical expression for the mean is valid regardless of the presence or absence of firing error. Right panel: standard deviation of damage fraction vs radius of area target. The analytical expression for the standard deviation (equations (11) and (12)) is valid only in the absence of firing error, which is true for the simulations in this figure.

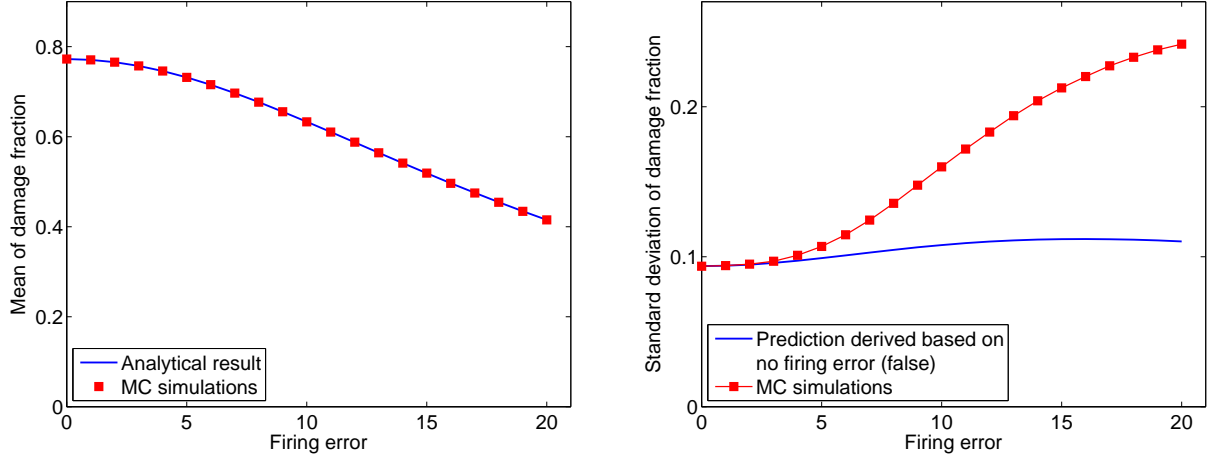


Figure 3: Statistics of the damage fraction for the case of a single shot against $N = 20$ normally distributed target elements with $s_1 = s_2 = 10$, $d_1 = d_2 = 0$ and $(b_1, b_2) = (15, 25)$. The firing error is defined as $\sigma_1 = \sigma_2$. Left panel: mean of damage fraction vs firing error. The analytical expression for the mean is valid regardless of the presence or absence of firing error. Right panel: standard deviation of damage fraction vs firing error. The analytical expression for the standard deviation (equations (11) and (12)) is valid only in the absence of firing error, which is false for the simulations in this figure. The results of Monte Carlo simulations show that the actual standard deviation of the damage fraction is larger than the value predicted by applying equations (11) and (12) with non-zero $(\sigma_1, \sigma_2, d_1, d_2)$.

When both the independent error (\vec{X}_j , $j = 1, 2, \dots, M$) and the dependent error (\vec{Y}) of the M weapons are absent, random variables $\{\chi_k, k = 1, 2, \dots, N\}$ are independent of each other. In this situation, we can calculate analytically the standard deviation of damage fraction (random variable). The variance of damage fraction has the expression

$$\begin{aligned} \text{var} [q_{\text{damage}}(\text{area target}, M \text{ weapons})] &= \text{var} \left[\frac{1}{N} \sum_{k=1}^N \chi_k \right] \\ &= \frac{1}{N^2} \sum_{k=1}^N \text{var} [\chi_k] = \frac{1}{N} G(1 - G) \end{aligned} \quad (10)$$

where shorthand notation G is defined as

$$G \equiv G(\sqrt{\sigma_1^2 + s_1^2}, \sqrt{\sigma_2^2 + s_2^2}, d_1, d_2, b_1, b_2, \{\vec{r}_j, j = 1, 2, \dots, M\}) \quad (11)$$

Note that this expression for the variance is valid only in the absence of dependent and independent errors, for which we have $(\sigma_1, \sigma_2, d_1, d_2) = 0$. The standard deviation of damage fraction is

$$\text{std} [q_{\text{damage}}(\text{area target}, M \text{ weapons})] = \sqrt{\frac{1}{N} G(1 - G)} \quad (12)$$

When either the independent errors or dependent error or both are present, the standard deviation of damage fraction is larger than the value predicted by applying equations (11) and (12) with non-zero $(\sigma_1, \sigma_2, d_1, d_2)$. We demonstrate this behavior numerically in Figures 2 and 3 below. We consider the model problem in which a single shot is fired against an area target of $N = 20$ normally distributed elements. Monte Carlo simulations are carried out with 10^6 runs for each set of parameter values and in each of the two situations below, yielding accurate numerical results to compare with theoretical predictions.

In Figure 2, there is no firing error; the damage fraction is affected by the radius of area target (the standard deviation of target elements distribution). In this case, both the predicted mean and the predicted standard deviation of damage fraction are valid. As a result, the accurate Monte Carlo simulations agree with the theoretical predictions.

In Figure 3, the radius of area target is fixed at $s_1 = s_2 = 10$; the damage fraction is affected by the firing error (the total effect of dependent and independent errors; for a single shot, there is no need to distinguish dependent and independent errors). In this case, only the predicted mean of damage fraction is valid. The predicted standard deviation calculated by applying equations (11) and (12) with non-zero $(\sigma_1, \sigma_2, d_1, d_2)$ is invalid since equations (11) and (12) are derived based on the assumption of zero firing error. The right panel of Figure 3 clearly demonstrates the deviation of the accurate Monte Carlo simulations from the invalid theoretical prediction.

4 Optimal aiming points for an area target

Next we investigate the optimal aiming points for the case of multiple weapons against an area target of normally distributed elements. We use MATLAB build-in function “fmin-

search” [5] together with formula (9) to find aimpoints which yields the largest damage fraction. In this study, in addition to finding the unconstrained overall optimal aiming positions, we also consider optimizations over a set of given constrained patterns of aiming points. The goal is to find simple and efficient “empirical” methods for calculating nearly optimal aiming positions. This approach greatly simplifies the numerical complexity of finding the optimal aiming points at the price of obtaining an approximate optimum. We consider 6 constrained patterns of aiming positions as listed below.

- Pattern A1: M points on an ellipse, uniform in parameter angle.

Specifically, the M aiming points are mathematically described by

$$\theta_j = \theta_1 + \frac{(j-1)}{M} 2\pi, \quad j = 1, 2, \dots, M \quad (13)$$

$$(x_j, y_j) = R \left(\sqrt{\eta} \cos \theta_j, \frac{1}{\sqrt{\eta}} \sin \theta_j \right) \quad (14)$$

This constrained pattern has three parameters: θ_1 , R and η , over which we are going to optimize the average damage fraction. Here θ_1 is the parameter angle for weapon 1. R is the effective radius of the ellipse, satisfying

$$R = \sqrt{\frac{\text{area of ellipse}}{\pi}}$$

whereas η is the aspect ratio of the ellipse, satisfying

$$\eta = \frac{\text{major axis}}{\text{minor axis}}$$

- Pattern A2: 1 point at center and $(M - 1)$ points on an ellipse, uniform in parameter angle.

One aiming point is placed at the center. The rest $(M - 1)$ aiming points are distributed along an ellipse, uniformly in parameter angle θ , as described by equations (13) and (14) where M is replaced by $(M - 1)$. This constrained pattern has three parameters: θ_1 , R and η .

- Pattern A3: 2 points on the x -axis and $(M - 2)$ points on an ellipse, uniform in parameter angle.

Two aiming points are placed, respectively, at $(x_a, 0)$ and $(-x_a, 0)$. The rest $(M - 2)$ aiming points are distributed along an ellipse, uniformly in parameter angle θ , as described by equations (13) and (14) where M is replaced by $(M - 2)$. This constrained pattern has 4 parameters: θ_1 , R , η , and x_a .

- Pattern B1: M points on an ellipse, uniform in polar angle.

The M aiming points are mathematically described by

$$\phi_j = \phi_1 + \frac{(j - 1)}{M} 2\pi, \quad j = 1, 2, \dots, M \quad (15)$$

θ_j determined by the condition that the two vectors

$$\left(\sqrt{\eta} \cos \theta_j, \frac{1}{\sqrt{\eta}} \sin \theta_j \right) \text{ and } (\cos \phi_j, \sin \phi_j) \text{ point in the same direction} \quad (16)$$

$$(x_j, y_j) = R \left(\sqrt{\eta} \cos \theta_j, \frac{1}{\sqrt{\eta}} \sin \theta_j \right) \quad (17)$$

This constrained pattern has three parameters: ϕ_1 , R and η .

- Pattern B2: 1 point at center and $(M - 1)$ points on an ellipse, uniform in polar angle.

One aiming point is placed at the center. The rest $(M - 1)$ aiming points are distributed along an ellipse, uniformly in polar angle ϕ , as described by equations (15), (16) and (17) where M is replaced by $(M - 1)$. This constrained pattern has three parameters: ϕ_1 , R and η .

- Pattern B3: 2 points on the x -axis and $(M - 2)$ points on an ellipse, uniform in parameter angle.

Two aiming points are placed, respectively, at $(x_a, 0)$ and $(-x_a, 0)$. The rest $(M - 2)$ aiming points are distributed along an ellipse, uniformly in polar angle ϕ , as described by equations (15), (16) and (17) where M is replaced by $(M - 2)$. This constrained pattern has four parameters: ϕ_1 , R , η , and x_a .

In numerical simulations below, we choose the parameter values as follows.

$$M = 1 \sim 12, \quad \text{number of weapons}$$

$$(b_1, b_2) = (60, 100), \quad \text{parameters in Carleton damage function}$$

$(\sigma_1, \sigma_2) = (5, 5)$, standard deviation (s.d.) of dependent error in firing errors

$(d_1, d_2) = (5, 5)$, s.d. of independent errors in firing errors

$s = s_1 = s_2 = 15 \sim 300$, radius of area target (s.d. of elements distribution)

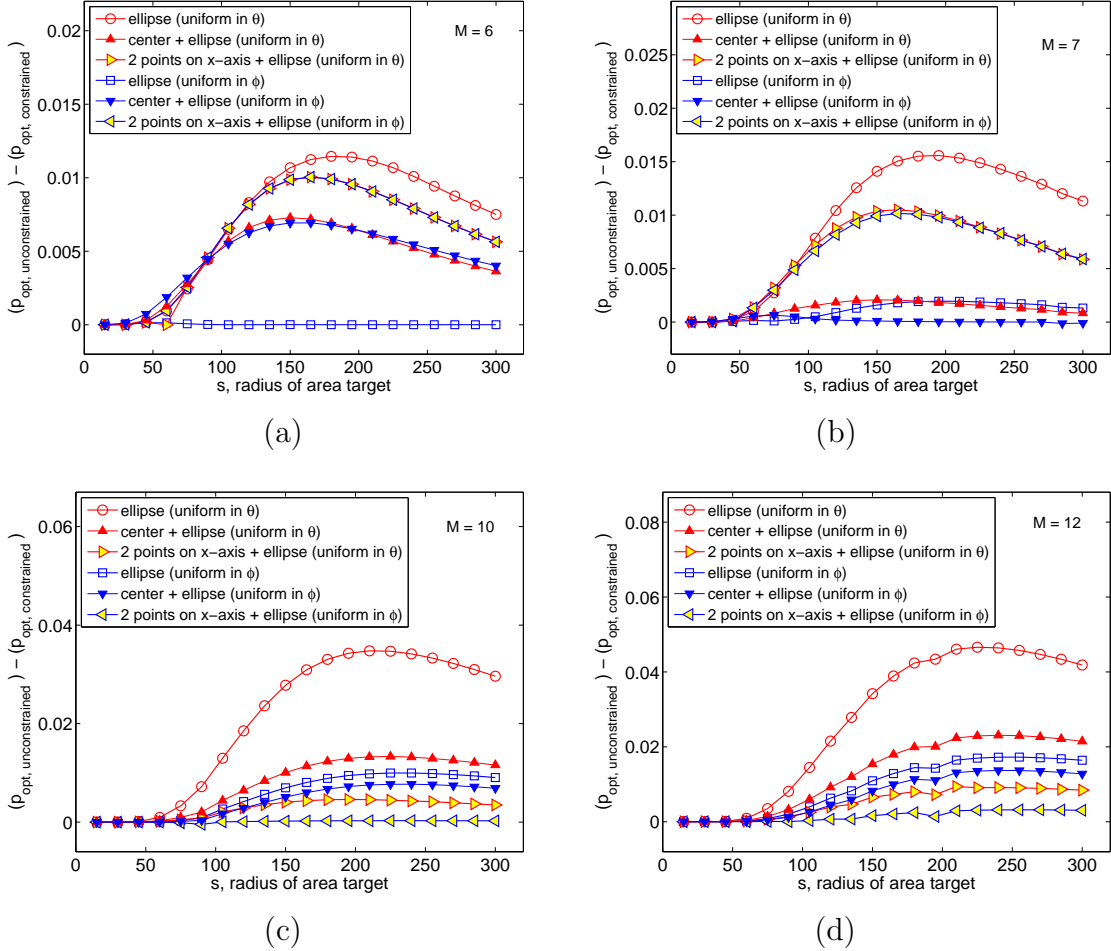


Figure 4: Difference in optimal damage fraction (p_{opt}) between constrained and unconstrained optimizations as a function of area target radius (s) for various numbers of weapons (M).
(a) $M = 6$. (b) $M = 7$. (c) $M = 10$. (d) $M = 12$.

We compare the results of optimization over constrained patterns with those of the overall optimization. Figure 4 plots the difference in optimal (maximum) damage fraction (p_{opt}) between constrained and unconstrained optimizations as a function of area target radius (s) for various numbers of weapons (M). The difference shows how accurate it is to optimize over a given pattern. For $M \leq 6$ (panel (a) of Figure 4), the best approximate optimal

damage fraction is achieved by distribute aiming points over an ellipse, uniformly in polar angle (Pattern B1 described above). At $M = 7$ (panel (b) of Figure 4), the best approximate optimal damage fraction is achieved by placing an aiming point at center and placing the rest six aiming points over an ellipse, uniformly in polar angle (Pattern B2) . This is also true for $M = 8$ and $M = 9$. As the number of weapons increases, at $M = 10$ (panel (c) of Figure 4), the best approximate optimal damage fraction is achieved by placing two aiming points on the x -axis and the rest eight aiming points over an ellipse, uniformly in polar angle (Pattern B3). The constrained optimum over Pattern B3 remains very accurate at $M = 12$ weapons (panel (d) of Figure 4).

In summary, as M increases, the best pattern of aiming points for obtaining approximately the highest damage fraction goes from Patterns B1 to B2 to B3. This transition is clearly demonstrated in Figure 5 where the difference in optimal damage fraction (p_{opt}) between constrained and unconstrained optimizations is shown as a function of M at $s = 150$ (radius of area target).

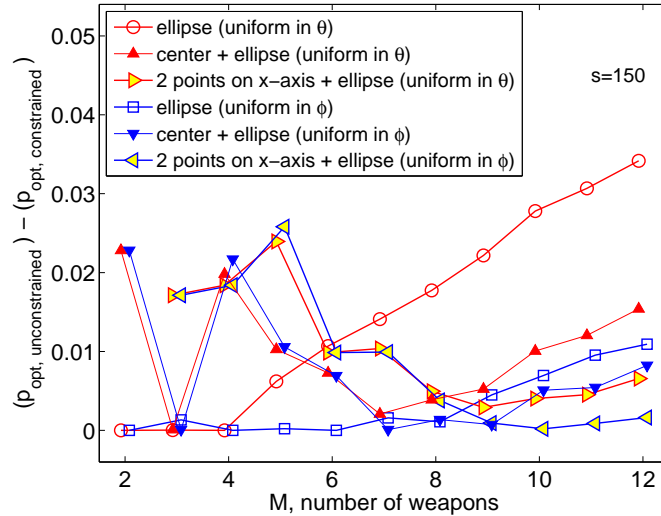


Figure 5: Difference in optimal damage fraction (p_{opt}) between constrained and unconstrained optimizations as a function of M at $s = 150$ (radius of area target). In the horizontal direction, all points should have integer values. To visually display points that are on top of each other, they are shifted slightly in the horizontal direction in the plot.

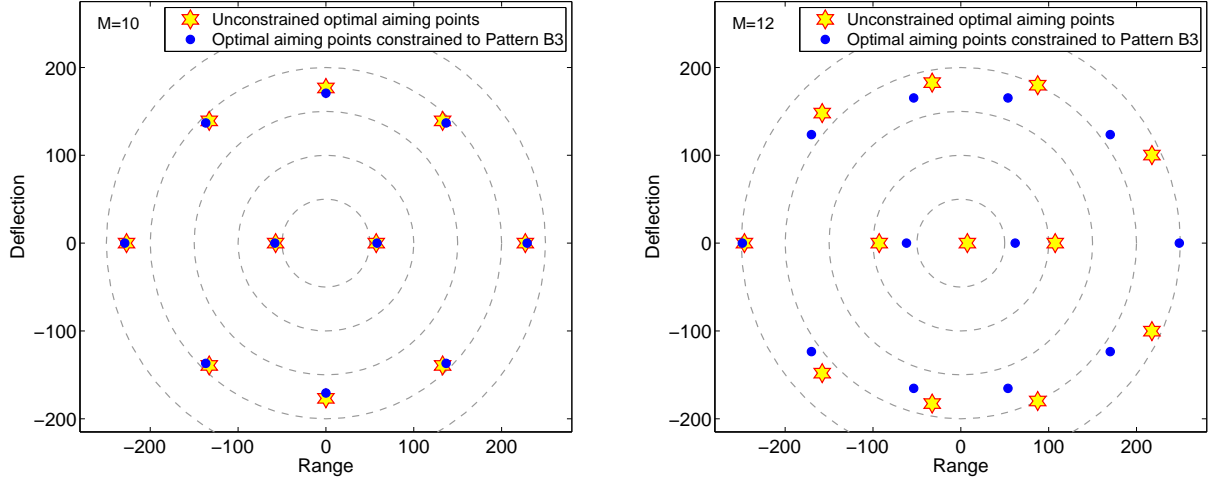


Figure 6: Comparison of unconstrained optimal aiming points and optimal aiming points constrained to Pattern B3. Left panel: two sets of optimal aiming points for $M = 10$, yielding $p_{\{\text{opt, unconstrained}\}} = 0.772604$ and $p_{\{\text{opt, Pattern B3}\}} = 0.772398$, respectively. Right panel: two sets of optimal aiming points for $M = 12$, yielding $p_{\{\text{opt, unconstrained}\}} = 0.814997$ and $p_{\{\text{opt, Pattern B3}\}} = 0.813372$, respectively.

Figure 6 compares the unconstrained optimal aiming points and the optimal aiming points constrained to Pattern B3, respectively for $M = 10$ and $M = 12$ at $s = 150$. At $M = 10$, the optimal aiming points of Pattern B3 match almost exactly the unconstrained aiming points. At $M = 12$, the optimal aiming points of Pattern B3 deviate from the unconstrained aiming points. Despite the apparent discrepancy between these two sets of optimal aiming points, the corresponding damage fractions are still very close to each other: the optimal damage fraction for Pattern B3 is $p_{\{\text{opt, Pattern B3}\}} = 0.813372$ while the overall optimal damage fraction is $p_{\{\text{opt, unconstrained}\}} = 0.814997$. The difference between these two damage fraction values is less than 0.2%. It is important to notice out the difference in computational complexity between these two optimizations. While the constrained optimization over Pattern B3 has 4 variables, the unconstrained optimization for $M = 12$ weapons has 24 variables, which converges much slower than the constrained optimization.

The optimal aiming points constrained to Pattern B1 for $M = 6$, the optimal aiming points constrained to Pattern B2 for $M = 7$ and the corresponding unconstrained optimal aiming points are displayed in Figure 7.

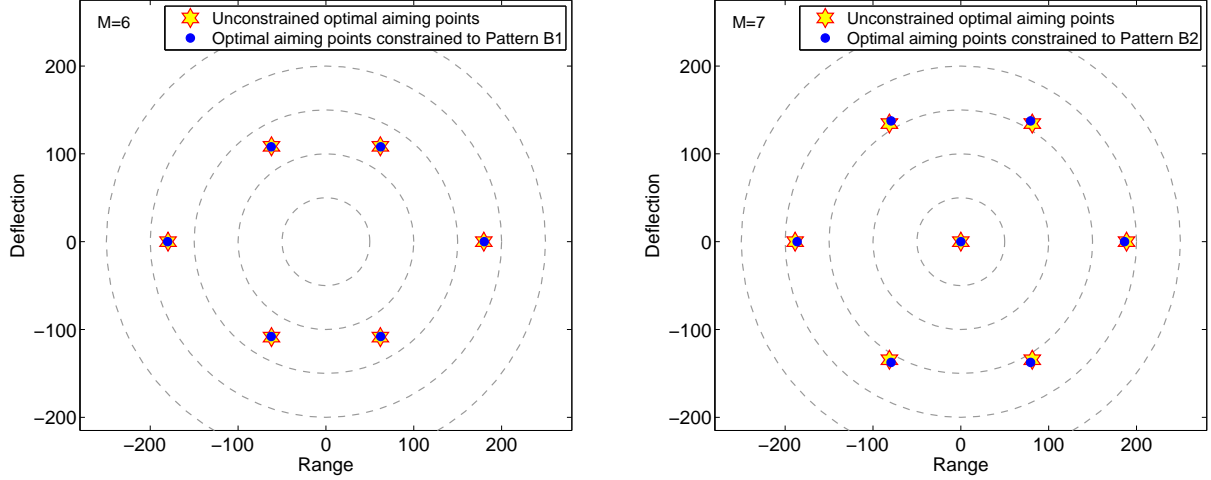


Figure 7: Left panel: unconstrained optimal aiming points and optimal aiming points constrained to Pattern B1 for $M = 6$ weapons. Right panel: unconstrained optimal aiming points and optimal aiming points constrained to Pattern B2 for $M = 7$ weapons.

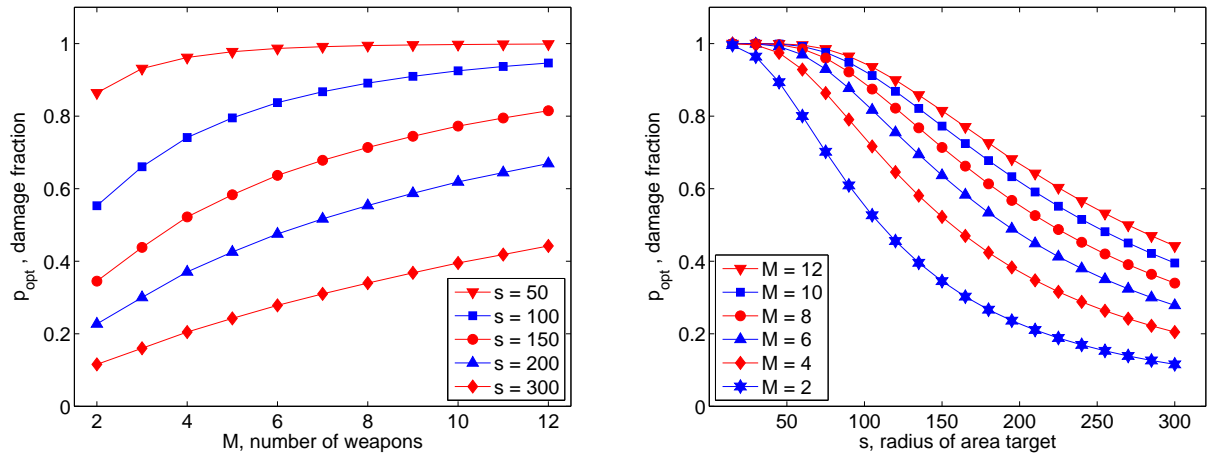


Figure 8: Damage fraction corresponding to the optimal aiming points. Left panel: damage fraction as a function of M . Right panel: damage fraction as a function of s .

Figure 8 plots the optimal damage fraction, respectively, as a function of M for several values of s (left panel), and as a function of s for several values of M (right panel). For a

fixed value of s , the optimal damage fraction increases with the number of weapons, M ; for a fixed value of M , the optimal damage fraction decreases as the radius (s) of area target is increased (i.e., damage fraction is lower for a larger area target). Both of these results are reasonable and consistent with our intuition.

A practical question regarding resource allocation is the following. Given the radius of area target (s), what is the minimum number of weapons needed to achieve a given threshold of damage fraction? This question is answered in Figure 9. Figure 9 shows that for any given threshold of damage fraction, the minimum number of weapons needed is an increasing function of the area target radius (i.e., larger area target requires larger number of weapons), which again is reasonable and consistent with our intuition.

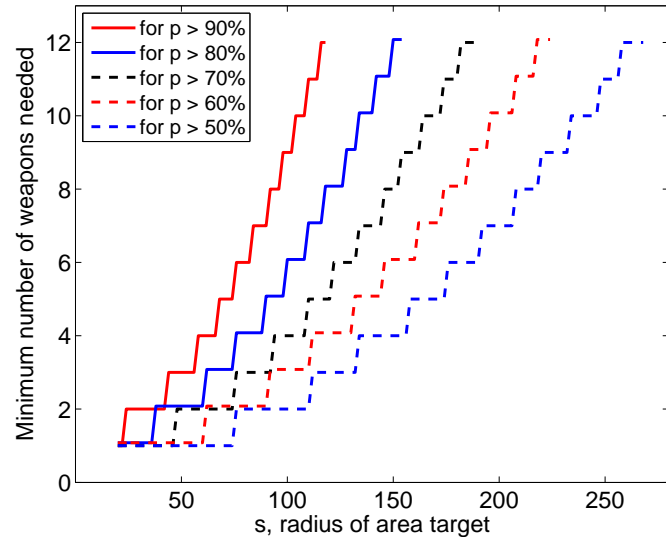


Figure 9: Minimum number of weapons needed for achieving a given threshold of damage fraction vs. radius of area target. In the vertical direction, all flat steps should have integer values. To visually display steps from different curves that are overlap with each other, they are shifted slightly in the vertical direction in the plot.

5 Scaling laws for optimal aiming points and optimal damage fraction with respect to area target radius

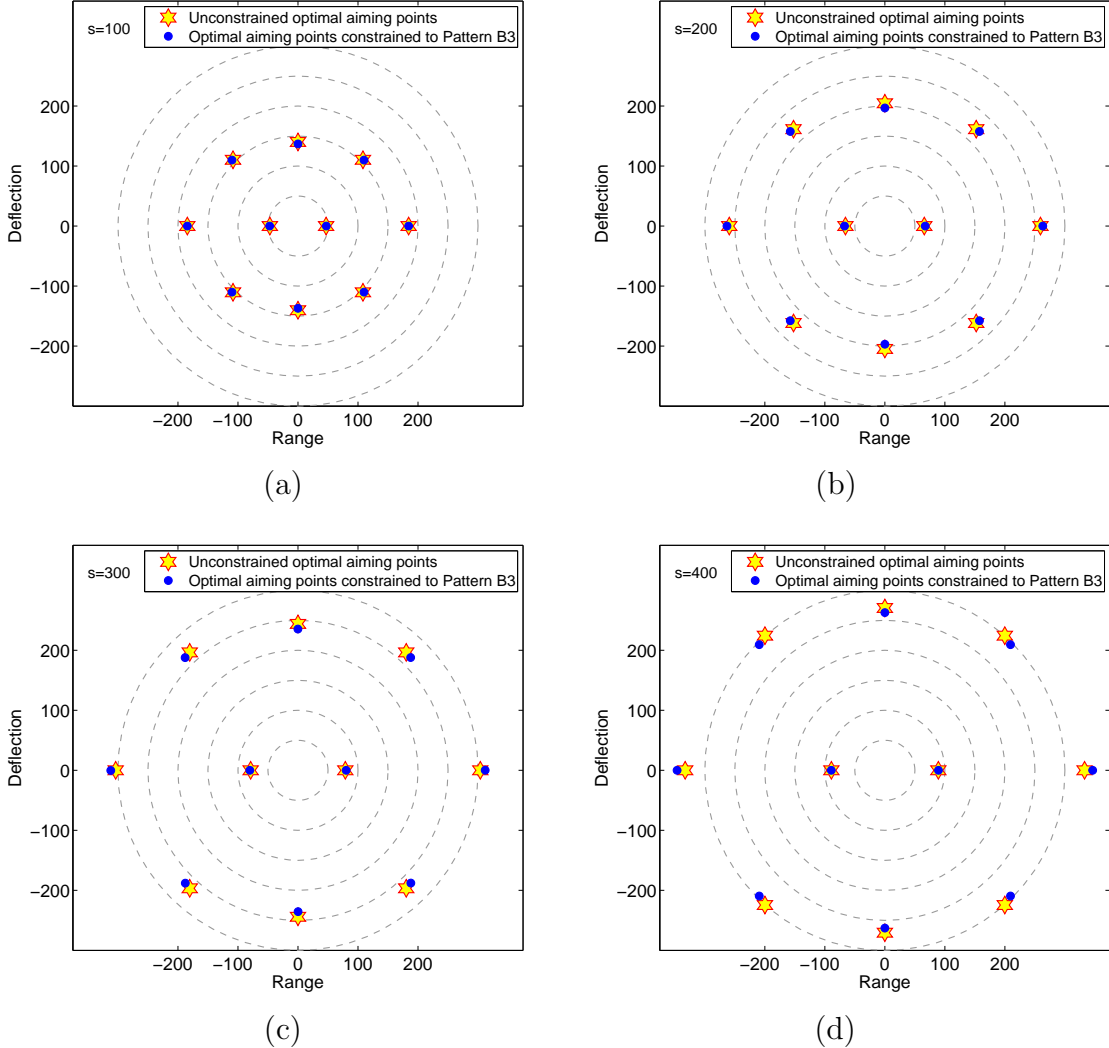


Figure 10: Sets of optimal aiming points for $M = 10$ weapons for several values of area target radius (s). (a) $s = 100$. (b) $s = 200$. (c) $s = 300$. (d) $s = 400$.

Finally, we study how the optimal aiming points change with s , the radius of area target, and explore if there is a scaling law relating sets of optimal aiming points at different values of s . We start by examining the optimal aiming points for 4 different values of area target

radius. The 4 panels in Figure 10 show the optimal aiming points for $M = 10$ weapons, respectively, for $s = 100$, $s = 200$, $s = 300$ and $s = 400$. The spreading size of optimal aiming points increases as the radius of area target (s) is increased. However, the increase does not follow a simple proportional linear relationship. Figure 10 indicates that the increase in the spread size of optimal aiming points is less than linear with respect to the area target radius. This can be explained intuitively as follows. When the radius of area target is increased, the set of aiming points needs to cover a larger region. On the other hand, to maximize the damage fraction, the killing areas associated with individual weapons also need to maintain a certain degree of overlapping with each other. These two needs contradict each other and cannot be both accommodated simultaneously with a fixed number of weapons (M) as the area target radius is increased. Thus, it is expected that as the radius of area target is increased, the spread size of optimal aiming points will increase less than linearly. Here we avoid using the term “radius of optimal aiming points” because the distribution of aiming points is not circularly symmetric.

For the purpose of investigating the spread size of aiming points quantitatively, we define the size of a set of M aiming points $\{\vec{r}_j, j = 1, 2, \dots, M\}$ mathematically as

$$L_{AP} \equiv \sqrt{\frac{1}{M} \sum_{j=1}^M |\vec{r}_j|^2} \quad (18)$$

To explore how the size of optimal aiming points scales with the area target radius, we plot these two quantities against each other in a log-log plot in the left panel of Figure 11, which also includes a fitting function of the form $L_{AP} \propto \sqrt{s}$. The log-log plot along the fitting function indicate that the size of optimal aiming points (L_{AP}) approximately is proportional to the square root of area target radius (\sqrt{s}). This observation suggests that we should normalize the aiming points by the square root of area target radius and introduce the scaled aiming points as

$$\vec{r}_j^{(\text{scaled})}(s) \equiv \frac{1}{\sqrt{s}} \vec{r}_j(s) \quad (19)$$

The right panel of Figure 11 compares sets of scaled optimal aiming points of Pattern B3 for $s = 100$, $s = 200$, $s = 300$ and $s = 400$. The comparison demonstrates that not only the spread size of optimal aiming points scales as \sqrt{s} , the distribution of optimal

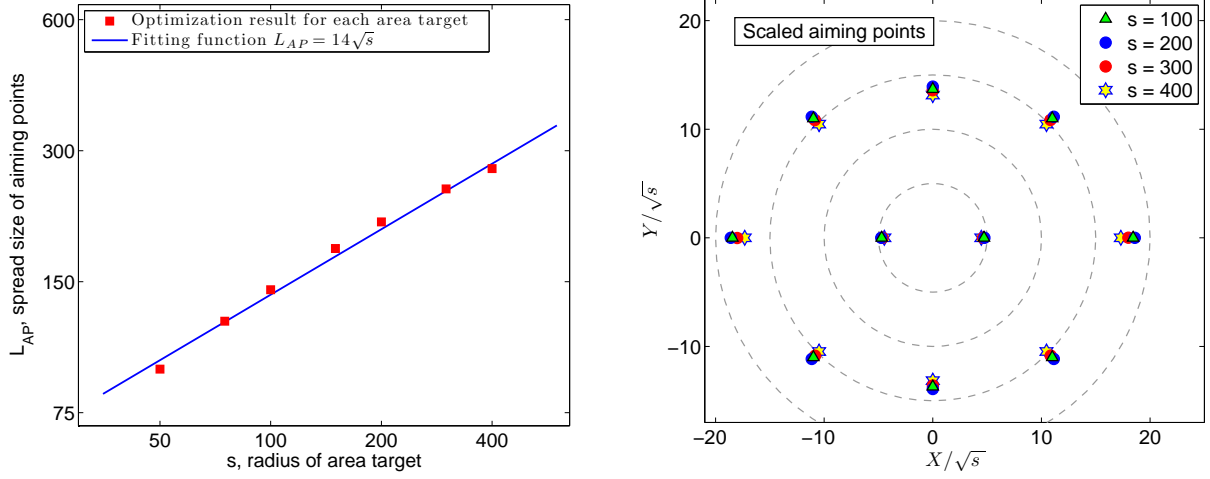


Figure 11: Comparison of optimal aiming points for different values of area target radius. Left panel: spread size of optimal aiming points vs. radius of area target in a log-log plot. Right panel: sets of scaled optimal aiming points of Pattern B3 for $s = 100$, $s = 200$, $s = 300$ and $s = 400$.

aiming points after scaling is approximately invariant with respect to the area target radius. Mathematically, we have observed that approximately

$$\vec{r}_j^{(\text{scaled})}(s) \text{ is invariant with respect to } s \quad (20)$$

This scaling property gives us an even more efficient way of calculating optimal aiming points. We only need to calculate the optimal aiming points for an area target of typical/representative radius: $\{\vec{r}_j(s_0), j = 1, 2, \dots, M\}$. We use $s_0 = 150$ in our study. For an area target of radius s , we simply calculate/predict a set of nearly optimal aiming points from $\{\vec{r}_j(s_0)\}$ using the scaling law.

$$\vec{r}_j(s) = \sqrt{\frac{s}{s_0}} \vec{r}_j(s_0) \quad (21)$$

We evaluate the performance of this efficient method by examining the damage fraction values achieved by these sets of nearly optimal aiming points. Specifically, for each area target, we calculate the damage fraction values corresponding to three sets of aiming points

- aiming points calculated in the unconstrained optimization

- aiming points calculated using scaling law (21)
- all aiming points = $(0, 0)$

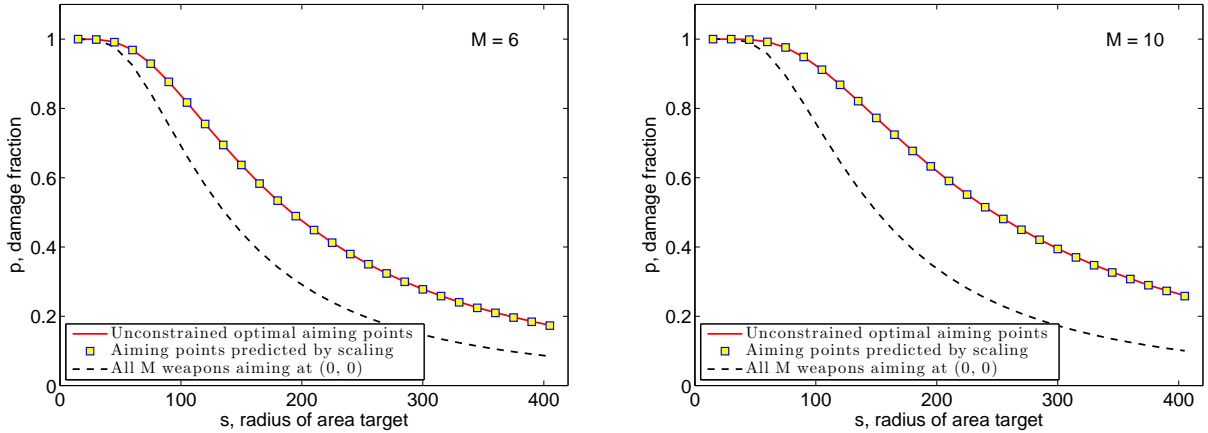


Figure 12: Comparison in damage fraction performance of 3 sets of aiming points: i) aiming points calculated in the unconstrained optimization, ii) aiming points calculated using scaling, and iii) all aiming points = $(0, 0)$. Left panel: $M = 6$ weapons. Right panel: $M = 12$ weapons.

Figure 12 compares the damage fraction values caused by the 3 sets of aiming points described above for $M = 6$ weapons (left panel) and for $M = 10$ weapons (right panel). The damage fraction achieved by the set of nearly optimal aiming points calculated using scaling is indistinguishable from that achieved in the unconstrained optimization (true optimum) while the damage fraction corresponding to all weapons aiming at $(0, 0)$ is much lower. Therefore, we conclude that scaling law (21) is an efficient and accurate method for calculating a set of nearly optimal aiming points.

6 Concluding remarks

We have studied the average damage fraction of an area target by multiple weapons. The area target was assumed to consist of normally distributed elements. Using the analytical expression of the average damage fraction, we compared various distribution patterns of

the aimpoints and gave optimal patterns for different number of weapons. Scaling laws for optimal aimpoints and optimal damage fraction with respect to the radius of the area target were derived. One prospective future research is to extend our current work to an area target of uniformly distributed elements. Another avenue for future research is to consider an area target where the elements are assigned different values and seek optimal aimpoints in order to minimize the total average surviving value.

7 Disclaimer

The authors would like to thank TRAC-Monterey for supporting this work and Center for Army Analysis (CAA) for bringing this problem to our attention. The views expressed in this document are those of the authors and do not reflect the official policy or position of the Department of Defense or the U.S. Government.

References

- [1] Eckler, A. and Burr, S. (1972). Mathematical Models of Target Coverage and Missile Allocation, Military Operations Research Society.
- [2] Washburn, A. and Kress, M. (2009). Combat Modeling. Dordrecht; New York; Springer.
- [3] Driels, M. (2014). Weaponeering: Conventional Weapon System Effectiveness, 2nd edition, American Institute of Aeronautics and Astronautics (AIAA) Education Series, Reston, VA.
- [4] Wang, H., Moten, C., Driels, M., Drundel, D., and Zhou, H. (2016). Explicit exact solution of damage probability for multiple weapons against a unitary target, American Journal of Operations Research, in press

- [5] Lagarias, J.C., Reeds, J.A., Wright, M.H., Wright, P.E. (1998) Convergence properties of the Nelder-Mead simplex method in low dimensions, SIAM Journal of Optimization, 9(1): 112-147

MATLAB Code

Damage probability for multiple weapons against a unitary target

```
1 function [p]=prob_ex_sol(M, ra ,b ,d ,sig )
2 %
3 % By Hongyun Wang <hongwang@soe.ucsc.edu>
4 % University of California , Santa Cruz
5 % and Hong Zhou , Naval Postgraduate School , Monterey
6 %
7 % This code calculates the kill probability against a single
8 % target at (0, 0) , by M weapons with given aimpoints , distribution
9 % of dependent error , distribution of independent errors , and
10 % the lethal area (Carleton damage function)
11 %
12 % Input :
13 % M: number of weapons
14 % ra: M x 2 matrix containing aimed positions of M weapons
15 % b=[b(1), b(2)]: parameters in Carleton damage function
16 % d=[d(1), d(2)]: std of independent error in 2 directions
17 % sig=[sig(1), sig(2)]: std of dependent error in 2 directions
18 %
19 % Output :
20 % p: kill probability by M weapons
21 %
22 bs=b.^2;
23 ds=d.^2;
24 ss=sig.^2;
25 %
26 nc=2^M-1; % number of all combinations
27 cf=zeros( nc ,M);
28 tem=uint32 ([1:nc] ');
29 for k=1:M,
30 cf (: ,k)=bitget (tem ,k) ;
31 end
32 ka=sum( cf ,2) ;
33 %
34 tma=(cf*ra (: ,1) ).^2./ka;
35 tmb=cf*ra (: ,1) .^2;
36 F1=sqrt( bs(1)/(bs(1)+ds(1)) ).^ka.* ...
37 sqrt( (bs(1)+ds(1))./(bs(1)+ds(1)+ss(1)*ka) ).* ...
38 exp( (tma-tmb)/(2*(bs(1)+ds(1))) - tma./(2*(bs(1)+ds(1)+ss(1)*ka)) );
39 %
40 tma=(cf*ra (: ,2) ).^2./ka;
41 tmb=cf*ra (: ,2) .^2;
42 F2=sqrt( bs(2)/(bs(2)+ds(2)) ).^ka.* ...
43 sqrt( (bs(2)+ds(2))./(bs(2)+ds(2)+ss(2)*ka) ).* ...
44 exp( (tma-tmb)/(2*(bs(2)+ds(2))) - tma./(2*(bs(2)+ds(2)+ss(2)*ka)) );
45 %
46 p=sum(-(-1).^ka.*F1.*F2);
47 %
48 %
```

Damage probability for area target with M aimpoints placed along an ellipse uniformly in polar angle (EUPA)

```

1 function [z]=p_eupa_G(M, r, eta, c0, b, d, sig, s)
2 %
3 %% By Hongyun Wang <hongwang@soe.ucsc.edu>
4 %% University of California , Santa Cruz
5 %% and Hong Zhou, Naval Postgraduate School , Monterey
6 %
7 %% This code calculates the damage fraction against an area target
8 %% of normally distributed target elements around (0, 0) , by M weapons
9 %% with aimpoints placed along an Ellipse Unifromly in Poar Angle (EUPA).
10 %% The set of aimpoints is specified by 3 parameters: major and minor
11 %% axes of the ellipse , and the off-set angle
12 %% Later (in "p_op_eupa_G.m"), an optimal set of aimpoints is calculated
13 %% by maximizing the damage fraction over the 3 parameters.
14 %
15 % Input:
16 % M: number of weapons
17 % r: average radius of ellipse = sqrt(major axis * minor axis)
18 % eta: aspect ratio of ellipse
19 % c0: c0*pi = off-set angle
20 % b=[b(1), b(2)]: parameters in Carleton damage function
21 % d=[d(1), d(2)]: std of independent error in 2 directions
22 % sig=[sig(1), sig(2)]: std of dependent error in 2 directions
23 % s=[s(1),s(2)]: std of target elements distribution in 2 directions
24 %
25 % Output:
26 % z: damage fraction
27 %
28 phi=c0*pi+[0:M-1]'/M^2*pi;
29 x0=cos(phi)/sqrt(eta);
30 y0=sin(phi)*sqrt(eta);
31 %x0=cos(phi)/sqrt(eta);
32 %y0=sin(phi)*sqrt(eta);
33 r0=sqrt(x0.^2+y0.^2);
34 x=(r*sqrt(eta))*x0./r0;
35 y=(r/sqrt(eta))*y0./r0;
36 ra=[x, y]; % matrix containing aimed positions of M weapons
37 %
38 ss=sqrt(sig.^2+s.^2);
39 [pex]=prob_ex_sol(M,ra,b,d,ss);
40 z=pex;
41 %
42 %

```

Optimized Damage probability for area target with M aimpoints placed along an ellipse uniformly in polar angle (EUPA)

```

1 function [z]=p_op_eupa_G(M, b, d, sig, s)
2 %
3 %% By Hongyun Wang <hongwang@soe.ucsc.edu>
4 %% University of California , Santa Cruz
5 %% and Hong Zhou, Naval Postgraduate School , Monterey
6 %
7 %% This code maximizes the damage fraction and calculates the optimal
8 %% aimpoints when an area target of normally distributed target elements
9 %% around (0, 0) is attacked by M weapons with aimpoints placed along
10 %% an Ellipse Unifromly in Poar Angle (EUPA)
11 %% In the constrained optimization , the set of aimpoints is specified by
12 %% 3 arameters: major and minor axes of the ellipse , and the off-set angle.
13 %% The damage fraction is maximized over the 3 parameters.
14 %
15 % Input :
16 % M: number of weapons
17 % b=[b(1), b(2)]: parameters in Carleton damage function
18 % d=[d(1), d(2)]: std of independent error in 2 directions
19 % sig=[sig(1), sig(2)]: std of dependent error in 2 directions
20 % s=[s(1),s(2)]: std of target elements distribution in 2 directions
21 %
22 % Output :
23 % z: optimal solution (a structure containing maximum damage fraction ,
24 % optimal aimpoints , ... )
25 %
26 u0=[log(40), log(2), 0];
27 G=@(u) -p_eupa_G(M, exp(u(1)), exp(u(2)), u(3), b, d, sig, s);
28 options = optimset('TolX',1e-8,'TolFun',1e-16, ...
29 'MaxIter',2000,'MaxFunEvals',2000,'Display','off');
30 [u, fval, flag, output]=fminsearch(@(u) G(u), u0, options);
31 %
32 pmax=fval;
33 ap=[exp(u(1)+0.5*u(2)), exp(u(1)-0.5*u(2)), u(3)];
34 rx=ap(1);
35 ry=ap(2);
36 phi=ap(3)*pi+[0:M-1]/M*2*pi ;
37 x0=cos(phi)/rx;
38 y0=sin(phi)/ry;
39 r0=sqrt(x0.^2+y0.^2);
40 x=rx*x0./r0;
41 y=ry*y0./r0;
42 %
43 z=struct('M',M, 'pmax',pmax, 'rx',ap(1), 'ry',ap(2), 'phi_1',ap(3), ...
44 'x',x, 'y',y, ...
45 'flag',flag, 'output',output);
46 %

```

Maximum damage probability of M weapons against N targets using the optimized EUPA methodology

```
1 %%  
2 %% By Hongyun Wang <hongwang@soe.ucsc.edu>  
3 %% University of California , Santa Cruz  
4 %% and Hong Zhou, Naval Postgraduate School , Monterey  
5 %%  
6 %% This code calculates and plots the maximum damage fraction vs  
7 %% the area target size.  
8 %% It also plots the optimal aimpoints for a given area target size  
9 %% PROBLEM SETUP:  
10 %% An area target of N normally distributed target elements around (0,0)  
11 %% is attacked by M weapons. The size of area target is defined as the  
12 %% standard deviation of the target element distribution.  
13 %%  
14 clear  
15 clf reset  
16 %  
17 M=6;      % Number of weapons  
18 N=20;     % Number of target elements  
19 %  
20  
21 b=[60,100]; % parameters in Carleton damage function  
22 d=[5,5];    % std of independent error in 2 directions  
23 sig=[5,5];   % std of dependent error in 2 directions  
24 sa=[15:15:300];  
25 % A sequence of values for the area target size.  
26 % For each value , we maximize the damage fraction  
27 s0=150;  
28 % Area target size for which the optimal aimpoints are shown  
29 %  
30 m=size(sa,2);  
31 p_eupa=zeros(1,m);  
32 for k=1:m,  
33 s=sa(k)*[1,1];  
34 z=p_op_eupa_G(M, b, d, sig, s);  
35 p_eupa(k)=z.pmax;  
36 end  
37 %  
38 figure(1)  
39 clf reset  
40 set(gcf, 'position',[50 100 560 420])  
41 axes('position',[0.15,0.15,0.75,0.75])  
42 %  
43 plot(sa, p_eupa, 'linewidth',2.0)  
44 set(gca, 'fontsize',14)  
45 axis([0,305, 0, 1.1])  
46 xlabel('Area target size')  
47 ylabel('Maximum damage fraction')  
48 text(100, 1.0, [num2str(M), ' weapons against an area ...  
target'], 'fontsize',14)
```

```

49 %
50 figure(2)
51 clf reset
52 set(gcf, 'position',[600 200 560 420])
53 axes('position',[0.15,0.15,0.75,0.80])
54 %
55 s=s0*[1, 1];
56 z=p_op_eupa_G(M, b, d, sig, s);
57 x=z.x;
58 y=z.y;
59 plot(x, y, 'bh', 'linewidth',1.0, 'markerfacecolor','y', 'markersize',14)
60 hold on
61 %
62 ct0=[0:64]/64*2*pi;
63 x0=cos(ct0);
64 y0=sin(ct0);
65 plot(50*x0,50*y0, '—', 'linewidth',1.0, 'color',0.6*[1, 1, 1])
66 plot(100*x0,100*y0, '—', 'linewidth',1.0, 'color',0.6*[1, 1, 1])
67 plot(150*x0,150*y0, '—', 'linewidth',1.0, 'color',0.6*[1, 1, 1])
68 plot(200*x0,200*y0, '—', 'linewidth',1.0, 'color',0.6*[1, 1, 1])
69 %
70 set(gca, 'fontsize',14)
71 axis([-200,200,-180,180])
72 axis equal
73 set(gca, 'xtick',[-200:100:200])
74 set(gca, 'ytick',[-200:100:200])
75 xlabel('Range direction')
76 ylabel('Deflection direction')
77 text(-150, 160, ['Optimal aimpoints of ', num2str(M), ' ...
    weapons'], 'fontsize',14)
78 %
79 %

```

Carleton Damage Function Exact Solution in R

Cardy Moten III

December 27, 2016

Purpose

The purpose of this report is to explain the supporting code for the equations developed in Wang et al. (2016a; 2016b). Dr. Hongyn Wang and Dr. Hong Zhou originally developed the code used in this report in MATLAB.

M Weapons firing at a single target

Description

The code in this section calculates the damage probability against a single target at $(0, 0)$, by M weapons with given aim points, distribution of dependent error, distribution of independent errors, and the lethal area (Carleton damage function).

Inputs

- M : Number of weapons.
- ra : $M \times 2$ matrix containing aimed positions of the M weapons.
- $b = [b_1, b_2]$: parameters in the Carleton damage function that represent the effective weapon radii in the range and deflection directions, respectively.
- $d = [d_1, d_2]$: standard deviation of the independent error in two directions.
- $sig=[sig_1, sig_2]$: standard deviation of dependent error in two directions.

Output

p : damage probability of the M weapons aimed at a single target at $(0,0)$.

Function Code

The code for the function of the exact solution is below. This code follows the details, specifically equations 6-8, documented in Wang et al. (2016a). The code will execute the following:

1. Compute squared values for parameters b, d , and sig .
2. Declare a variable for the total number of hit combinations.
3. Create a matrix to store all the hit combinations. The number of rows will be equal to the number of combinations, and the number of columns will equal the number of weapons fired.
4. Create a variable that is equal in length to the number of hit combinations.
5. For each row and column of the combinations fired matrix:
 - (a) Compute the bit value of the current index in the matrix.
 - (b) For example, if we fire two weapons at a target, the combinations fired matrix will contain three rows and two columns. The bit values for each row would be $(1,0)$, $(0,1)$, and $(1,1)$ respectively to represent a hit from weapon 1, weapon 2, and weapons 1 & 2 respectively.

6. Compute the row sum of the combinations fired matrix.
7. Compute the impact points in the x-direction.
8. Compute the average independent error.
9. Compute the impact points in the y-direction.
10. Compute the average dependent error.
11. Compute the final damage probability.

```

prob.ex.sol <- function(M,ra,b,d,sig){
  bs <- b^2; ds <- d^2; ss <- sig^2;
  nc <- 2^M-1 #Number of total hit combinations
  cf <- matrix(0,nrow=nc,ncol=M) #Matrix to store all hit combinations
  tmpCombinations <- 1:nc
  for (j in 1:M){
    #register hit and miss combinations
    for(k in 1:nrow(cf)){cf[k,j] <- as.numeric(intToBits(tmpCombinations[k]))[j]
    }
  }
  ka <- rowSums(cf) #Total hits per combination of weapons

  #Impact points in the x-direction
  tma <- (cf%*%ra[,1])^2/ka
  tmb <- cf%*%(ra[,1])^2

  #Equation 6 of the exact solution paper
  F1 = sqrt(bs[1]/(bs[1]+ds[1]))^ka * sqrt((bs[1]+ds[1])/((bs[1]+ds[1])+ss[1]*ka)) *
    exp((tma-tmb)/(2*(bs[1]+ds[1])-tma/(2*(bs[1]+ds[1]+ss[1]*ka)))

  #Impact points in the y-direction
  tma <- (cf%*%ra[,2])^2/ka
  tmb <- cf%*%(ra[,2])^2

  #Equation 7 of the exact solution paper
  F2 = sqrt(bs[2]/(bs[2]+ds[2]))^ka * sqrt((bs[2]+ds[2])/((bs[2]+ds[2])+ss[2]*ka)) *
    exp((tma-tmb)/(2*(bs[2]+ds[2])-tma/(2*(bs[2]+ds[2]+ss[2]*ka)))

  #Equation 8 of the exact solution paper
  p <- sum(-(-1)^ka*F1*F2)
  return(p)
}

```

We will Compute the single shot damage probability for one weapon with the following parameters from Wang et al. (2016a):

- M = 1
- ra = [0,0]
- b = [15.4640, 23.3628]
- d = [5,5]
- sig=[30, 30]

```
M <- 1; ra <- matrix(c(0,0),ncol=2); b <- c(15.4640,23.3628); d <- c(5,5); sig <- c(30,30);
prob.ex.sol(M,ra,b,d,sig)
```

```
## [1] 0.2760992
```

M weapons firing at an area target.

The code in this section calculates the kill probability where M weapons are used against an area target centered at $\vec{x}_{target} = (0, 0)$, consisting of N discrete elements, normally distributed around the target center. For this section, we will implement the code that depicts M aiming points on an elliptical target, uniform in polar angle as described in equations 15-17 of Wang et al. (2016b).

Kill probability for an area target

Description

This code calculates the damage fraction against an area target of normally distributed target elements around $(0, 0)$, by M weapons with aim points placed along an Ellipse Uniformly in Polar Angle (EUPA). The set of aim points is specified by three parameters: weapon effective radius in the ellipse (r), aspect ratio of the ellipse (η), and the off-set angle (c_0).

Input

- M : number of weapons
- r : average effective radius of ellipse = $\sqrt{\text{major axis} * \text{minor axis}}$
- η : aspect ratio of ellipse
- c_0 : $c_0 * \pi$ = off-set angle
- $b = [b_1, b_2]$: parameters in Carleton damage function
- $d = [d_1, d_2]$: standard deviation of independent error in 2 directions
- $\sigma_g = [\sigma_{g1}, \sigma_{g2}]$: standard deviation of dependent error in 2 directions
- $s = [s_1, s_2]$: standard deviation of target elements distribution in 2 directions

Output

z : damage fraction

Function Code

To compute the damage probability over an elliptical target area, conduct the following:

1. Compute a vector off-set angles for each weapon.
2. Compute the off-set impact points scaled by the aspect ratio in the x and y direction.
3. Compute the radius of the scaled impact points.
4. Compute the x and y coordinates of the actual impact points.
5. Generate a matrix of the impact points.
6. Compute the standard deviation of the weapon error and target locations.
7. Compute the average damage probability.

```
p.eupa <- function(M,parameters,b,d,sig,s){  
  #Equation 15 of the area target paper  
  phi <- parameters[3]*pi+(0:(M-1))/M*2*pi #offset angle  
  if(parameters[2]==0){  
    parameters[2] <- .Machine$double.eps^(2/3)  
  }  
  if(parameters[2]<0){
```

```

parameters[2] <- abs(parameters[2])
}
#Equation 16 of the area target paper
x0 <- cos(phi)/sqrt(parameters[2])
y0 <- sin(phi)*sqrt(parameters[2])
r0 <- sqrt(x0^2+y0^2)

#Equation 17 of the area target paper
x <- (parameters[1]*sqrt(parameters[2]))*x0/r0
y <- (parameters[1]/sqrt(parameters[2]))*y0/r0

ra = cbind(x,y)
ss = sqrt(sig^2+s^2)
pex <- prob.ex.sol(M,ra,b,d,ss)
return(-pex)
}

```

Note, we are making the final probability negative, because we will minimize this value in the next section.

Optimal aimpoints and Kill probability for an area target

The code below performs a constrained optimization of an elliptical target area that will produce nearly optimal aiming points. The parameters we are optimizing are the effective radius (r), aspect ratio (η), and the off-set angle (c_0). According to Wang et al., “This approach greatly simplifies the numerical complexity of finding the optimal aiming points at the price of obtaining an approximate optimum” (2016b). In MATLAB Wang et al. (2016a; 2016b) used the *fminsearch* function for this optimization. In R, a similar function is found in the *pracma* package.

The code below executes the following:

1. Set the starting conditions for the optimization.
2. Optimize to find the effective radius (r), aspect ratio (η), and off-set angle (c_0).
3. Store the maximum probability.
4. Generate a vector of the optimal parameters (r, η, c_0).
5. Generate the average radius in the x and y direction.
6. Generate a vector of off-set angles.
7. Compute the off-set impact points scaled by the aspect ratio in the x and y direction.
8. Compute the radius of the scaled impact points.
9. Compute the x and y coordinates of the actual impact points.
10. Store the following values in a list:
 - (a) Number of weapons.
 - (b) Max damage probability.
 - (c) x -axis effective radius (range direction).
 - (d) y -axis effective radius (deflection direction).
 - (e) Off-set angle.
 - (f) x -axis aiming points.
 - (g) y -axis aiming points.

```

if(!require(pracma)){
  install.packages("pracma")
}

```

```

## Loading required package: pracma

p.optim.eupa <- function(M,parameters=c(40,0,2),b,d,sig,s){
  u0 <- parameters
  opt.values <- fminsearch(p.eupa,c(u0[1],u0[2],u0[3]),M=M,b=b,d=d,sig=sig,s=s,
                           tol=1e-8,maxiter = 2000)
  pmax <- -opt.values$fval
  u <- opt.values$xval
  ap <- c(u[1]+0.5*u[2],u[1]-0.5*u[2],u[3])
  rx <- ap[1]
  ry <- ap[2]
  phi <- ap[3]*pi+(0:(M-1))/M*2*pi
  x0 <- cos(phi)/rx
  y0 <- sin(phi)/ry
  r0 <- sqrt(x0^2+y0^2)
  x <- (rx*x0)/r0
  y <- (ry*y0)/r0
  z <- list(M=M,pmax=pmax,rx=ap[1],ry=ap[2],phi_1=ap[3],x=x,y=y)
  return(z)
}

```

Maximum Damage Fraction vs. Target Area Size

The code below is an analysis of the relationship of the size of the area target versus the maximum damage probability. The initial conditions are below

- M = 6 weapons
- N = 20 targets
- b = [60, 100]
- d = [5, 5]
- sig=[30, 30]
- sa = sequence from 15 to 300 in increments of 15 to represent the size of the area target.

The code and supporting plot is below. As shown in the graphic, as the size of the target increases, the damage probability decreases as expected.

```

M <- 6; N <- 20; b <- c(60,100); d <- c(5,5); sig <- c(5,5);

#Generate a sequence of values for the area target size and
#an area target size (s0) to show the optimal aim points

sa <- seq(15,300, by= 15)

m <- length(sa)
p_eupa <- numeric(m)
for(k in 1:m){
  s <- sa[k]*c(1,1)
  z <- p.optim.eupa(M=M,b=b,d=d,sig=sig,s=s)
  p_eupa[k] <- z$pmax
}
plot(0,0,type="n",xlim=c(0,305),ylim=c(0,1.1),xlab="Area Target Size",
      ylab="Maximum damage fraction")

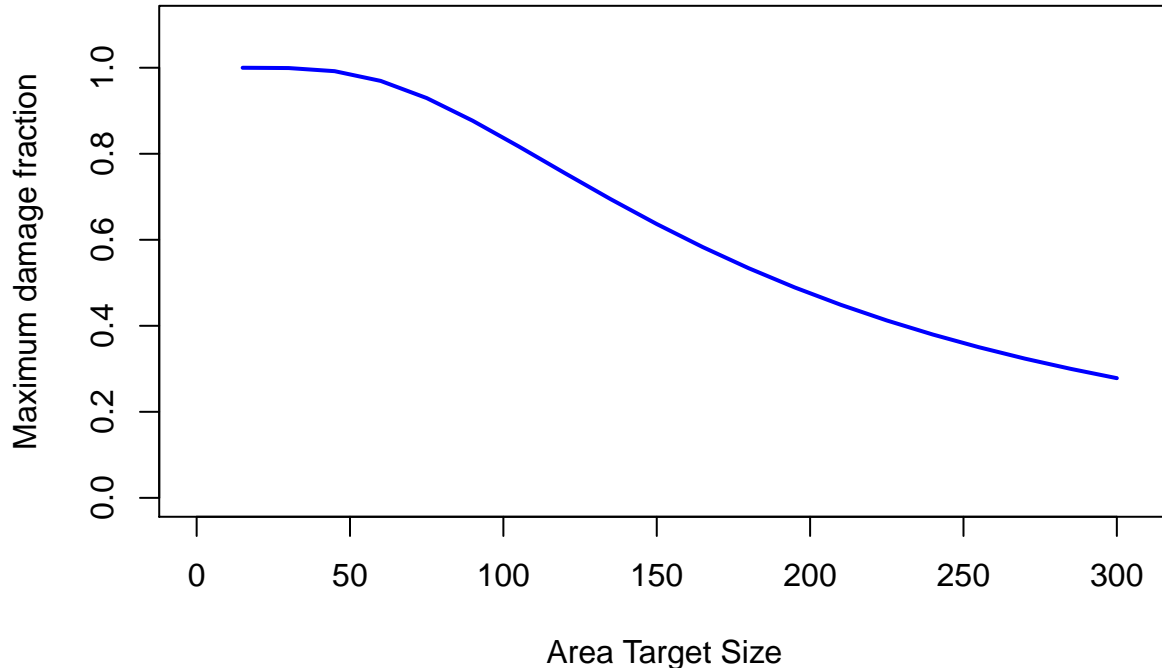
```

```

lines(sa,p_eupa,col="blue",lwd=2)
title(paste(M," weapons against an area target",sep=""))

```

6 weapons against an area target



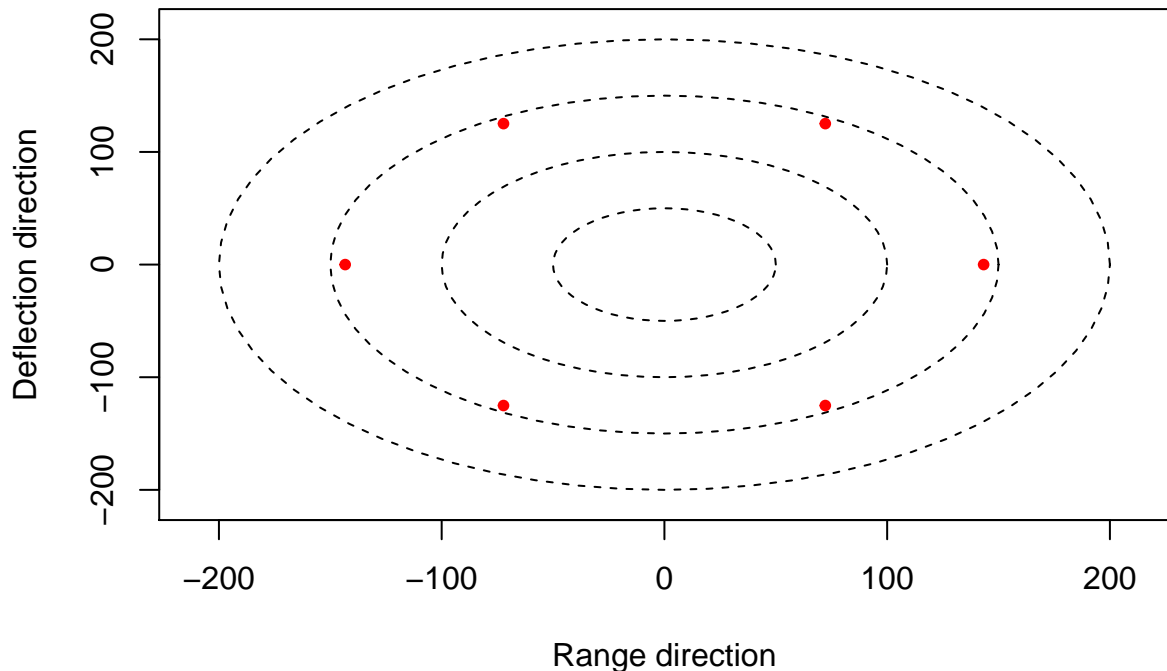
This final section of code plots the locations of the optimal aiming points using the same initial conditions of the previous analysis, however, the plot will focus on a target area size of 150 units².

```

s0 <- 150
s <- s0*c(1,1)
z <- p.optim.eupa(M=M,b=b,d=d,sig=sig,s=s)
x <- z$x
y <- z$y
ct0 <- (0:64)/64*2*pi
x0 <- cos(ct0)
y0 <- sin(ct0)
plot(0,0,type="n",xlim=c(-210,210),ylim=c(-210,210),xlab="Range direction",
      ylab="Deflection direction")
lines(200*x0,200*y0,type="l",lty=2)
lines(150*x0,150*y0,type="l",lty=2)
lines(100*x0,100*y0,type="l",lty=2)
lines(50*x0,50*y0,type="l",lty=2)
points(x,y,pch=20,col="red")
title(paste("Optimal aimpoints of ",M," weapons",sep=""))

```

Optimal aimpoints of 6 weapons



References

- Wang, Hongyun, George Labaria, Cardy Moten, and Hong Zhou. 2016b. "Average Damage Caused by Multiple Weapons Against an Area Target of Normally Distributed Elements." TRAC-Monterey.
- Wang, Hongyun, Cardy Moten, Morris Driels, Don Grundel, and Hong Zhou. 2016a. "Explicit Exact Solution of Damage Probability for Multiple Weapons Against a Unitary Target." *American Journal of Operations Research* 6 (06). Scientific Research Publishing: 450.

Appendix D

Response Surface Methodology

Response surface methodology results

Precision Guided Munitions Project Notes

Title: Algorithm Development for the Combat Sample Generator (COSAGE) Model

Darryl Ahner and Andrew McCarthy, Air Force Institute of Technology

Project Goals

The United States military has been using precision-guided artillery rounds (as opposed to “conventional” rounds) in recent years, but analytical methods enabling effect analysis and tradeoffs between precision and conventional munitions are lacking. The main goal of this project is to develop an algorithm and methodology to accurately represent the high explosive (HE) precision munitions using the Carlton Damage Function.

The motivation for this effort is to accurately model the desired and undesired effects of precision munitions. The algorithm will be developed for use in the Combat Sample Generator (GOSAGE) Model in use by the TRADOC Analysis Center – Monterey Naval Postgraduate School and the Center for Army Analysis – Army G-3. The COSAGE model simulates ground combat between a large number of U.S., Ally, and Enemy weapon systems over a 48-hour period and produces engagement results for U.S. versus Enemy and or Ally versus Enemy interactions.

The algorithm developed during this effort will provide the Army G-3 a better representation of precision munitions effects in their Joint Integrated Contingency Model (JICM) simulation.

Modeling Combat – Initial Setup

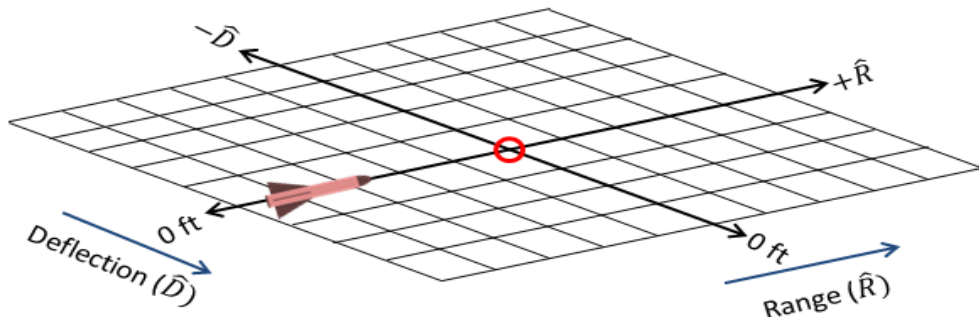


Figure 1: Range and Deflection Grid

When speaking about the grid or the firing area, everything is approached from the perspective of the person firing the artillery round. To start with, some fixed point is established as the origin. The “Range” direction is determined using a straight line from the weapon to the target. The “Deflection” direction is perpendicular to this line, and also intersects the origin.

The entirety of the analysis is in metric units (meters). The standard data is that TLEs, lethal areas, and other measures are provided with in metric units.

For simulation probability results, a square, uniform grid is used. There is a specified distance between each grid point in the range direction and that same distance between grid points in the deflection direction. The size of the grid is arbitrary, but in order to get the most out of limited computer memory, should be as small as possible while still simulating all important distribution characteristics.

Modeling combat – Damage

The Carleton Damage Function is given by the equation:

$$P(K) = D_0 \exp\left(-D_0 \frac{(d - d_{aim})^2}{2b_1^2}\right) \exp\left(-D_0 \frac{(r - r_{aim})^2}{2b_2^2}\right)$$

where

- $P(K)$ is the probability of being killed by that munition strike. To be more general, instead of saying “kill”, “destroyed” is better. This is because not all targets are living. $P(K)$ is a probability and therefore has to be between 0 and 1.
- D_0 is the $P(K)$ for a direct hit. This is a function of both the target and the weapon system and ranges from 0 to 1. For example, if the weapon system has a 50% chance of destroying the target with a direct hit, D_0 is equal to 0.5
- $d - d_{aim}$ is the distance between the point in question and where the munition detonated in the deflection direction
- $r - r_{aim}$ is the same concept, just in the range direction
- b_1 and b_2 represent in some way how far away you have to be from where the munition lands to be safe. To calculate these two numbers, you need to know the Lethal Area (A_L) of the munition and the aspect ratio of the dangerous area. To figure out the aspect ratio, you need to know θ .
- θ is the impact angle of the munition. This is the impact angle relative to the ground plane; if the munition detonates while pointing straight at the ground, $\theta = 90^\circ$. If the munition blows up parallel to the ground, $\theta = 0^\circ$.

$$a = \max(1 - 0.8 \cos \theta, 0.3) \quad b_1 = \sqrt{\frac{a * A_L}{2\pi}} \quad b_2 = \frac{b_1}{a}$$

If the lethal area (A_L), the impact angle (θ), and the direct hit effectiveness (D_0), is known, the Carleton Damage Function estimates $P(K)$ for any point relative to the explosion point. According to Klopčić (1990), the Carleton Damage Function does an excellent job of estimating damage done far away from the blast point. However, that same paper indicates the function underestimates damage in close proximity as can be seen when the Carlton Damage function is plotted (Figure 2).

The Cookie Cutter function is another modeling tool used frequently by the U.S. military. It assigns everything in close proximity to detonation the same $P(K)$ and everything farther away with a $P(K)$ of 0.

Klopovic(1990) indicates the cookie cutter function is a woefully poor estimator of outlying damage, but actually better than the Carleton Damage Function for close proximity damage modeling.

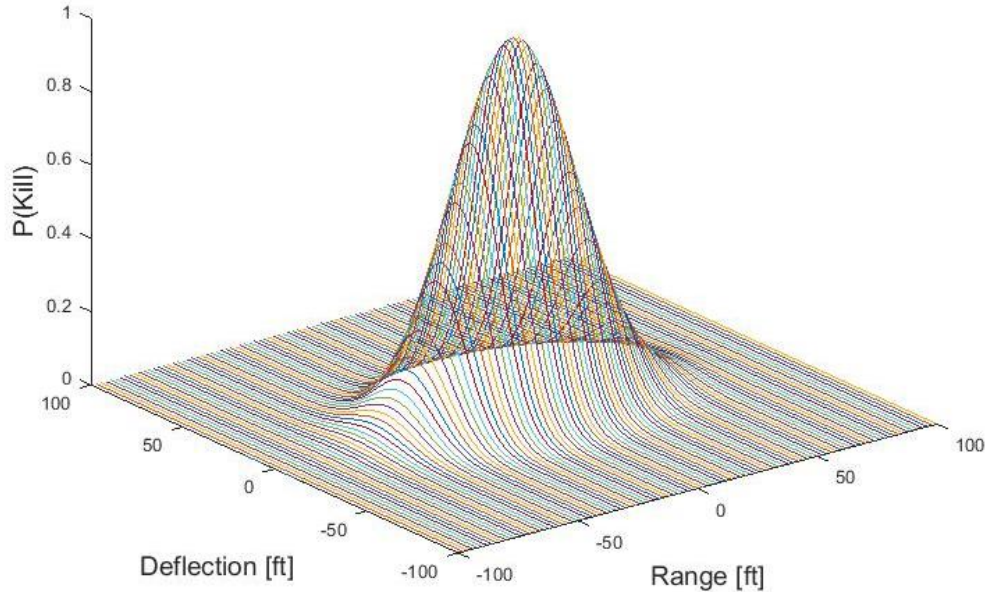


Figure 2: Carlton Damage Function

In summary, the Carleton Damage Function tends to underestimate damage in close proximity to the detonation point, but does an excellent job approximating damage far from detonation point, while the Cookie Cutter Function is simple to implement, but underestimates effects of munitions on distant targets. We therefore combine them taking the best characteristics from each. In order to maximize how realistic our simulation is, we use this combined function which is called the Klopovic Hybrid Function:

$$P(K) = \begin{cases} D_0 & \text{if "close"} \\ D_0 \left(\exp \left(D_0 \frac{(d - d_{aim})^2}{2b_1^2} \right) \exp \left(D_0 \frac{(r - r_{aim})^2}{2b_2^2} \right) \right) & \text{if "not close"} \end{cases}$$

Deciding whether or not you are “close” depends on a fourth input, the Core Lethal Area (A_{L0}). Using this hybrid approach we can take into account not only the inputs, but also the how environmental conditions may affect those inputs as indicated in Figure 3.

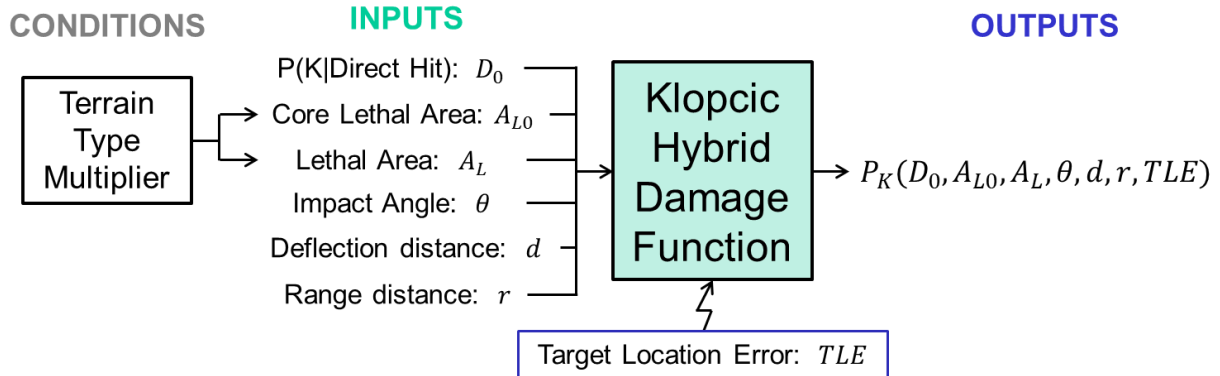


Figure 3: Klopovic Hybrid Function Inputs and Outputs

The Core Lethal Area and Lethal Area are functions of the weapon system and the terrain. The direct hit effectiveness, D_0 , is a function of the weapon system and the target type. This hybrid function will be the basis of analysis going forward and can be used for several different estimates of interest. A three shot hybrid result is illustrated in Figure 4 where total probability of kill as a function of location is depicted.

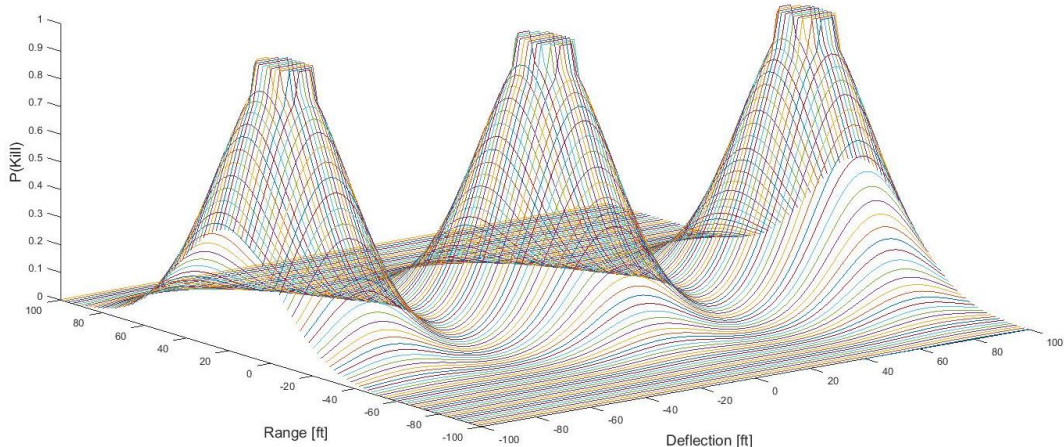


Figure 4: Klopovic Hybrid Function

As seen by the calculation, a closed form probability of kill can be obtained except that target location error exists. This uncertainty changes the deflection and range variables from fixed inputs (d, r) to random variables $(d+\delta, r+\rho)$ where $\delta, \rho \sim \text{Uniform}(-\text{TLE}, \text{TLE})$ as seen in Figure 5. To account for the effects of this target location error random variable, several simulation runs are executed with the target location represented by uniformly distributed location errors from 0 to the maximum reported target location error. In this way, the average effect of a munition can be determined. That effect can take the form of an object being in one of four states.

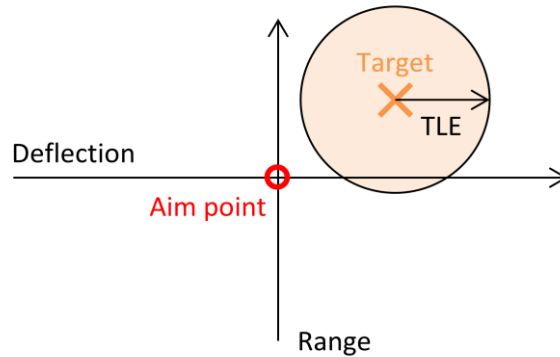


Figure 5: Effect of Target Location Error

Modeling Combat – States of Combatants

There are four separate states that an object can exist:

- Unaffected – The object (whether enemy or non-enemy, mobile or immobile) is functioning at the top of its game. It is at full power.
- Killed – The object is completely destroyed and the prospects of rebuilding or replenishing the object are only plausible in the long term.
- Wounded – An enemy or non-enemy who is not killed, but is slightly damaged. It is not functioning at the highest level of effectiveness, but is still armed and dangerous.
- Suppressed – The object is not killed, but is temporarily unable to defend itself. This changes as a function of time, but is considered constant for the short time frame of this simulation. For example, if an enemy is held down and cannot return fire, that enemy is considered to be suppressed.

If an object is destroyed (“killed”), it is not wounded or suppressed. However, an enemy can be both wounded and suppressed or either one alone. Being wounded and being suppressed are independent of one another. A wounded enemy is no more likely to be suppressed than a healthy enemy. The interrelation of these states is represented in Figure 5.

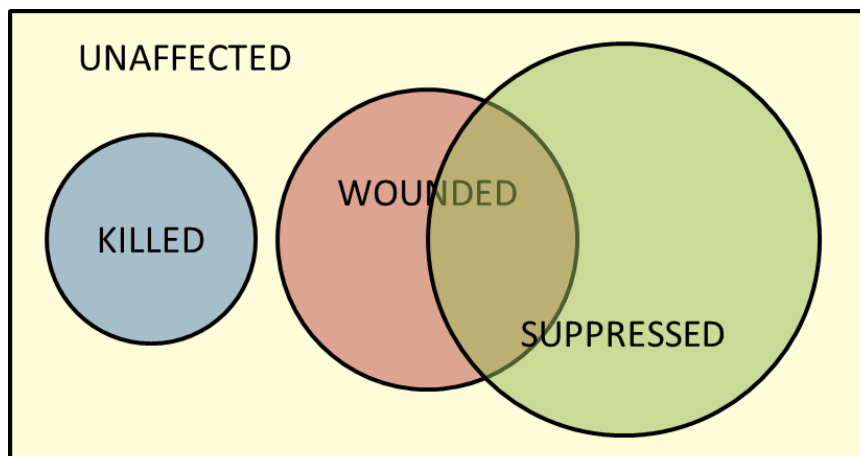


Figure 5: Interrelation of Targeted Object's States

The formula for estimating the probability that a combatant is killed is described earlier. To calculate the probability that an enemy is wounded, the same logic is applied as for this probability $P(W)$, only the “Wounding” Lethal Area of the weapon is larger than the Lethal Area for the $P(K)$ calculation. To arrive at the “Wounding” Lethal Area , the lethal area of the weapon is multiplied by some factor dependent on type of munition. Because a wounded object cannot also be killed, the Klopctic Hybrid analysis for wounding actually calculates $P(W|K^c)$, not $P(W)$. This quantity must be multiplied by the probability of not being killed:

$$P(W) = (1 - P(K)) * P(W|K^c)$$

The logic for calculating the probability of being suppressed works similarly. The Suppression lethal area of the weapon is the original lethal area of the weapon multiplied by some factor. Generally, this factor is larger than the wounding lethal area factor. Because suppression is independent of being wounded, $P(S)$ is just multiplied by the probability of not being killed. The equation is:

$$P(S) = (1 - P(K)) * P(S|K^c)$$

Algorithm Development – Spreadsheet Simulation

KlopcticHybrid.xlsx is the macro-enabled spreadsheet used to model the damage done by a munition or group of munitions while taking in account the uncertainty caused by target location error. Excel was chosen to do all of the modeling due to its wide availability. It is limited in how much resolution you can examine the outcome, but offers the user an intuitive set of inputs.

We describe the setup of the simulation in general here. The grid setup and weapon characteristics were discussed earlier and are needed to calculate the Klopctic Hybrid function. The battlefield characteristics are used to add a terrain factor to the weapon lethal area. Open, level terrain corresponds to a factor of 1, while other terrain (wooded, urban, uneven) takes values less than 1 and shrinks the lethal area of the weapon.

The user sets a number of enemies and places them in the formation chosen by the user. Another important input related to enemy location is the Target Location Error (TLE). TLE is not needed to set the grid or calculate $P(K)$ at each point, but is a major factor in the analysis, especially when determining whether to use PGMs or conventional rounds.

The value of TLE quantifies the uncertainty in target location. In the real world, a spotter or sensor of some kind is needed to determine enemy locations, but it is hard if not impossible to be exact. For example, if the spotter is fairly certain the target is within a circle of radius 10 meters from where we think it is, the TLE is 10 meters. The target is equally likely to be anywhere within 10 meters of the reported location.

To account for TLE in the spreadsheet, a macro called PofK goes through the entire grid point by point, adds up all the P(K) values that are within the TLE for the target in question, and then divides by the number of grid points in that space.

The number of munitions launched and how they are aimed is the last input section, but to meet the first goal of the project, the analysis is restrained to analysis of single munitions. To describe how effective the munition strike is, several measures of effectiveness (MOEs) are listed. The expected number of kills simply adds up the probability of kill for each enemy in the simulation. The expected number of kills per munition divides the expected number of kills by how many munitions were launched. The average P(K) adds up the P(K) for every grid point and then divides by the number of grid points. Expected number of wounded and expected number of suppressed operate in the same fashion as expected number of kills.

Algorithm Development – Experiment Design

In order to measure the impact of each variable a Nearly Orthogonal Latin Hypercube (NOLH) design, a space filling design, is used to mitigate the large number of trials under various conditions while adequately capturing the full range of variability. An NOLH ensures the whole range of interest of each variable is considered, while having minimal correlation between input variables. This approach allows a full range of munition types to be considered without explicitly providing the particular performance parameters of munitions as long as the parameters are captured within the range of variables considered. A random design would ensure minimal correlation, but wouldn't guarantee that all possible values of each variable are equally represented. The actual values used are given in Table 1.

Table 1: Minimum and Maximum Variable Ranges

Input Variable	Minimum	Maximum
Deflection Distance	0 meters	50 meters
Range Distance	0 m	50 m
D_0	0.05	1.0
Lethal Area (A_L)	100 m ²	1500 m ²
Core Lethal Area	10% of A_L	60% of A_L
Terrain factor	0.5	1.0
Impact Angle	30°	90°
Target Location Error	2 m	91 m
Wound LA factor	1.1	2.5
Suppression LA factor	1.1	2.5

The choice of minimum and maximum for each variable in the NOLH is very important. The Core Lethal Area is not yet a measured concept, and was set to be anywhere from 10% of the Lethal Area to 60% of the Lethal Area. The terrain coefficient was set to be between 0.5 and 1, and the wounding and suppression factors were set to be between 1.1 and 2.5. None of these factors had a meaningful effect

on the eventual R^2 values. Impact Angle can only vary between 0° and 90° , but any angle between 0° and 30° provides the same result by the calculation. The assumptions of regression don't work well when a large subset of a predictor gives the same answer, so the range chosen was 30° to 90° .

That leaves distance in the range and deflection directions, the lethal area, D_0 and TLE. The minimum distance away is 0 meters. You can't get any closer than standing at the detonation point. The minimum TLE was set to 2 meters. If you have exact knowledge of the enemy's location, the TLE could be as small as 0, but 2 ensures that with the resolution of the spreadsheet, at least 1 point would be within the TLE.

Lethal Areas are classified, so the estimates are a relative shot in the dark. In the example that Major Moten gave us, the lethal area was $2,270 \text{ ft}^2$ (211 m^2). Based on this, the minimum value was set at 100 m^2 .

In terms of the maximum value for TLE and lethal area, we discussed with Mr. Robert Lillard of the Fires Center of Excellence whether our choices of maximum TLE and maximum lethal areas were representative of real values. A maximum lethal area of 1500 m^2 and a maximum TLE of 25m (for the most precise weapon system, Excalibur) were given a reasonable stamp of approval. It was then at our discretion to determine how much distance we want to analyze and what values of D_0 to use.

Variable	Min	Max
Deflection (d)	0 m	50 m
Range (r)	0 m	50 m
D_0	0.05	1
CLA	0.1	0.6
LA	100 m^2	1000 m^2
Tfactor	0.5	1
ImpAng	30°	90°
TLE	2 m	91 m

Table 2: Initial Experimental Range

There are three types of tube-launched artillery rounds in question: Excalibur, PTK, and conventional rounds. Deciding which one to fire is mostly a function of the TLE. If the TLE is 25 meters or less, two Excalibur rounds are fired at the target. These currently cost around \$5,000 per round, but presumably may become more expensive in the near future (\$15,000-\$20,000 or so). If the TLE is greater than 25 meters but less than 100 meters, PTK rounds are fired. These are not as precise as Excalibur, but are still

considered close to “precision-guided munitions”. How many are fired depends on the target, but these are generally fired in small groups.

Any TLE above 100 meters will be fired upon using conventional rounds, generally in groups of 30-40 rounds per attack. “Dumb” rounds cost around \$1000 per round. After this initial firing, there is a re-assessment period and the decision is made whether to attack again. Whatever kind of round is being fired, the target is called a unit. A unit could be anything from a small, single stationary object to several vehicles 50 to 75 meters apart.

The simulation of these weapon systems can be three-dimensional, but the algorithm should not be. The Carleton Damage Function is not designed to be a three-dimensional equation. Also, the Excalibur weapon is not designed to perform area fires, where many rounds are fired at a group of targets in a large area. Conventional rounds are best suited for this purpose.

$$P_K = f_1(d, r, D_0, A_L, A_{LO}, T, \theta, TLE)$$

Equation 1

Initial experimentation is conducted to determine the overall fit of a regression model to a full range of factors. If the model is sufficient at this point no further model would be required.

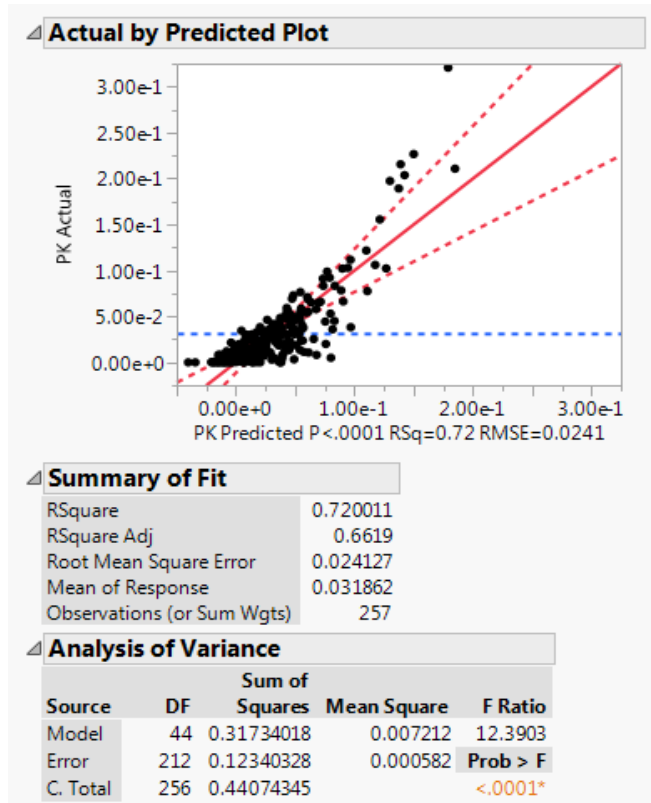


Figure 6: Initial Model

Algorithm Development – Experiment Results

A NOLH was constructed using the ranges in Table 2 for the initial experiment. The initial model fitted a response service that allowed polynomial of degree terms and two-way interaction terms to be considered by a step-wise regression and is a function of terms shown in Equation 1. This resulted in a marginal fit with an adjusted R^2 of .66 which is less than expected and is shown in Figure 6. Additionally, the data displayed a nonlinear relationship with the fitted function indicating a transformation of the data may be required. A square root transformation was applied to the dependent variable $P(k)$ to seek to correct this nonlinear relationship.

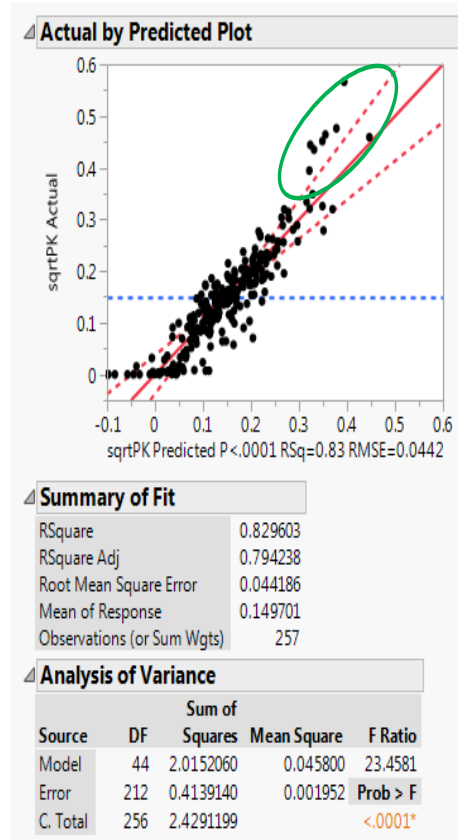


Figure 7: Initial Transformed Model $SQRT(P(k))$

The transformed $P(k)$ regression is shown in Figure 7. Despite the increased adjusted R^2 value of .79, there are concerns over whether this was a good fit across all variable values or whether it was just a good fit for very low $P(K)$ values far from the target and mediocre for close proximity points which have high $P(K)$ as shown for the circled values in Figure 7. To mitigate this, models were developed for different maximum values of TLE, Lethal Area, and distance from the origin (d and r). Specifically different models were developed for maximum TLEs of 15m, 50m, and 91m, maximum Lethal Areas of

500m², 1000m², and 1500m², and maximum d and r values of 10m, 15m, 20m, 25m, and 50m. In all, models were developed for 45 different testing configurations. The goal was to examine how R² is affected by simply changing the range of several key input variables using R² as the dependent variable. The result of this analysis was to verify that models with large TLEs, small Lethal Areas, and large values of d and r produce poor predictive models. While not surprising, it highlights that in order to develop a realistic model, the ranges of input variables had to be realistic and these parameter settings from the initial model do not add resolution to the model.

Using this insight, separate models were developed for Excaliber, PGM, and conventional munitions using values less than 25 meters, 100 meters, and 1000 meters respectively. Since from the original transformed model and further experimentation it was known that model fit may be effected by nonlinearity in some key variables, classification and regression trees were used to determine which variable created the most variability in the model. As shown for the dataset with TLE < 25, there is a natural break at the deflection of 12.6 meters. This process was subsequently used to divide the data as shown in Table 3.

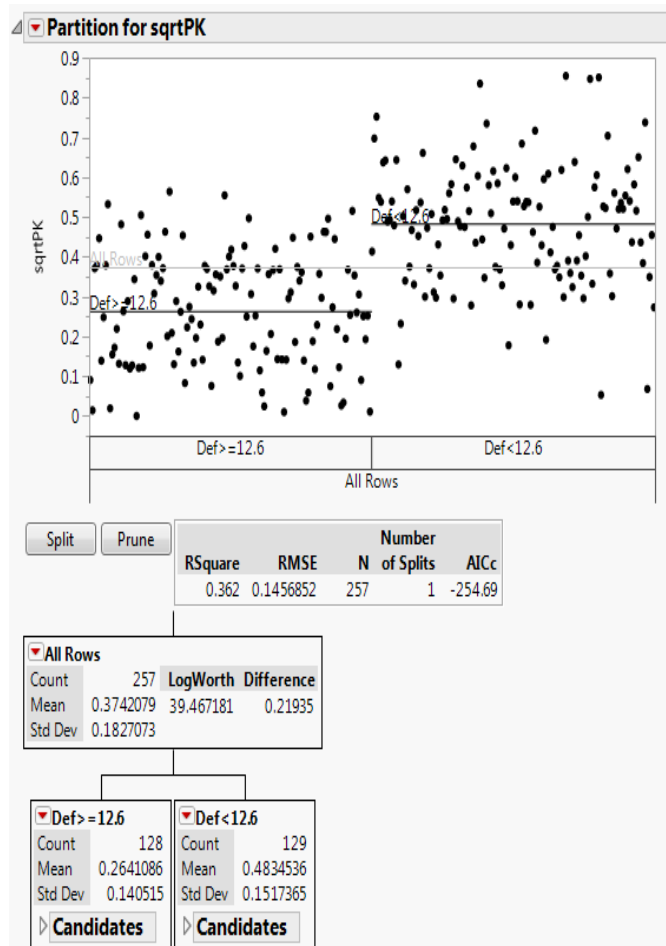


Figure 8: Classification and Regression Tree for TLE<25

This process is followed to develop models for both Excaliber and PGK munitions as shown in Figure 9 (See Appendices for equations) . This methodology creates the 4 models shown in Figure 9 with model goodness-of-fits that are both traceable and defendable for munition effects. The Fit adjusted R² values are shown with the highest R² values for the models with rounds landing closest to the target regardless of the lethal area which is the area of most importance. The Fit adjusted R² values are for the modeling of the square root of P(k). Validation R² values are for simulations of actual P(k) after the square root is transformed back to P(k). These validation runs used 500 randomly selected factor vectors. Again, the model performs extremely well for the area of most concern of higher P(k) values close to the target.

Model	Conditions
Model 1A	D and R < 12.6, TLE < 25
Model 1B	D or R > 12.6, TLE < 25
Model 2A	D and R < 25, 100 > TLE > 25
Model 2B	D or R > 25, 100 > TLE > 25

Table 3: Data Breakpoints for Models

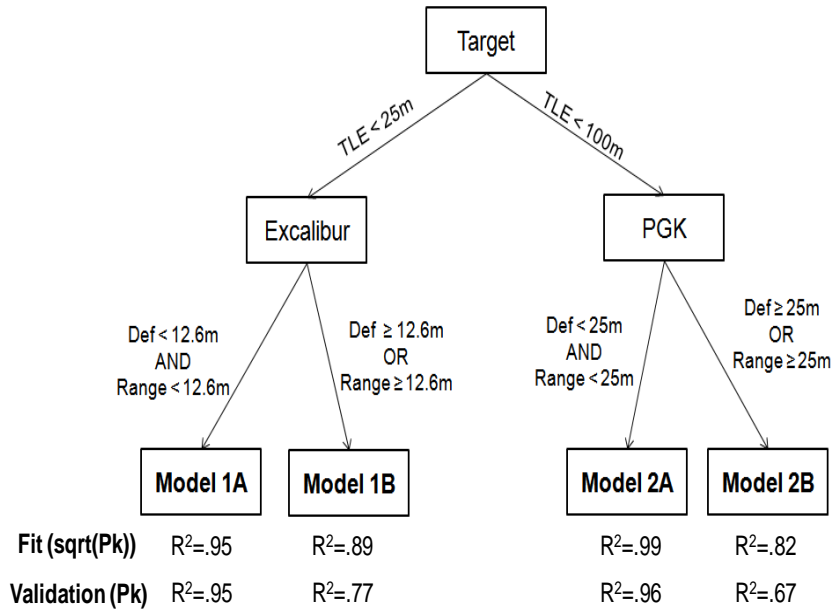


Figure 9: Final Model Goodness-of-Fit and Validation Results

Adjustment for Risk Averse Modeling

While the preceding models capture well the average P(k) effect of a single mention round, planners sometimes want to be risk averse do to civilians or proximity of sensitive objects to impact. As with any good regression model, the preceding models had errors in prediction that were verified to be normally distributed . For risk averse modeling, we use this normal distribution of errors to adjust our model. Based on the Model in use, a constant based on error distribution can be added to the model before it is

squared and then both the model function and added constant to predict a risk based $P(k)$ as shown in Equation 2.

$$\begin{aligned}\sqrt{P_K} &= f_2(d, r, D_0, A_L, A_{LO}, T, \theta, TLE) + C \\ P_K &= [f_2(d, r, D_0, A_L, A_{LO}, T, \theta, TLE) + C]^2\end{aligned}$$

Equation 2

The constant C is determined through a percentile plot of the error terms shown in Figure 10. Dependent on the level of risk aversion, C values for each model can be obtained. For Example, values for C are given for the 75th, 90th, and 99th percentile in Table 4.

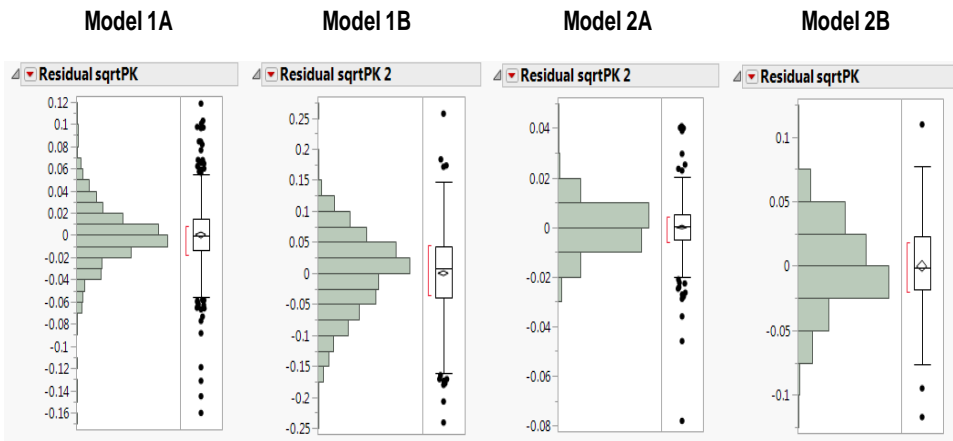


Figure 10: Error for Each Model

Model	75% Adj	90% Adj	99% Adj
1A	0.014	0.032	0.10
1B	0.04	0.077	0.15
2A	0.005	0.011	0.04
2B	0.022	0.041	0.10

Table 4: Error for selected percentiles for each model

Application of Models

To apply the models , traceable inputs for each scenario must be known. Given this information, each round is assumed to act independently. This model is typical in this type of modeling and does not account for a situation where one round may wound an individual and that same individual is "wounded". The number of rounds fired in each situation is left to the modeler; however, this modeling approach allows the modeler to begin to approach the question of how many rounds are enough to achieve the desired effect.

Conclusion

This effort developed an algorithm and methodology to accurately represent the high explosive (HE) precision munitions using the Carlton Damage Function for use with the COSAGE model to accurately model the desired and undesired effects of precision munitions. This effort should enable the COSAGE model to better simulate precision munition weapon effects in ground combat between a large number of U.S., Ally, and Enemy weapon systems over a 48-hour period and produce engagement results .

Similar models can be developed for probability of wounding and probability of suppression.

APPENDIX 1 – Excaliber Models

Trial 55		
Variable	Min	Max
Deflection	0 m	25 m
Range	0 m	25 m
D ₀	0.25	1
Lethal Area	100 m ²	1500 m ²
Core Lethal Area	0.1	0.6
Terrain Factor	0.5	1
Impact Angle	30	90
TLE	2	25

APPENDIX 1A– Excaliber Model 1A

SQRT(P(k) =

$$\begin{aligned}
 & 0.3151885 - 0.012095 * \text{DEF} - \\
 & 0.006095 * \text{RAN} + 0.2659346 * \text{D0} + 0.0215783 * \text{CLA} + 0.0002081 * \text{LA} + 0.1779652 * \text{TFACCTOR} + 0.0008161 * \text{IF}(\text{IMPANG} \\
 & < 30, 30, \text{IMPANG}) - 0.007863 * \text{TLE} - 0.000866 * (\text{DEF} - 5.73838)^2 - 0.000329 * (\text{RAN} - 5.77882)^2 - \\
 & 0.014571 * (\text{DEF} - 5.73838) * (\text{D0} - 0.62775) - 0.009837 * (\text{RAN} - 5.77882) * (\text{D0} - 0.62775) - 0.214067 * (\text{D0} - \\
 & 0.62775)^2 + 0.0000047582 * (\text{DEF} - 5.73838) * (\text{LA} - 804.634) + 0.0000035178 * (\text{RAN} - 5.77882) * (\text{LA} - \\
 & 804.634) + 0.0002606 * (\text{D0} - 0.62775) * (\text{LA} - 804.634) - 0.0000001878 * (\text{LA} - 804.634)^2 + 0.2768908 * (\text{D0} - \\
 & 0.62775) * (\text{TFACCTOR} - 0.75083) - 0.0000738 * (\text{LA} - 804.634) * (\text{TFACCTOR} - 0.75083) - 0.220381 * (\text{TFACCTOR} - \\
 & 0.75083)^2 + 0.0001185 * (\text{DEF} - 5.73838) * (\text{IF}(\text{IMPANG} < 30, 30, \text{IMPANG}) - 60.0127) - 0.00008652 * (\text{RAN} - \\
 & 5.77882) * (\text{IF}(\text{IMPANG} < 30, 30, \text{IMPANG}) - 60.0127) + 0.0014057 * (\text{D0} - \\
 & 0.62775) * (\text{IF}(\text{IMPANG} < 30, 30, \text{IMPANG}) - 60.0127) - 0.000022 * (\text{IF}(\text{IMPANG} < 30, 30, \text{IMPANG}) - \\
 & 60.0127)^2 + 0.0012364 * (\text{DEF} - 5.73838) * (\text{TLE} - 13.535) + 0.0004483 * (\text{RAN} - 5.77882) * (\text{TLE} - 13.535) - \\
 & 0.008522 * (\text{D0} - 0.62775) * (\text{TLE} - 13.535) - 0.000226 * (\text{TLE} - 13.535)
 \end{aligned}$$

For 30 degrees <= alpha <= 90

APPENDIX 1B– Excaliber Model 1B

SQRT(P(k) =

$$\begin{aligned}
 & 0.1821638 - 0.007924 * \text{DEF} - \\
 & 0.00459 * \text{RAN} + 0.000169 * \text{LA} + 0.160827 * \text{TFACCTOR} + 0.0003699 * \text{IF}(\text{IMPANG} < 30, 30, \text{IMPANG}) + 0.0023676 * \text{TLE} + \\
 & 0.000081642 * (\text{DEF} - 26.9887)^2 + 0.000089675 * (\text{DEF} - 26.9887) * (\text{RAN} - 26.9609) + 0.000024447 * (\text{RAN} - 26.9609)^2 - \\
 & 0.00128 * (\text{RAN} - 26.9609) * (\text{D0} - 0.62314) - 0.000003489 * (\text{DEF} - 26.9887) * (\text{LA} - 796.842) - \\
 & 0.000002 * (\text{RAN} - 26.9609) * (\text{LA} - 796.842) + 0.00006377 * (\text{D0} - 0.62314) * (\text{LA} - 796.842) - 0.00000006079 * (\text{LA} - \\
 & 796.842)^2 - 0.003067 * (\text{DEF} - 26.9887) * (\text{TFACCTOR} - 0.7495) + 0.0001227 * (\text{LA} - 796.842) * (\text{TFACCTOR} - 0.7495) - \\
 & 0.00003078 * (\text{RAN} - 26.9609) * (\text{IF}(\text{IMPANG} < 30, 30, \text{IMPANG}) - 60.0044) - 0.00004532 * (\text{RAN} - 26.9609) * (\text{TLE} - \\
 & 13.4792) + 0.0055151 * (\text{D0} - 0.62314) * (\text{TLE} - 13.4792) - 0.000003057 * (\text{LA} - 796.842) * (\text{TLE} - 13.4792)
 \end{aligned}$$

APPENDIX 2 – PGK Models

Trial 57		
Variable	Min	Max
Deflection	0 m	100 m
Range	0 m	100 m
D ₀	0.25	1
Lethal Area	100 m ²	1500 m ²
Core Lethal Area	0.1	0.6
Terrain Factor	0.5	1
Impact Angle	30	90
TLE	2	25

APPENDIX 2A– PGK Model 2A

SQRT(P(k) =

$$\begin{aligned}
 & 0.2118496 - 0.00056 * \text{DEF} - \\
 & 0.000298 * \text{RAN} + 0.0247488 * \text{D0} + 0.0001617 * \text{LA} + 0.1465859 * \text{TFACtor} + 0.0001839 * \text{IF}(\text{IMPANG}<30, 30, \text{IMP} \\
 & \text{ANG}) - 0.003926 * \text{TLE} - 0.00003766 * (\text{DEF}-9.1624)^2 - 0.00002676 * (\text{RAN}-8.86918)^2 - 0.000000894 * (\text{DEF} \\
 & -9.1624) * (\text{LA}-790.25) - 0.0000005558 * (\text{RAN}-8.86918) * (\text{LA}-790.25) + 0.0000192 * (\text{D0}-0.61069) * (\text{LA}-790.25) - \\
 & 0.00000007661 * (\text{LA}-790.25)^2 + 0.0000823 * (\text{LA}-790.25) * (\text{TFACtor}-0.74579) - 0.103632 * (\text{TFACtor} \\
 & -0.74579)^2 + 0.00000024725 * (\text{LA}-790.25) * (\text{IF}(\text{IMPANG}<30, 30, \text{IMPANG}) - 59.9399) + 0.0000414 * (\text{DEF} \\
 & -9.1624) * (\text{TLE}-58.6302) + 0.000044243 * (\text{RAN}-8.86918) * (\text{TLE}-58.6302) - 0.00068 * (\text{D0}-0.61069) * (\text{TLE} \\
 & -58.6302) - 0.00000211 * (\text{LA}-790.25) * (\text{TLE}-58.6302) - 0.001881 * (\text{TFACtor}-0.74579) * (\text{TLE}-58.6302) - \\
 & 0.00001285 * (\text{IF}(\text{IMPANG}<30, 30, \text{IMPANG}) - 59.9399) * (\text{TLE}-58.6302) + 0.000058223 * (\text{TLE}-58.6302)^2
 \end{aligned}$$

APPENDIX 2B– PGK Model 2B

SQRT(P(k) =

$$\begin{aligned}
 & 0.0578981 - 0.001659 * \text{DEF} - \\
 & 0.001348 * \text{RAN} + 0.0000672 * \text{LA} + 0.0735056 * \text{TFACtor} + 0.0011076 * \text{TLE} + 0.0000294 * (\text{DEF}-53.0857) * (\text{RAN} \\
 & -52.9462) - 0.000001108 * (\text{DEF}-53.0857) * (\text{LA}-805.155) - 0.0000007203 * (\text{RAN}-52.9462) * (\text{LA}-805.155)
 \end{aligned}$$

This page intentionally left blank.

Appendix E

References

- [1] Hongyun Wang et al. “Explicit Exact Solution of Damage Probability for Multiple Weapons against a Unitary Target”. In: *American Journal of Operations Research* 6.06 (2016a), p. 450.
- [2] Hongyun Wang et al. *Average damage caused by multiple weapons against an area target of normally distributed elements*. Tech. rep. TRAC-Monterey, 2016b.
- [3] Darryl Ahner and Andrew McCarthy. *Algorithm Development for the Combat Sample Generator (COSAGE) Model*. Tech. rep. Air Force Institute of Technology, 2016.

This page intentionally left blank.

Appendix F

Glossary

ARO	Army Research Office
CAPTTIM	Cognitive Alignment With Performance Targeted Training Intervention Model
IGT	Iowa Gambling Task
TRAC	Training and Doctrine Command Analysis Center
WCST	Wisconsin Card Sorting Test